Politecnico di Torino

Department of Electronic and Telecommunications

Master Degree in Electronic Engineering

Definition of different calibration methods for digital MEMS microphones

Metrological characterization of digital MEMS microphones and definition of a new sensitivity formulation

Relatore:
Prof.Alessio Carullo

Correlatori:
Dott. Andrea Prato
Dott. Alessandro Schiavi
Dott. Claudio Guglielmone

Candidato:
Nicola Montali

Aprile 2018

Everybody's a mad scientist, and life is their lab. We're all trying to experiment to find a way to live, to solve problems, to fend off madness and chaos.

David Cronenberg

Ai miei genitori e a mia nonna

Contents

List Of Symbols

C	capacitance
R	resistance
A	diaphragm surface
Z_{ac}	acoustical impedance
Z	electrical impedance
u	output voltage
ϵ_0	electrical permittivity
c	sound speed ($= 340m/sec$)
λ	wavelength
f	frequency
f_A	audio frequency
$f_C LK$	clock frequency
L_{eq}	equivalent continuous sound level
L_{Aeq}	equivalent continuous sound level A-weighted
L_p	sound pressure level
$dBSPL$	decibel refers to Lp
p	sound pressure (acoustic pressure)
$p0$	reference sound pressure ($= 20\mu Pa$)
$\hat{p}$	rms value of sound pressure
$Decimal_{16-bit-signed}$	decimal scale number converted from 16-bit signed binary data
$Dec\hat{i}mal_{16-bit-signed}$	rms value of 16-bit signed binary wave converted in decimal scale
$Decimalp_{16-bit-signed}$	peak value of 16-bit signed binary wave converted in decimal scale
$dBFS$	decibel full scale
FS	digital full scale of ADC
THD	total harmonic distortion
$THD + N$	total harmonic distortion plus noise
EIN	equivalent input noise (residual noise)
SNR	signal-to-noise- ratio
SNR	signal-to-noise- ratio
PSD	power spectral density

1 Introduction

Over the years MEMS technology (Micro-Electro-Mechanical-System) has allowed the creation of many devices with micro dimensions that previously required substantial mass and volume, such as accelerometers, gyroscopes and magnetometers. MEMS devices combine mechanical parts and electrical components. The first are used to transduce the measured quantity and the later to process the signal. In the audio system the first MEMS microphone has been reported in 1983 by G. Sessler and D. Hohm , and the first commercial MEMS was presented in 2002 by Knowles. From this point forward the study and the research on those devices never stopped.

Figure 1: *MEMS Microphones Application*

Thanks to the recent improvement on MEMS microphones, lot of progresses have been made: small dimensions, high resistance against soldering heat, high immunity to noise. Moreover the acoustic parameters are became more effective, making those devices comparable to professional sound meter and standard microphones. MEMS microphones nowadays are an essential component of any type of electronic device and they start to be used in different fields such as mobile phones, health-care, smart cities, traffic noise monitoring, automotive, home assistants, military etc... (see figure 1) [4]. Furthermore the latest improvements in audio processing in *digital* MEMS microphones has also included voice recognition, noise cancellation, wind cancellation and person identification making MEMS mic fundamental in modern virtual assistants like Alexa, Cortana, Siri, OK Google and Bixby [4].

From an economic point of view, MEMS microphones market is growing up. In the last few years MEMS microphones replaced the electret microphones. Figure 2 shows that the $CAGR$ (Compound Annual Growth Rate) for MEMS is about +11% with $5000 Munits$ (60% of microphone market) produced in 2017 meanwhile CAGR for ECM is decreasing with $3000 Munits$ (40% of the microphone market) in 2017.

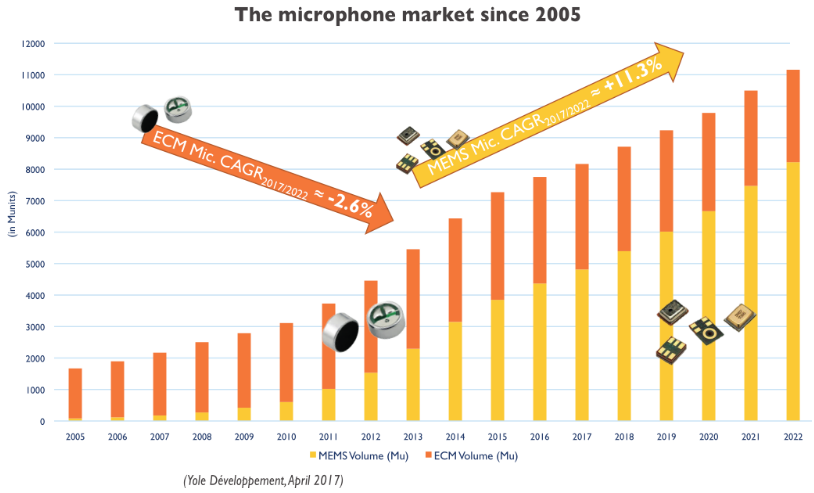

Figure 2: *ECM vs MEMS microphones*

Today μaudio market, including μspeaker and IC supplies, is an important business. In 2017, Yole Développement [4] estimates that the MEMS microphone market almost reached the \$1B milestone, with a value of \$993M. Combined with the \$700M electret condenser microphone (ECM) market, the acquisition of sound nowadays is almost equal to a \$2B value market.

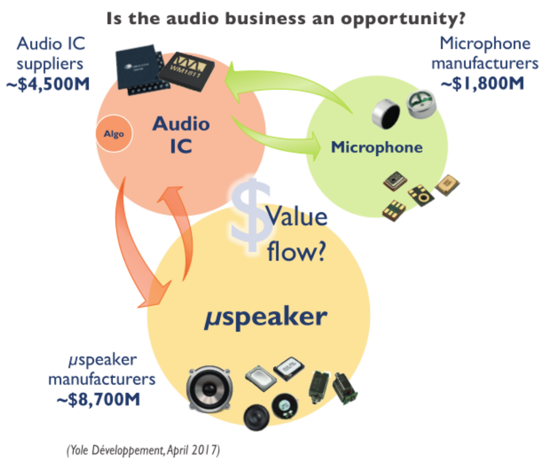

Figure 3: *Audio Market*

MEMS microphones are divided in analogs and digitals. Few years ago, analog microphones dominated the market. But nowadays digital MEMS microphones, are overtaking (see figure 4) . This is due because they offer big advantages such as a higher immunity to electromagnetic interference (EMI), coming, e.g., from a large LCD or Wifi antenna, a higher power supply rejection (PSRR), a higher SNR and the digital output facilitates digital signal processing [3]. As example in a system that only needs audio capture and not playback, like a surveillance camera, a digital output microphone eliminates the need for a separate audio converter and the microphone can be connected directly to a digital processor [6].

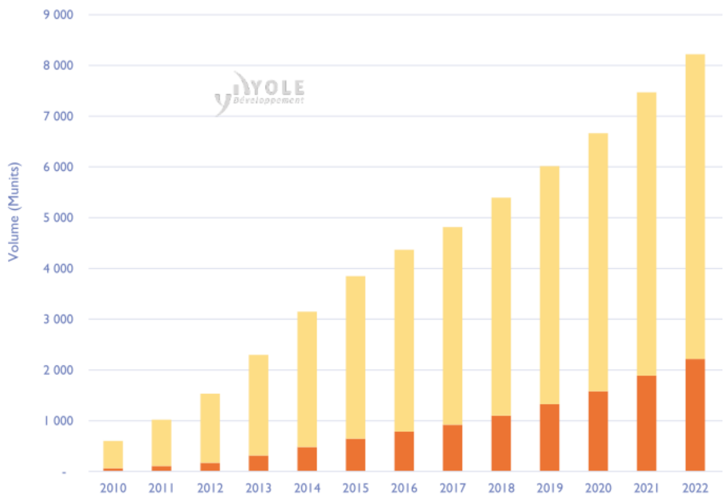

Figure 4: *Analog versus Digital MEMS Microphone breakdown volume - Munits - 2010/2022*

Nowadays one of the major environmental problem in urbanized regions is the noise annoyance [[4]]. The European Environmental Noise Directive [10] obliges each member state to make noise maps of their major highways and highly populated agglomerations. A noise map shows an estimation of long-term averaged noise levels with a fine spatial resolution.

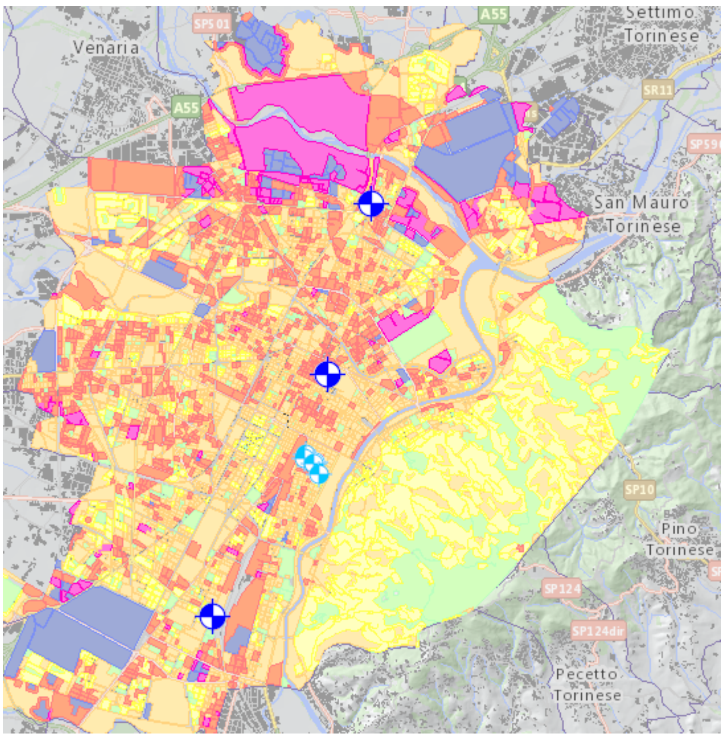

Figure 5: *Torino Noise Map [ARPA]*

However, producing accurate city noise maps is a hard task due to the high cost and number of sensors (class 1 sound level meter) that have to be placed and sometime any city areas are not covered. To overcome those problems MEMS microphones could be used. Thanks to their very low price and high performances those sensor could be placed all around the city and a well precise noise maps could be to obtained. Of course, this would mean to use MEMS microphone as measuring devices

and, as such, a calibration has to be performed.
At present the main problem of MEMS microphone is the lack of certification. Acoustic IEC normative haven't included yet a calibration method for MEMS microphones and, in order to use those devices in one of the previous applications out of a research context, a certification document is needed. The aim of this thesis is to calibrate and characterize one type of digital MEMS microphones trying to investigate different calibration methods by considering precision, accuracy, time and uncertainty. Unlike analog microphones output that is expressed in millivolt, digital MEMS have a digital output expressed in decimal bit, that is the binary number converted in decimal scale. As consequence of that a new definition of microphone sensitivity is needed. In this thesis different way to express it are shown. In $decimal\ Pa$ and in $dBFS$ (decibel-full-scale). Furthermore the principle microphones parameters will be characterized such as: frequency response, sensitivity, distortion, level stability, SNR (signal-to-noise-ratio), residual noise, 1/3 octave-band analysis and influence of temperature.

2 State of the art

2.1 Capacitive MEMS Microphones

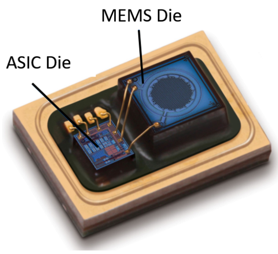

Figure 6: *Architecture of a MEMS microphone*

Capacitive MEMS microphones are dual-die device consisting of two chips. A sensor which converts the acoustic signal into an electrical one and the application-specific-integrated-circuit (ASIC) which is necessary for signal processing. As well as condenser microphones the acoustic sensor is a capacitor.

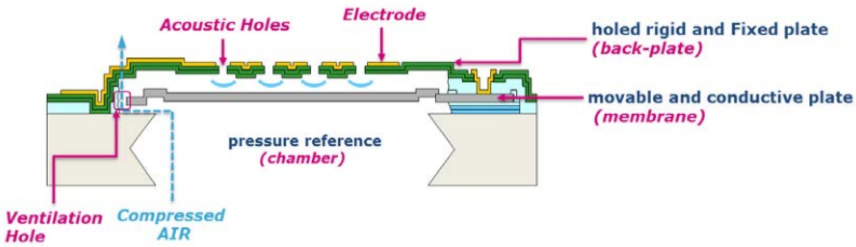

Figure 7: *Internal view of a MEMS microphone*

This last one consists of two silicon plates (see figure 7) where one is fixed (back-plate) while the other is movable (diaphragm). The backplate is a stiff perforated structure that allows air to pass through it, while the diaphragm is a thin solid structure that flexes in response to the change in air pressure caused by sound waves. The back-plate is covered by an electrode in order to make it conductive. Since the MEMS microphone behaves like a capacitor the membrane bending induces changes in the capacitance according to the law:

$$\Delta C = \frac{\epsilon_0 A}{d} \tag{1}$$

Where d is the distance between the two plates, A is the diaphragm surface and ϵ_0 is electrical permittivity. When an acoustic wave, that is an alteration in pressure, passes through the back-plate holes and flexes the diaphragm, it causes a variation of d and therefore on the value of ΔC, converting an acoustical signal into an electrical signal.
The interface circuit for a MEMS microphone, whose block diagram is shown in figure 8, typically consists of some sort of preamplifier that amplifies the small electrical signal coming through the capacitor and a charge pump that generates the bias voltage (V_{ref}) to the microphone.

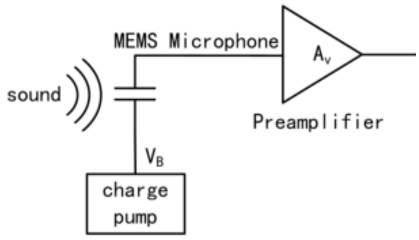

Figure 8: *Block Diagram of a capacitive MEMS microphones*

In order to provide a constant charge on the MEMS capacitors a very large resistor R_b ($G\Omega$) between the microphones and the charge pump is needed, see figure 9. Recalling the equation 1 the output voltage can be expressed as [11]:

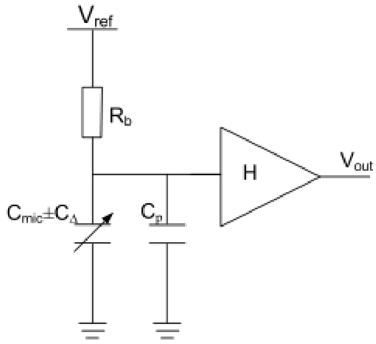

Figure 9: *DC bias scheme*

$$V_{out} = \frac{\pm C_\Delta \cdot V_{ref}}{C_{mic} + C_p \pm C_\Delta} \tag{2}$$

where $\pm C_\Delta$ is the capacitive variation of microphones, V_B is the bias voltage, C_{mic} is the capacitance of the MEMS capacitor when the membrane is not deflected and C_p us the parasitic capacitances. The membrane is fixed only at one side 7. On the other side a ventilation hole is present in order to make the air compressed in the back-chamber to flow out. Both the pressure chamber under the movable plate and this moving air effects allow the membrane to move inside and back to the quiet position.

Membrane and Backplate in detail

The microphone sensitivity is mainly influenced by the typology of the diaphragm and the backplate. The membrane has a circular shape with different diameter dimension depending on different technology process and design variant. The membrane material on MEMS capacitive microphone, metal, polysilicon, and Si_3N_4 etc. are all applicable [9]. The successful application is to use polysilicon due to its lower coefficient of thermal expansion.

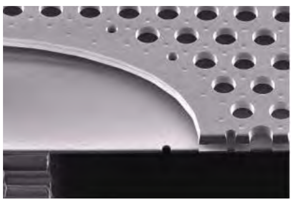

Figure 10: *Insight of Membrane and Backplate*

The backplate has the same shape of the membrane but present on their surface ventilation holes which differ on size and number depending on design. It is realized with highly tensile silicon nitride and thick polysilicon layer that gives enough rigidity to act as a reference electrode. The ventilation holes influences the microphone sensitivity in particular their number and dimension determine the lower corner frequency f_{low} in frequency response [2], which can be expressed by (3).

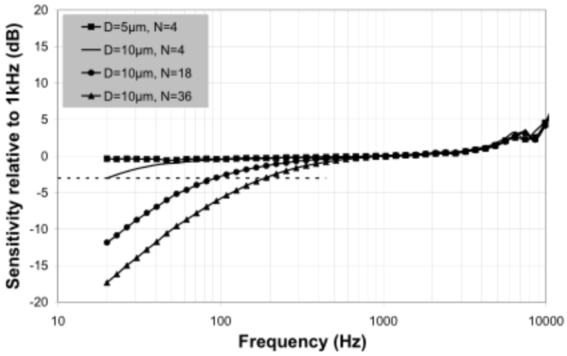

Figure 11: *Corner Frequency with different Number and Size of the Ventilation Holes*

$$f_{low} = \frac{1}{2\pi \cdot R_{vent} \cdot Cbv} \quad (3)$$

where R_{vent} is the equivalent acoustical resistance of the ventilation holes and C_{bv} is the acoustical compliance of the back volume. The corner frequency decreases with high acoustical resistance, which means smaller and less ventilation holes. The figure 11 shows that increasing the number and the dimensions of ventilation holes the sensitivity at low frequency is reduced due to an higher corner frequency [2].

2.1.1 Digital MEMS Microphones [8]

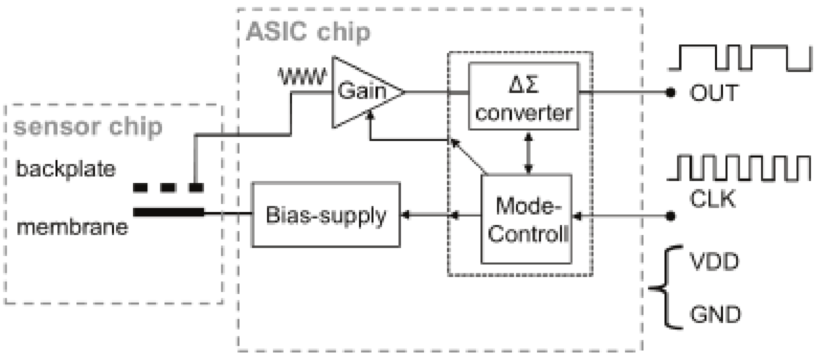

Figure 12: *Block Diagram of Digital MEMS*

As mentioned before the basic internal components of MEMS microphones are the bias supply and the preamplifier (figure 8). Digital MEMS microphones include also an ADC (analog to digital converter) which converts the analog signal that is previously captured by the sensor into a digital one. In order to work properly the ADC needs a clock signal which has to be provided from an external components such as a micro-controller with a I^2S connection. Different frequencies of this signal, provide different operation modes. The modes differ in their power consumption and some electro-acoustic parameters. The best acoustic parameters is obtained with the highest power consumption and is implemented only when records with high quality are needed. This mode is called high mode. Low mode operation with lower power consumption is available but the SNR(signal to noise ratio) decreases.

Digital MEMS microphones need 4 or 5 signals (see figure 13) to work: power supply, ground, clock as inputs and digital signal as output, the fifth is L/R which allows stereo recording but is not always needed. Digital MEMS are typically bigger than analog due to this many connections. Standard package dimension are $3x4x1mm^3$.

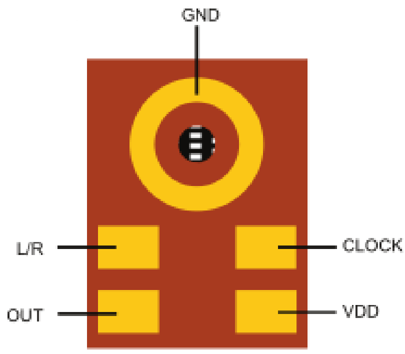

Figure 13: *Bottom View of Digital MEMS*

Sigma Delta Converter [5]

MEMS microphones' ADC is a $\Sigma\Delta$ converter. This kind of converter transform an input analog signal $X(s)$ into a PDM digital output $Y(s)$. PDM stands for pulse density modulation which is a 1 bit digital modulation. The figure 14 shows this kind of modulation.

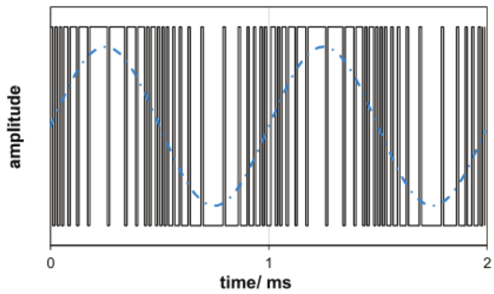

Figure 14: *Analog input signal and Digital output signal with PDM modulation [7]*

When the input signal has a large absolute slope , rapid changes between +1 and 0 are present. A small absolute slope gives less changes between +1 and 0 and a large amount of ones or zeros during that time. The scheme in figure 15 shows a block diagram of $\Sigma\Delta$ converter.

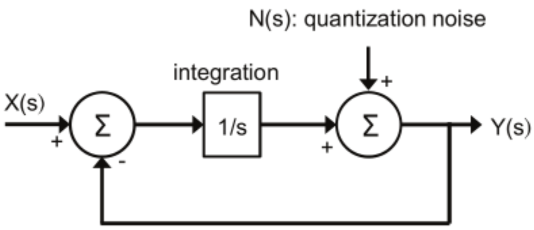

Figure 15: *Block Diagram of $\Sigma\Delta$-converter [7]*

The output $Y(s)$ is obtained with the sum of the integration step, which is a low pass characteristic transfer function, and the noise quantization step which has a high pass characteristic transfer function. The output $Y(s)$ in Laplace domain could be written as:

$$Y(s) = \frac{1}{s+1}X(s) + \frac{s}{s+1}N(s) \tag{4}$$

with $s = 2\pi j\omega f$. From equation (4) is possible to see that when $f \to 0$ only the signal $X(s)$ is present and $N(s)$ is null, instead when $f \to \infty$ the signal $X(s)$ is null and the output signal is equal only to the quantization noise $N(s)$. This behavior can be seen in figure 16. and is a consequence of an oversampling technique which deals with $\Sigma\Delta$ converter. The reason to use this kind of ADC in MEMS microphone is that the quantization noise is shifted to frequencies that are higher than the audio frequencies (from 20Hz to 20kHz). The order of the $\Sigma\Delta$-converter defines how strong this effect is.

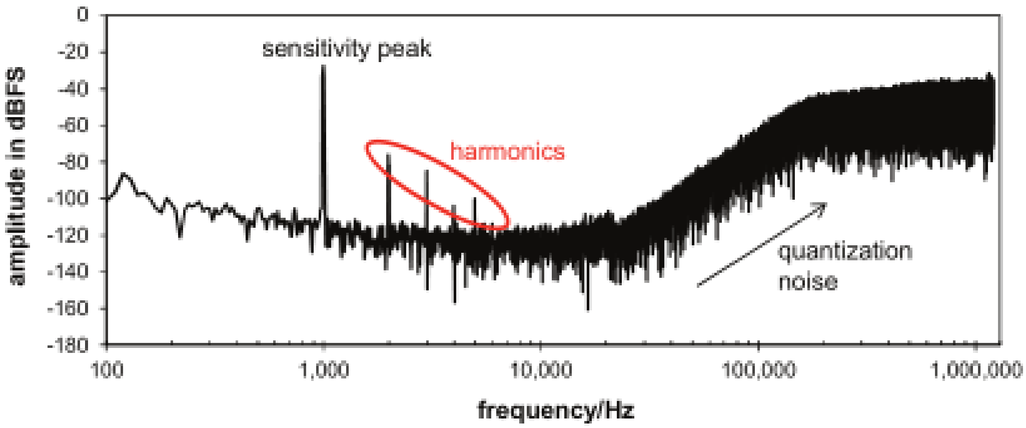

Figure 16: *Spectrum of the output signal of a digital MEMS microphone in high mode exited with a 1 kHz signal with 1 Pa [7]*

Once the digital signal is generated by the converter, is necessary to convert it again to the analog domain. To do that a low pass filter and a decimator filter are implemented. The former is needed to transform the digital oversampled signal in an analog signal. The latter to reduce the number of data analog points and convert the signal in the audio band frequency of 24kHz. The frequency of the PDM, which is the clock input of the microphone, must be a multiple of the final audio output frequency needed from the system. For example, if the audio output signal is required with a frequency of 30 kHz, with a decimation of 80 it needs to provide a clock frequency of 2.4 MHz.

$$f_A = \frac{f_{CLK}}{DecimatorFactor} = \frac{2.4MHz}{80} = 30kHz$$

The output of digital MEMS is expressed in *Decimal* unit which means the conversion in decimal scale of binary data. In equation 5 a digital binary number on 16 bit signed converted in its decimal number is shown.

$$1000101100011111_{16} = -29921_{10} \tag{5}$$

Figure 17 shows a 1kHz digital sine wave generated with and ADC of 16 bit signed. In spite of typically standard microphones that the output is in millivolts referred to an RMS (root-mean-square) value of sine signal (mV_{RMS}), in digital MEMS the output is expressed in Decimal unit referred to the peak value of the signal. As example 16 bit signed sine wave means a signal whose values are between $2^{16-1} = -32768 < x < 2^{16-1} - 1 = +32767$ Decimal. This means that, without considering distortions, the maximum value of digital MEMS coincides with the full scale of the digital convert, that in the case of 16 bit signed is 2^15.

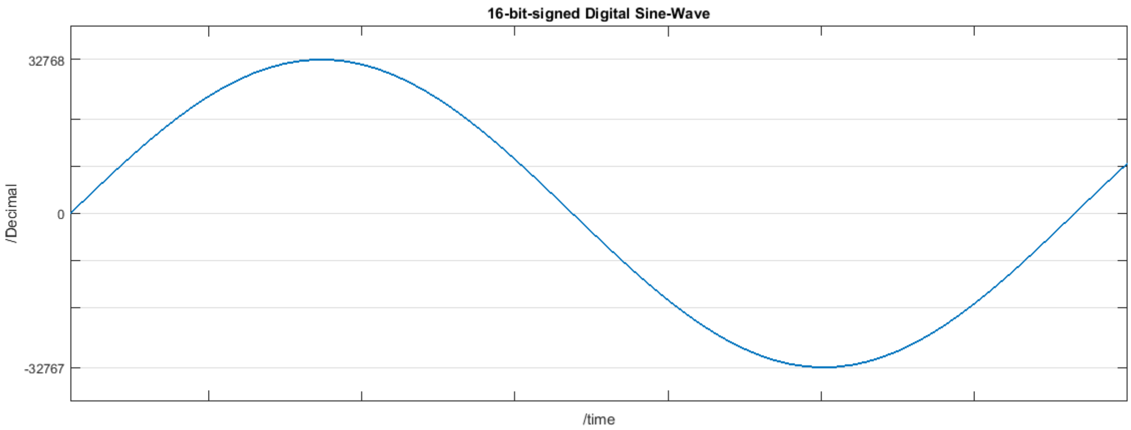

Figure 17: *Digital Sine Wave of 16 bit signed*

2.1.2 Analog MEMS Microphones

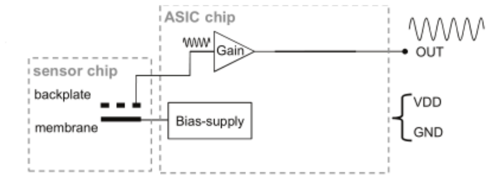

Figure 18: *Block Diagram of an Analog MEMS [7]*

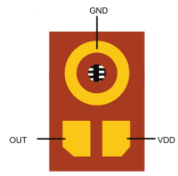

Figure 19: *Top View of an Analog MEMS*

Inside analog MEMS (see figure 18) the bias-supply voltage and the preamplifier are always present. But in spite of digital ones they have an analog output. As consequence, they have a smaller pad and fewer connection. Typically the number of connections, see figure 19, are three (VDD, GND, OUT) and the dimensions are $2.5x3.35x0.98mm^3$. Since the output is a voltage signal any block conversion are not necessary. The output of analog MEMS is expressed in mV.

2.2 Principle Acoustic Parameters of Microphones

Microphones are characterized by different acoustic parameters which describe some of their technical aspects, such as: sensitivity, directionality, SNR, acoustic overload point, dynamic range, frequency response and THD (total armonic distorsion). Some of those values are equal both for standard microphones and MEMS microphones, some are different because of digital output in digital MEMS microphones.

2.2.1 Sensitivity

The sensitivity is the electrical output signal produced by the microphone to a given acoustic pressure in the input. The reference is an acoustic signal of 1 Pa_{RMS} or 94 dBSPL (dB sound pressure level) at the frequency of 1kHz. For analog MEMS the sensitivity is expressed in dBSPL referred to mV_{RMS}/Pa. For digital MEMS, as mentioned before, the output is expressed in Decimal referred to the full scale of digital converter and its number of bits.
As consequence, the sensitivity of digital MEMS microphone could be equally referred to the full scale. A value expressed in dBSPL is made to coincide with the digital full scale and the sensitivity is generally expressed in $-dBFS$, which means how many decibel under the full scale value is the *peak value* of the acoustic signal. If 120 dBSPL coincides with the digital full scale, -20 dBFS means $F.S. - dBFS = dBSPL- > 120 - 20 = 100dBSPL$.

Another possible way to define sensitivity is taking into account, as for standard microphones, the RMS value of digital sine wave and to express the sensitivity in $Dec\hat{i}mal_{16-bit-signed}/Pa$. This concept will be developed in section 3.2.1.

2.2.2 Directivity

The directivity specifies the sensitivity of the microphones with respect to the incident angle of the acoustic wave. This parameter is expressed by polar diagrams figuring the sensitivity pattern response in space. MEMS microphones are typically omnidirectional which means that the sensitivity is the same in every position of the sound source.

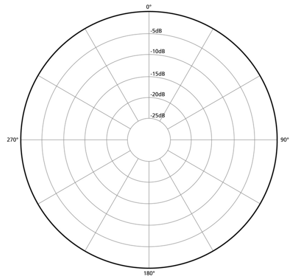

Figure 20: *Omnidirectional Directivity of a typical MEMS microphone*

2.2.3 Signal to Noise Ratio

SNR or signal to noise ratio specifies the difference in dB between reference signal and the amount of residual noise of the microphone output. The reference signal is an acoustic pressure of 94 dBSPL at 1kHz. The noise signal is the residual noise measured in anechoic environment. This parameters include the noise coming both from MEMS sensor and from ASIC. This last noise is negligible respect to the noise coming from the sensor. This kind of noise is typically calculated as a global level over a band of 20 Hz to 20 kHz with an A-weighted filter. This kind of acoustic filter includes a correction factor that corresponds to the human ear's sensitivity to sound at different frequencies. In particular (see figure 21) produces a strong attenuation at low frequencies, a flat response in the middle frequencies and small attenuation at high frequencies.

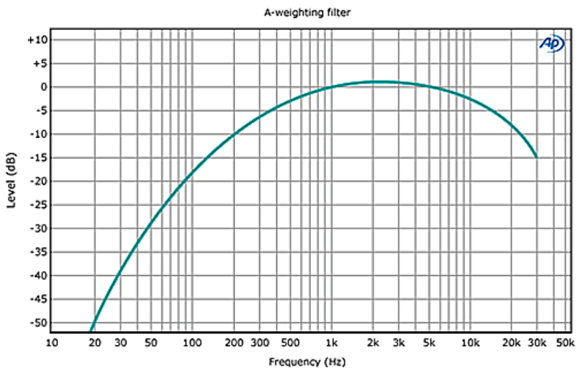

Figure 21: *A-Weighted filter*

Typical SNR values for MEMS microphones are about 63 dB.

2.2.4 Equivalent Input Noise

Equivalent input noise (EIN) is the output noise level of the microphone, expressed in dBSPL, when a theoretical external noise source, which correspond to the residual noise, is placed at the microphone's input. The EIN can be expressed by:

$$EIN[dBSPL] = acoustic_overload_point(F.S) - dynamicrange \tag{6}$$

Input acoustic signals with dBSPL lower than the EIN can not be read by the MEMS microphone. This value define the lowest boundary of the dynamic range.

2.2.5 Total Harmonic Distortion

Total harmonic distortion plus noise (THD + N) is the level of the output distortion respect to a given pure tone at the input. This specification is given as a percentage value and is expressed by the ratio between the power of the successive N harmonics plus the power of noise and the power of the fundamental:

$$THD + N(\%) = \frac{\sum_{n=1}^{N} Power(Harmonics) + Power(Noise)}{Power(Foundamental)} \tag{7}$$

THD +N, rather than just THD, is shown because at lower acoustic amplitude it is almost impossible to distinguish the distortion measured from the microphone noise floor.

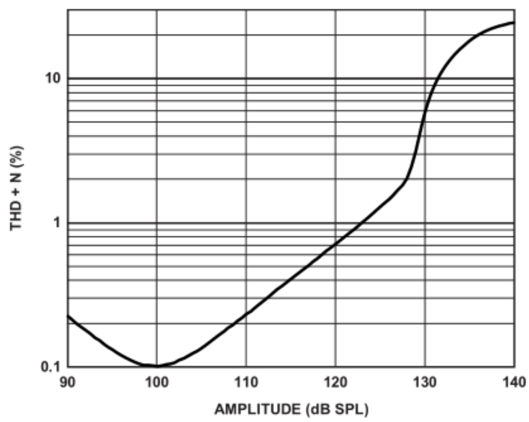

Figure 22: *THD + N for a MEMS microphones [Invensense]*

2.2.6 Acoustic Overload Point

The IEC-61094-4 normative specifies that *the upper limit of the dynamic range shall be stated in terms of the sound pressure level which, throughout the frequency range from 160 Hz to 1000 Hz, results in a total harmonic distortion of 3%* [1]. In the case of digital MEMS the acoustic overload point, AOP, is the sound pressure level (L_p) at which the digital output reaches the digital full scale and gives +0 Decimal. This value correspond to a distortion of about 10-12 % which is different from 3 %. Acoustic pressure with values higher than this specification cause nonlinear distortion of the output signal (see figure 24). In this thesis two way of calculating the AOP are shown in the next chapter.

2.2.7 Dynamic Range and Level Linearity

The dynamic range is the difference between the minimum and maximum signal that the microphone is able to generate keeping its response linearly. The minimum signal is the smallest signal that microphone can generate distinctly from noise that is called *EIN*. The maximum signal is the biggest signal the microphone can generate with small distortion (10 %), so is the AOP. The level linearity is the function which describes how much is linear the L_p read by the microphone between the dynamic range. At certain value of dB L_p the digital mems reaches the plateau, which is the ADC saturation.

2.2.8 Frequency Response

Frequency response of a microphone indicates the sensitivity variation in dB with respect to frequency. Typically there is a frequency band in which the response is linear and two region of deviation: one at low frequency and one at high frequency. In

MEMS microphones the roll of region at LF is due to the ventilation hole in the back cavity and to the geometry parameters of the holes in the backplate (see figure 11). The deviation in the HF is, instead, due to an Helmotz resonator of the inlet.

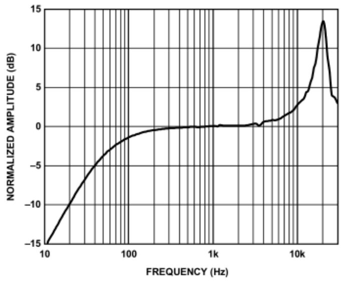

Figure 23: *Typical Frequency Response of MEMS microphones [InvenSense]*

In order to better understand all the parameters expressed before figure show the relation for digital and analog world of MEMS microphone.

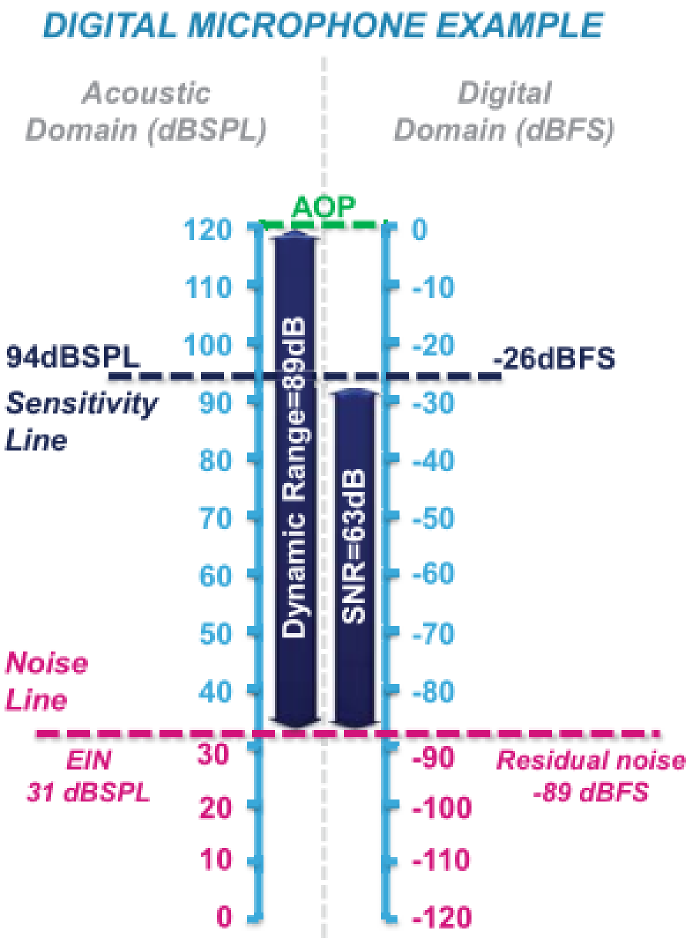

Figure 24: *Acoustic Parameters for Digital MEMS [ST]*

2.2.9 Stability

The stability of a measurement microphone is a very important feature, and distinguishes measurement microphones from other microphones. Two types of stability are typically analyzed, long term and short term stability. Long term stability deals with the microphone diaphragm changes as a function of heat and time. A decrease in mechanical tension of the diaphragms leads to a permanent change in the sensitivity of a microphone. At normal room temperature for laboratory microphone this effect is of the order of 1 dB per 1000 years.
Short term stability deals with some minor variations in sensitivity that will occur due to thermal or mechanical shock.

2.2.10 Influence of Temperature

The sensitivity of the microphone is only slightly affected by the ambient temperature. It is usually not necessary to compensate for this influence, unless the microphone is subjected to very high or very low temperatures. Typical mean temperature coefficient of B&K microphones are very small at between -0.002 and -0.007 $dB\ °C$ averaged over the temperature range to -10 to 50 $°C$. The sensitivity decreases with temperature as shown in figure 25.

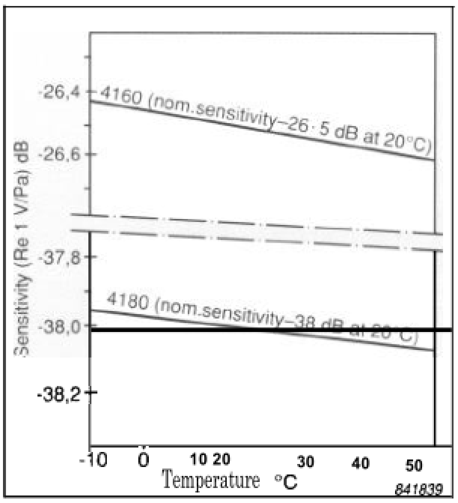

Figure 25: *Effect of temperature on microphone sensitivity*

2.2.11 Influence of Vibrations

When a microphone is vibrating due to different causes, it produces a small output voltage whose magnitude is related to the mass per unit area of the diaphragm. The sensitivity of a microphones to vibration is quantified in terms of equivalent sound pressure level. The magnitude of this effect is of the order of 65 dB at $1m/s^2$.

2.3 An Overview on Standard Calibration Methods for Microphones

The principle standards methods for microphone calibration are describe by the International Electrotechnical Commission (IEC). This corporation elaborates regulations that have to be followed in order to certify a microphones. For example it describes the kind of microphones that have to be used, the environment specification in which the measurement have to be carried out, the kind of sound source that has to be adopted, the sound that has to be generated, etc... . *For all these situations essentially all commonly used measurement and reference standard microphones are condenser microphones. Nowadays a normative for the calibration for MEMS microphones does not exist.*
Typically sound is measured in many different places and sound fields can be very different, but there are three basic standard situations. Sound field produced within cavities, whose dimensions are smaller than about a quarter of the sound's wavelength

that is called a *pressure-field*. Sound field generated inside an anechoic rooms or outside in a big open space, where sound may propagate freely without reflecting objects that is called *free-field* . Sound field generated in a reverberation room with reflecting walls that is called *diffuse-field*. Between those kind of filed situations two principal typologies of microphones calibrations exist: primary calibration by reciprocity and secondary calibration by comparison. The main difference is that a primary calibration does not require a reference microphone and is the more accurate procedure to calibrate laboratory microphone. The calibration by comparison need a reference microphone that has to be previously calibrated with the primary calibration.

2.3.1 Pressure-Field Primary Calibration by Reciprocity

The microphones calibration by reciprocity is the primary method to calibrate microphones. The reference normative is the CEI EN 61094-2 and CEI EN 61094-3. Reciprocity calibration is based on the measurement of the transfer function between two or three microphones that are operated as a source and a microphone respectively. The basic principle is that a microphones is a reciprocal sound-to-electricity transducer which means that it can work as a microphones, converting an acoustical input to an electrical output, and as a sound source, converting an electrical input to an acoustical output. The sensitivities of each of a set of three microphones are determined from the results of three independent measurements made with pairs of microphones, where one is the transmitter ant the other the receiver, connected by an acoustic coupler, with no pairwise combinations ([8]). For each combination two microphone are coupled together in an acoustic chamber (see figure 27 and 26) and their sensitivities is obtained by the combination of two transfer functions: the ratio between the output voltage (u_B) of one microphone and the input current of the other (u_A), that is the electrical impedance (Z_{AB}) and the acoustical impedance (Z_{ac}) of the coupler.

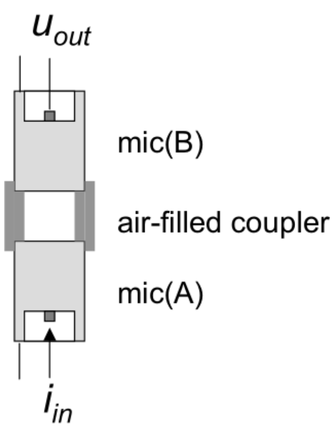

Figure 26: *Microphones coupled by air-filled cavity for pressure response calibration*

Figure 27: *Measurement chamber designed for reduction of noise and for pressurisation*

The following equation describes reciprocity methods:

$$Z_{AB} = \frac{u_B}{i_A} = M_A Z_{ac} M_B = M_A M_B = \frac{Z_{AB}}{Z_{ac}} \tag{8}$$

By repeating the measurement with an other combination and by combining the finale equations, the sensitivity of the microphone under test is determined. The problem of using this technique with MEMS microphones is that this kind of microphone do not behave like a sound source. As consequence, the MEMS microphone work just as a receiver and the other two the microphones as a transmitter and receiver .

2.3.2 Pressure-field secondary calibration by comparison

The sensitivity and frequency response of a microphone may be either obtained by comparison with a reference microphone that has already been calibrated with a reciprocity calibration. This kind of calibration is carried out in a pressure-field which means inside an active coupler (see the figure 28) or –close enough to the sound source in order to consider the acoustic field a pressure field (see the figure 29).

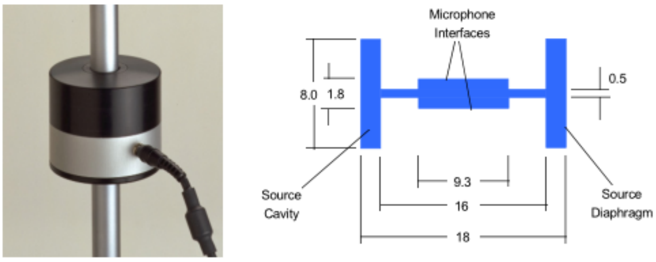

Figure 28: *Active Coupler with built-in sound source (left). Cross-sectional view of its air-filled cavity (right)*

Comparison calibration of pressure sensitivity is covered by *IEC61094-5*[[1]].The standard describes all the procedures that have to be followed and also the way of mounting the microphones. In all cases they are aligned up their axes of symmetry with their diaphragms or protection grids facing each other in a distance of typically 1 mm. This is done in order to have the same pressure field at both microphones. Once the microphones have been placed a certain number of sine waves are generated. For each of them the value of sound pressure level in Pa from the reference microphone and the output sensitivity in mV or Decimal units from the microphone under test have been recorded. The frequency response is obtained by calculating the ratio of those two values. The frequency generated could be selected with an octave band step (one-third, one-sixth, etc..) from 20 Hz to 20 kHz.

Figure 29: *Pressure-Field comparison nearby the Sound Source with MEMS microphone*

2.3.3 Free-field calibration by comparison

The key concept is the same of pressure-field calibration: a calibrated reference microphone and a microphone under test are exposed to the same sound-field. By calculating the ratio of their open circuit output voltage, the ratio of their sensitivities is obtained. The main difference is that in this case the sound is propagated in a free-field which means three wave-length away from the sound source. Two way of doing this calibration are possible. One using sequential excitation and an other using simultaneous excitation. The typical configuration is using an anechoic environment with the sound source mounted in the floor and the microphone floating upon the speaker (see figure 30). The kind of calibration is rarely used since it requires many time to prepare the measurement setting. The most common calibration is the pressure calibration and from that is derived a correction coefficient used to transform the sensitivity in pressure filed to the sensitivity in free field.

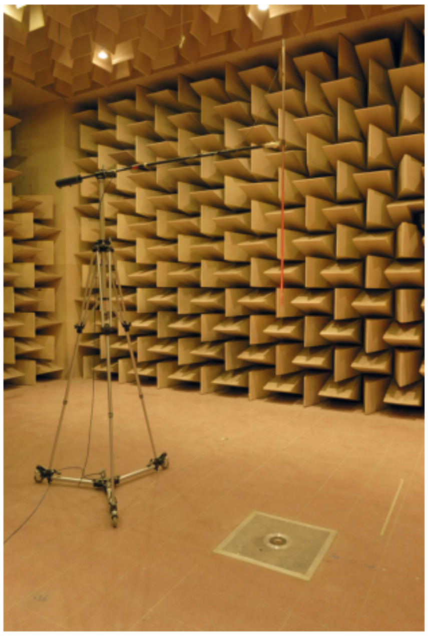

Figure 30: *Free-Field Configuration in Hemi-Anechoic Chamber*

2.3.4 Sound level calibrators

Figure 31: *Sound Calibrator Type 4231*

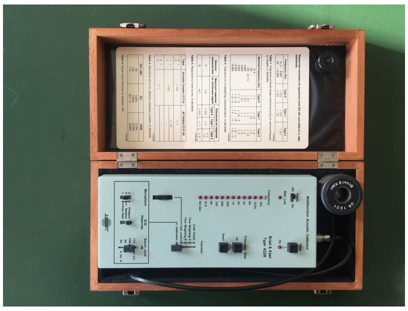

Figure 32: *Sound Calibrator Type 4226*

Sound level calibrators are sound sources that produce known sound pressure level at single known frequency (*Sound Calibrator Type 4231*, figure 31) or at different frequencies (*Sound Calibrator Type 4226*,figure 32). The most common calibrator type is the "feed-back calibrator". It contains a sound source that is a microphone that works with extremely high stability and independence of variations in static pressure and temperature. One cavity of 1" or 1/2" where to insert the microphone to be tested is present on the top of the calibrator and when fitted on a microphone it gives a continuous sound pressure level. The sound is stable if the air-flow in the coupling volume are inhibited. This condition is easily reached with standard microphones because of the calibrator geometry is made for them. As regards MEMS microphones that are smaller than standard microphone, a specific adapter has to be built. This concept will be developed in section 3.3. Sound level calibrator are well-suited for reference standards for comparison calibration.

3 Measurements Methodology

In this section are listed the measurements performed for digital MEMS calibration and how the acquisition of digital data are implemented. The results are shown in the next chapter. The results are described in the next chapter.

3.1 Digital Data Acquisition

Digital MEMS microphones need at least 4 signals to work: power supply (VDD),ground (GND), data and clock (CLK). Unlike analog MEMS, they need a micro-controller which generates the clock signal, VDD, GND and acquires digital data. In this thesis the micro-controller and the digital MEMS microphone adopted are *32F769I DISCOVERY* and *MP34DT05-DS* respectively.

Figure 33: *32F769I DISCOVERY*

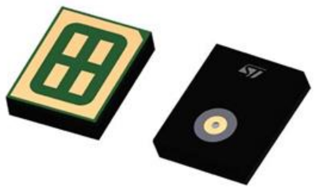

Figure 34: *MP34DT05-DS*

The micro-controller has been programmed to generate a clock of $3MHz$ and a power supply of $3.5V$. In this condition, digital MEMS microphones works in HIGH MODE, which means higher performances and power consumption. Digital signals are sampled with a sampling frequency of $48kHz$ and acquired using the I^2S protocol (see section 2.1.1). The digital data are expressed by 16 bit signed. To acquire data a PC is needed, since the micro-controller has *USB* connection to be powered and programmed. A simple graphic interface programmed with Visual Studio has been implemented to make the acquisition easier, see figure 35.

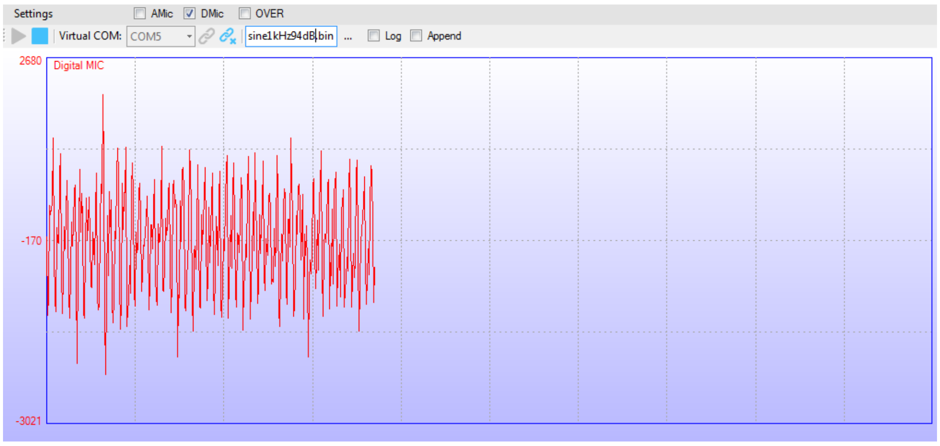

Figure 35: *Visual Studio Graphic Interface*

The wave that is shown in the graphic, is an example of a signal which shows if the microphone is correctly working. To record data a log button must be pressed and a binary file will be generated with the name inserted in the white cell next to the log button. During the acquisition phase a buffer is filled with a certain number of digital data, that is one every $20\mu sec$ since the sampling frequency is 48kHz. The binary file is then elaborated with *Matlab*. As consequence, all the data processing are not performed in real time but signals are firstly acquired and then analyzed.

3.2 Analysis of Digital Data

Starting from the binary file the elaboration with Matlab is done trying to emulate audio analyzer, in particular Time, FFT and RTA analysis.

3.2.1 Time

The typical signals analyzed are stationary and periodic signals like sine waves or stationary and random noise. As mentioned in 2.1.1 digital sine wave is a sine signal with the range depending on the digital full scale. The ADC in micro-controller generates 16 bit signed data, so the upper and lower limits of digital signal are:

$$2^{16-1} = -32768 < x < 2^{16-1} - 1 = +32767 \tag{9}$$

Time domain signal could be an important analysis to understand if the signal is acquired in a correct way. In particular it is possible to see saturation with a clipped area and the influence of low frequency which modulate the signal. Furthermore by plotting the entire acquired signal it is possible to see if spike noises are present. Typically when this kind of noise appeared at the end of the signal it is removed by taking less samples, even if it appeared in the middle the measure is repeated. This kind of noise were more common when measures are taken in the office since the noise coming from the surrounding environments is more frequent than the anechoic room. Typical situations could be a closing door which causes pressure variation in the room.
The analysis in time domain is performed also every time a filter in time series is required, in particular for the frequency response in $Decimal_{16-bit-signed}\hat{}/Pa$ and 1/3 octave bands (see respectively 2.1.1 and 3.8).

Frequency Response

As mentioned in 2.2.1, the sensitivity of digital MEMS microphones could be expressed in dBFS, considering the signal peak value , or in Decimal/Pa, considering the RMS value. This last formulation is taken into account since, from a metrological point of view, is important to give a reference for digital MEMS more similar to standard microphones, where the sensitivity is expressed in mV_{RMS}/Pa. Furthermore the value of real acoustic signals are typically expressed by considering the RMS value. Special when stationary random signal have to be analyzed, the equivalent level, i.e. the equivalent level A-weighted or linear, Fast, Slow, Imp etc..., has to be computed by considering the RMS
To calculate the frequency response in $Dec\hat{i}mal_{16-bit-signed}/Pa$ a digital pass-band filter in time domain is implemented. The bandwidth is chosen narrow enough to consider all the signal energy at the specific frequency. In particular the filter bandwidth is centered in the frequency of interest and the two lateral endpoints are ±10% of this frequency. In example when the frequency at 1000 Hz has to be analyzed the bandwidth of the filter is centered at 1000 Hz and the lateral endpoints are at 990 Hz and 1010 Hz. Once the signal is filtered the RMS value is computed with the following formulas:

$$Dec\hat{i}mal_{16-bit-signed} = \sqrt{\frac{1}{N}\sum(Decimalp_{16-bit-signed})^2} \tag{10}$$

where N are the number of samples in the digital waveform, and decimal is the value, converted from the signed 16-bit binary number, of those samples.

3.2.2 FFT

The most common representation of the *analysis* of the acoustic signal comes trough the frequency analysis. This is done by calculating the *Fast Fourrier Transformation* that is defined by:

$$X(f) = \int_{-\inf}^{+\inf} x(t)e^{-2i\pi ft}\delta t \tag{11}$$

where X(f) is the signal in frequency domain, x(t) the same signal in time domain. Moreover in order obtain more accuracy two type of windowing filter are implemented: Hanning and Flat-Top.

Windowing

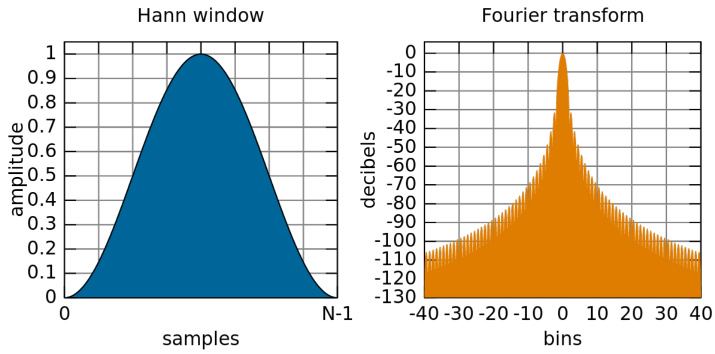

Figure 36: *Hanning Filter*

The Hanning window is characterized by a narrow main lobe and the subsequent side-lobes are characterized with a fast slope in the amplitude which make the filter very selective in frequency. This kind of window is used to improve frequency accuracy and remove spectral leakage. In fact typically signal analyzed present a non-integer number of cycles in the analysis window of the fft. As consequence, the discontinuities at the boundaries cause frequency energy leakage in the original signal. The Hanning window reduces discontinuities at the endpoints of the waveform providing a more frequency defined spectrum.

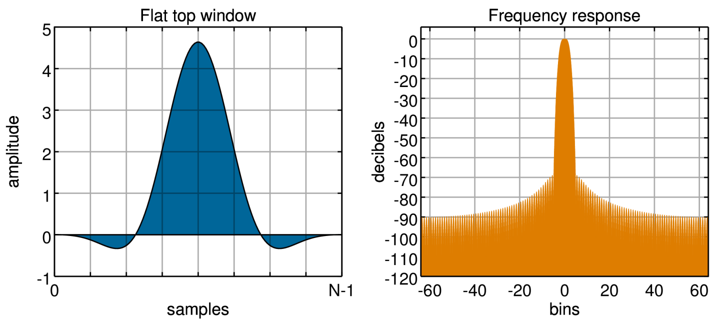

Figure 37: *Flat-Top Filter*

Flat-Top window's spectrum is characterize by a nearly flat main lobe which reduces maximum amplitude error because make the signal indifferent to the position of the frequency signal compared to spectral resolution. As consequence, a more accurate in the peak value is reached. Flat-Top window is the most used window filter in microphones calibration since the peak amplitude of the spectrum is fundamental to calculate the frequency response.
In parallel with fft, also the Power Spectrum Density is computed by the equation (12):

$$PSD_X(f) = X(f)X^*(f) \tag{12}$$

PSD describes how much power of a signal is distributed over frequency. It converts complex fft function in to real domain loosing phase information which is not important in acoustic calibration.
To analyze digital sinewave and calculate the sensitivity, four types of fft are implemented: standard fft, standard fft with hanning window and with flattop filter, PSD with flattop. Every fft is obtained by an average a certain number of fft calculated every 2^N points of the digital waveform in time domain. As shown in the figure 38 the time signal is segmented in k rectangular window of 2^N number of pints with an overlap factor of 50 %. For every window a Hanning or Flat-Top is applied and then a fft or PSD function is calculated.

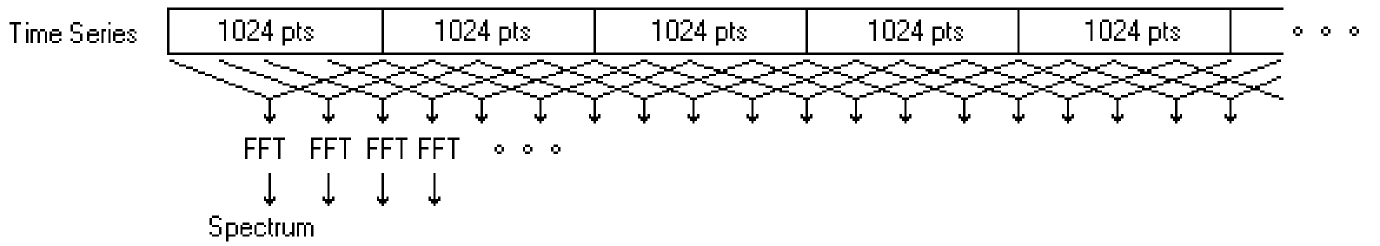

Figure 38: *Overlap Process*

The 50 % overlap factor is decide in order to increment the accuracy in the spectrum average without loosing samples, and the power of 2 for the window size is chosen to achieve the best performance from Matlab fft calculation. The k number of average step depends on the number of samples of digital waveform and the number of points of the rectangular window. Once the signal is filtered by the Hanning or Flat-Top windows it has to be normalized by normalization factors that are respectively 0.215 for Flat-Top and 0.5 for Hanning. The figure 39 shows the four type of spectrum calculated by the previous algorithm of an acoustic signal of 94 dB at 1kHz. The Y-axis scale is in decibel scale. Recalling that PSD is a squared number to obtain the value the square root has to be taken. In decibel domain this means calculating $10 * log10(Y)$. The spectrum in figure 39 shows just the fundamental frequency at 1kHz.

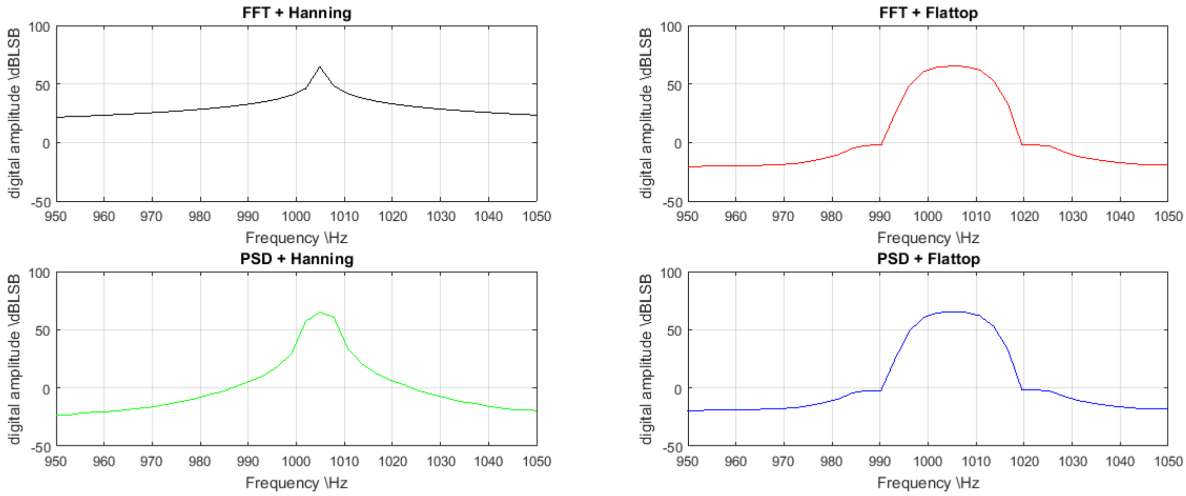

Figure 39: *Four Types of Spectrum Analysis - Fundamental Frequency*

In the graphics on the left it is possible to see the effect of the hanning window that makes the shape of the fundamental frequency narrower than flat-top with the peak value centered at the signal frequency that is 1005 Hz. The flat-top, on the right, is smoother than hanning with the peak value that covers the fundamental frequency 1005 Hz $\pm 15 Hz$. Moreover the PSD, bottom-left and bottom-right, both with Hanning and Flat-Top, makes the energy of the signal condensed at the signal frequency, while in standard fft energy is more spread over the frequencies. This effect is more visible in the graphics on the left, with Hann window, where the frequency energy from 1kHz to 950 Hz in the standard fft decrease very low and is about 25 dB at 950 Hz. The frequency energy in PSD decrease faster and reaches the -20 dB at 950 Hz.
In more cases could be also useful to calculate the spectrum over the full range of frequencies. This is done in particular to observe the behavior of the successive harmonics and also to verify if disturbing signal are present. In the case of this thesis the micro-controller used is equipped with an LCD screen which generates a an acoustic signal at *11870 Hz*. This signal is not an upper harmonic of the acoustic signal at 1kHz because is not at 12 kHz. Therefore 12^{th} harmonic already exist in the

spectrum. The figure 40 in the graphic on the bottom-right shows the disturbing signal at 11870 Hz with the amplitude of 9 dB bigger than the 12^{th} harmonic with an amplitude of -16 dB. Even if this signal is an unwanted signal does not corrupt the measure since the fundamental signal at 1kHz is bigger than 60 dB.

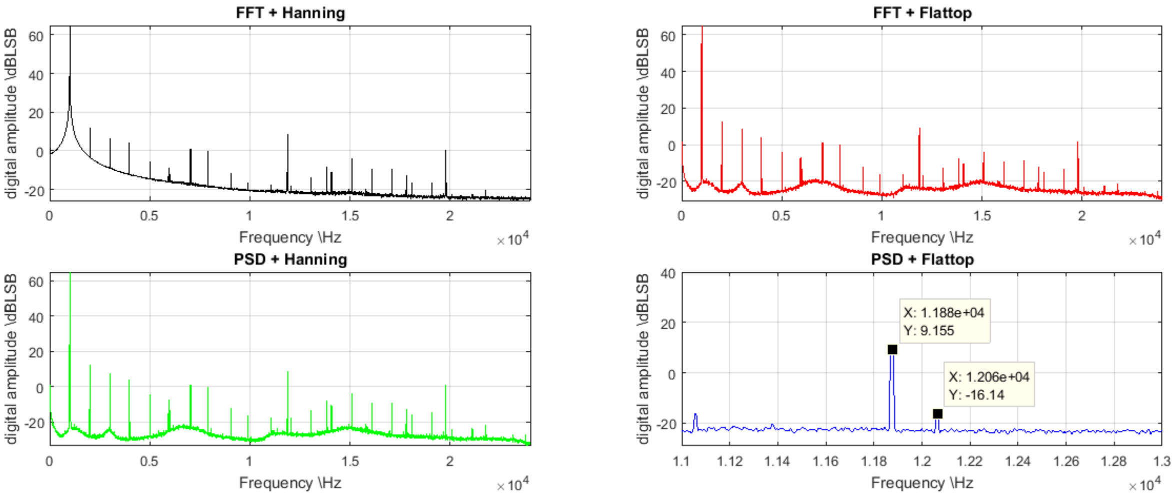

Figure 40: *Four Types of Spectrum Analysis - Complete Range*

Frequency Response

To calculate the frequency response refers to *dBFS*, the PSD spectrum with Flat-Top filter (see figure 41 *PSD+Flattop*) is use, since a more accuracy in the peak value is preferred. The spectrum is in linear scale and since the PSD is a squared value the square root is taken.

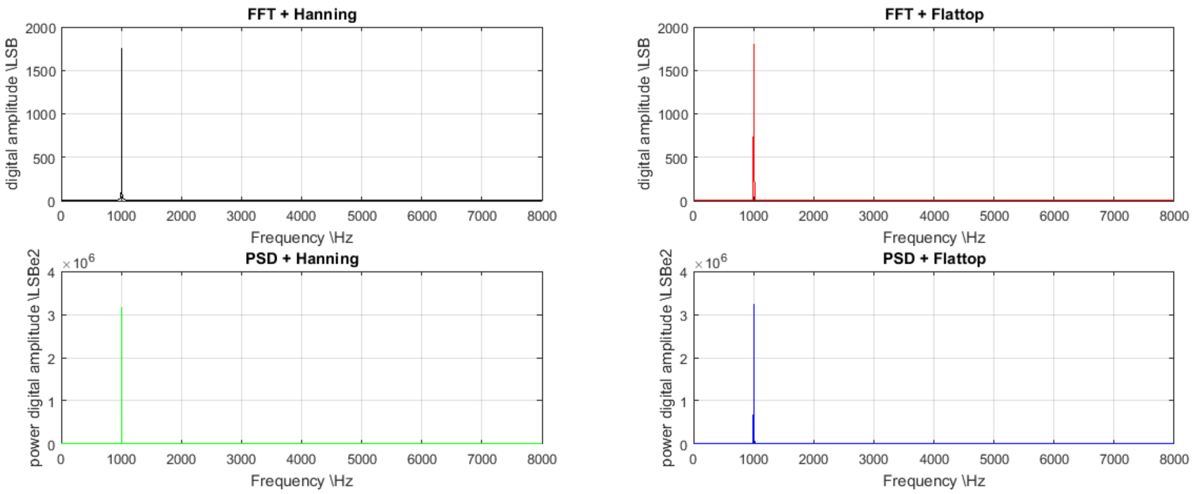

Figure 41: *Four Types of Spectrum Analysis - Linear Scale*

The peak amplitudes from the four type of spectrum shown in figure 41 are listed in table 1. The difference from fft with Hann and fft Flat-Top is about 50 decimal unit, from PSD with Hann and PSD with Flat-Top is about 20 decimal units and from PSD with Flat-Top and FFT with Flat-Top is about 20 μ , so is quite the same value.

	FFT + Hann.	**FFT + F.T.**	**PSD + Hann.**	**PSD + F.T.**
Peak Value	1749.150181	1797.934368	1778.793548	1797.934383

Table 1: *Differences in Peak Value taken from the Different Spectrum*

3.2.3 $\frac{1}{3}$ Octave Band Analysis

An important analysis to evaluate the behavior of an acoustic signal, typically stationary and random, is the octave band spectrum analysis. The input signal is filtered in time domain with a certain number of pass-band filter centered at specific frequencies. The number of pass-band filters and the number of center frequencies depend on the type of octave band chosen for the analysis. Typically values are 1/3, 1/6, 1/12, 1/24 octave bands. The 1/3 octave band spectrum has 30 center frequencies.
The percentage filters bandwidth is constant for all frequencies. The relative frequency difference between a center frequency and the next one is constant too. This means that, along the acoustic frequency spectrum *20Hz-20kHz*, the signal is equally distributed in constant frequency bands. Once the signal is filtered, the RMS (root mean square) is evaluated. The spectrum band analysis typically include also the continuous equivalent level (L_eq) and the continuous equivalent level A-weighted (L_{Aeq}). To represent the band spectrum, a bar graphic is chosen in order to make the energy contribution in each frequency clearer, as shown in figure 42. The y-axes is expressed in logarithm scale.

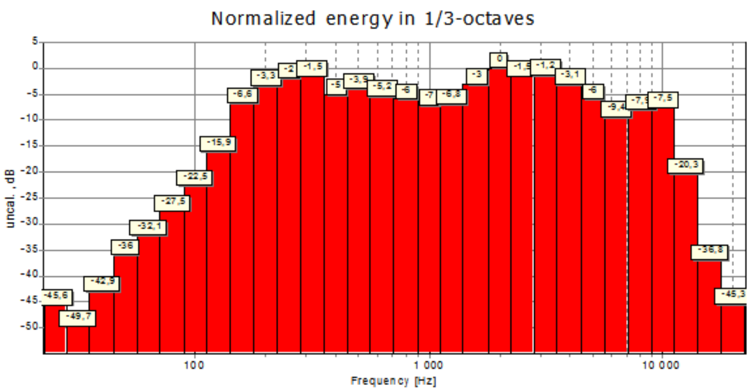

Figure 42: *1/3 band spectrum*

The octave band spectrum analysis for digital MEMS microphones is computed with *Matlab*. The pass-band filters implemented are Butterworth filter of 2Nth-order with the sampling frequency of 48kHz and the center frequencies equal to all the preferred frequencies between 20 to 20kHz, see Appendix A.

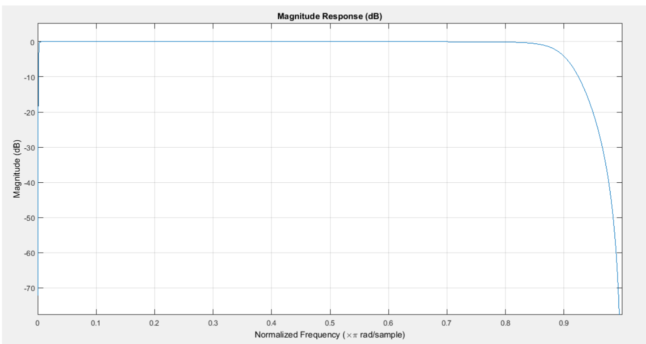

Figure 43: *Butterworth filter of 2Nth-order*

Since the sampling frequency is very high to sample the low-frequency signal, to reduce processing overhead a decimation by 2 is implemented. After the filter process the RMS is calculated obtaining the $\hat{Decimal}_{16-bit-signed}$ value of the digital signal in time domain filtered in the specific frequency band. To convert it in Pascal, two ways are possible: the first is to divide every RMS values by the sensitivity calculated in $\hat{Decimal}_{16-bit-signed}\ Pa$ per every 1/3 frequency band, the latter is to divide every RMS values by the sensitivity just at 1kHz for all the 1/3 frequency band. Both way are considered and the results are shown in the next chapter. Once the value in Pascal is obtained is converted in dB with the formula

$$Lp = 20log10(\frac{p}{p_0})dB$$

where p_0 is the static pressure that is $20\mu Pa$. The equivalent value is calculated by taking the square root of the sum of all the single rms levels dived for each band squared.

$$L_{eq} = \sqrt{\sum (L_{RMS})^2}$$

The equivalent value A-weighted is calculated in the same way but in addition to the pass-band filter the A-weighted filter is applied. The A-weighted filter is implemented with Matlab with *bilinear transformation*. To better understand the algorithm used a flow chart graphic is shown in figure 44.

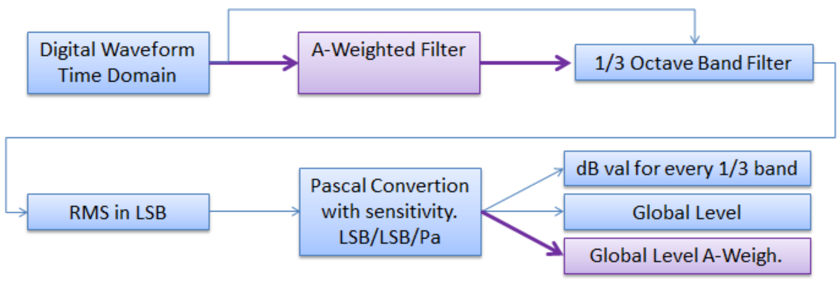

Figure 44: *1/3 Band Spectrum Flow Chart*

The plot obtained with *Matlab* is shown in the figure 45, where a red noise is analyzed.

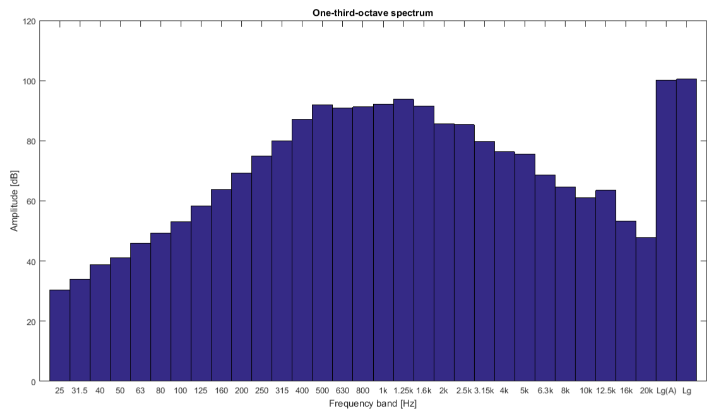

Figure 45: *Red Noise 1/3 octave band spectrum*

3.3 MEMS Microphone Adapter

Figure 46: *Front View of MEMS Adapter*

Figure 47: *Top View of MEMS Adapter*

In order to make the calibration more accurate, an adapter for MEMS microphone is built. The adapter should look like the standard $\frac{1}{2}''$ pre-amplifier for B&K microphone. It is fabricated with a PVC cylinder with about the same diameter of the laboratory microphone, 13 mm. The MEMS microphone was inserted at one side of the cylinder and on the other side there were the cables. Moreover a silicon glue is doused in on the bottom of the cylinder and a small dose is inserted also on the front side of the cylinder below the MEMS in the inside part. A strip of tape is wrapped outside around the MEMS border and the cylinder. All this steps are done for two reasons: the first is to avoid air leakages which causes unwanted acoustic resonance in the frequency response. The latter is that without an adapter is impossible to make a calibration for MEMS microphone in an acoustic coupler or with a sound calibrator since it does not correctly couple and the acoustic feedback is not achieved.

3.4 Frequency Response

Refers to section 2.3.2 for theory concept.
All the types of frequency response are obtained by calibration by comparison in a pressure-field. This was consequence of that the digital MEMS elaboration was not done in real time and the calibration by reciprocity requires that both three microphone are able to acquire simultaneously. Furthermore the free-filed calibration by comparison was avoid since digital MEMS is always equipped with the micro-controller and it could generate acoustic reflections. So the calibration by comparison was done in three different way, in hemi-anechoic room, with a sound calibrator and with an active coupler. According to the type of the calibration, different test benches with different instruments are provided. Different sine waves are generated according to the sound source potentiality. As consequence, different type of precision and computational work are obtained. Some kind of calibration are more precise and accurate but need more time and more instruments. Some other are less accurate but also need less time and less instruments. But regardless of the calibration way the algorithm is the same for all and will be describe in the next section.

3.4.1 Hemi-Anechoic Room

INSTRUMENT	VALUE	MANUFACTURER	TIC. TYPE	U(y)
reference microphone	L_p	Bruel & Kjaer	4191	0.2 dB
MEMS microphone UT	LSB/Pa - dBFS	ST	MP34DT05-DS	
spectrum analyzer	Hz/L_p	Onosokki	DS-3200	0.015 dB
signal generator	Hz	Bruel & Kjaer	1049	0.001 Hz
sound source amplifier		Rotel	RA-05-SE	
microphone amplifier		Bruel & Kjaer	5935	
cables RGB				
2 PCs				
2 Tripod Booms				
Software	Remote Connection	Team Viewer 12		

Table 2: *Differences in Peak Value taken from the Different Spectrum*

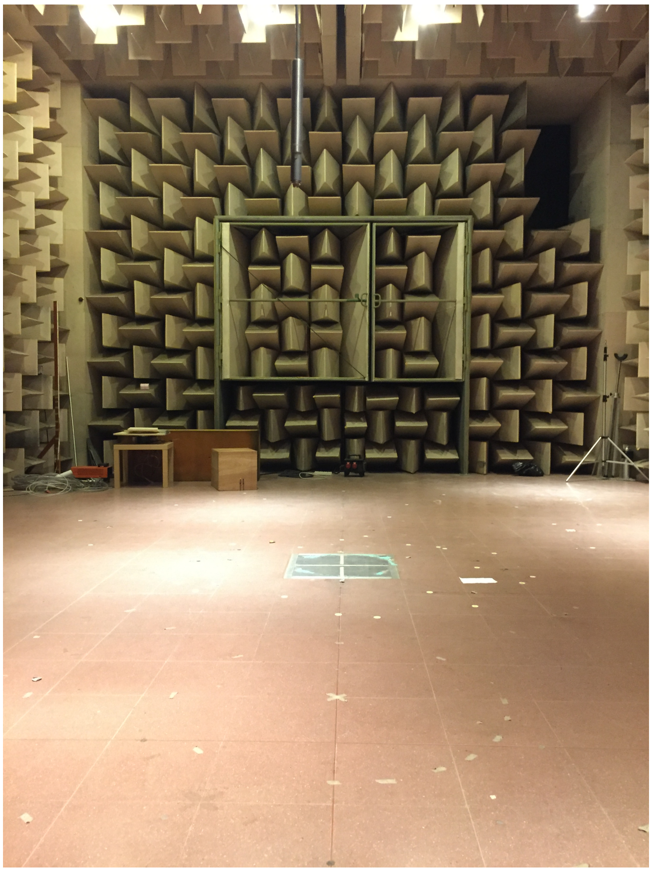

Figure 48: *Hemi-Anechoic Room of INRiM*

The measurement environment was the hemi-anechoic room of INRiM (figure 48), that is a $350m^2$ room with the walls fully covered by sound-absorbing wedges. Thanks to that the sound in this room is never reflected (except for the floor) and sound propagation is generated only by direct sound waves. Moreover since this room is suspended on big steel spring the noises, in particular vibrations at very low frequency, coming from the outside do not flow through the room. Every time this chamber was used to implement a measure was previously heated until a temperature of 20° was reached.

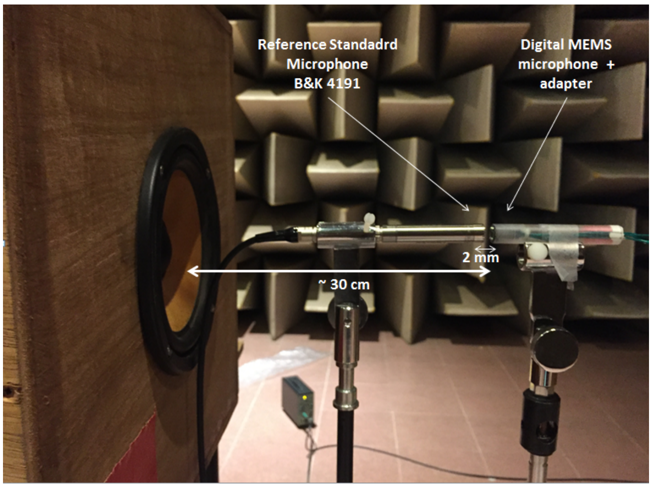

Figure 49: *MEMS calibration in Anechoic Room*

The MEMS microphone and the reference microphone are placed coaxially with to the center of the loudspeaker, whit their membranes spaced of 1 mm so that both microphone acquire the same pressure level. A range of frequency is chosen and for every frequency the L_p read by the microphone under test and the reference microphone is acquired. The value of the MEMS microphone is acquired from the outside of the anechoic-room with a remote connection. The value of the reference microphone is acquired by the OnoSokki sound analyzer from the outside of the anechoic-room with a BNC cable connection. The Onsokki sound analyzer showed the power spectrum with a Flat-Top windows like the analysis implemented by Matlab for digital MEMS data. The frequency range selected is the following.

- from 20 Hz to 1kHz - 1/3 *octave band step*
- from 1kHz to 6 kHz - 1/6 *octave band steps*
- from 6kHz to 20kHz - 1/12 *octave band steps*

For each frequency the L_p of the specific frequency generated by the sine generator was recorded in a text file. The accuracy in frequency on the spectrum analyzer depends on the number of points and on the full scale of the frequency axes. This means that if a small difference in frequency between the frequency read on the spectrum and the one generated by the sine generator is due to the spectrum parameter and not to the reference microphone that has a very high precision. For MEMS acquisition the algorithms explained in section 3.2 was used.
The acquisition time was about 1 minute at low frequency and gradually smaller until the last frequency that is 30 seconds. This was done because low frequency need more time to be correctly sample. The values in L_p generated by the sound source were between 85-100 L_p, depending on the frequency. Higher value for high frequency. As provided by the IEC normative two position of the microphones are implemented, the first with reference mic closer to the sound source and the MEMS mic on the other side (L_{12}), the later with reverse positions (L_{21}). This is done to exclude electrical uncertainty in the measurement. Since the IEC normative refers to standard microphone which the same dimensions (or al least small difference in the membrane), when MEMS microphones, that have a significant smaller diaphragm than reference microphone, have to be tested, it is necessary to take into account this issue.

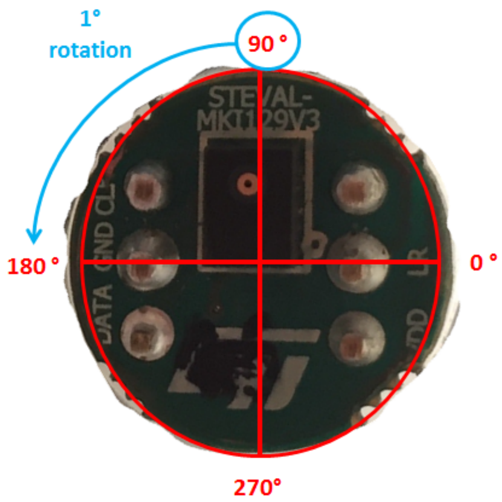

Figure 50: *MEMS Orientations*

A possible solution is two implement four positions of the MEMS for each of the two setups of the microphones. Starting with the membrane at the top, 90 ees, the mic is turned of 90 degrees to make it oriented respectively at 180, 270 and 0 degrees as shwon in figure 50
Since the diaphragm of digital MEMS is so small, the effect of diffraction in particular at high frequencies is present. By rotating the MEMS this effects is partially avoided. In total, 52 frequencies times 4 positions of the MEMS times 2 positions of the microphones i.e. about 400 values are evaluated.

3.4.2 Sound Calibrator

INSTRUMENT	VALUE	MANUFACTURER	TIC. TYPE	U(y)
reference microphone	L_p	Bruel & Kjaer	4191	0.2 dB
sound calibrator	Hz-L_p	Bruel & Kjaer	4226	0.5 dB
cables RGB				
1 PCs				

Table 3: *Differences in Peak Value taken from the Different Spectrum*

The MEMS microphone is inserted in the Bruel & Kjaer 4226 sound calibrator which generates very accurate L_p, 94-104-114 dBSPL, at different frequency. The possible frequency range is the following.

- from 20 Hz to 20kHz - 1/3 *octave band step*

Unlike anechoic room, in this case the measurement environment was a silence office. Just one PC is required without remote connection. No sound speaker, tripod boom, reference microphone and long cables are used since the sine wave are generated only by the 4226 sound calibrator with its inside sound sources. As consequence, the test bench was easier than anechoic calibration, furthermore less frequencies are taken. The MEMS adapter is inserted in the sound calibrator 4226 and thanks to the PVC built adapter the calibration is implemented without significantly air leakages. The sound calibrator 4226 allows three possible values for the sound pressure level, 94,104,114 dB. Trying to eliminate noise floor coming from the outside of the calibrator, since the measurement took place in an office, the pressure field used for all the frequency were 104 dB. As for hemi-anechoic calibration, 3.4.1, four position for the MEMS microphones are implemented, 90, 180, 27 and 0 degrees.

Unlike anechoic-room in this case is not possible, and also unnecessary to change the position of MEMS microphone and the reference one since this last is a sound source built-in the calibrator. 11 frequencies times 4 positions, in total 44 values are evaluated.

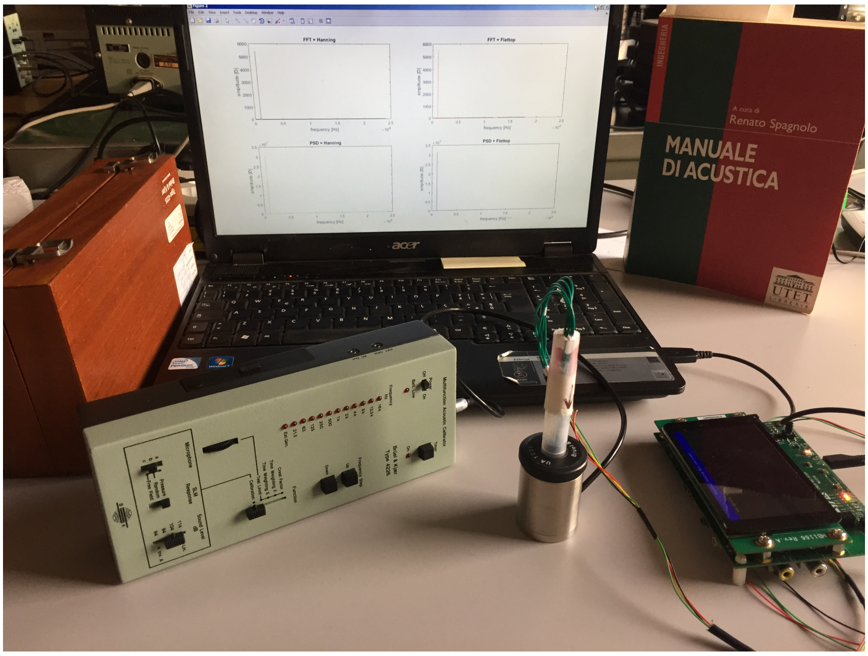

Figure 51: *MEMS calibration with Sound Calibrator*

3.4.3 Active Coupler

INSTRUMENT	VALUE	MANUFACTURER	TIC. TYPE	U(y)
reference microphone	L_p	Bruel & Kjaer	4180	??? dB
MEMS microphone UT	LSB/Pa - dBFS	ST	MP34DT05-DS	
spectrum analyzer	Hz/L_p	Onosokki	DS-3200	0.015 dB
signal generator	Hz	Bruel & Kjaer	1049	0.001 Hz
sound source	L_p	Bruel & Kjaer	WA0817	
sound source amplifier	L_p	Bruel & Kjaer	??????	
microphone amplifier		Bruel & Kjaer	5935	
cables RGB				
2 PCs				

Table 4: *Test Bench for Active Coupler Calibrator*

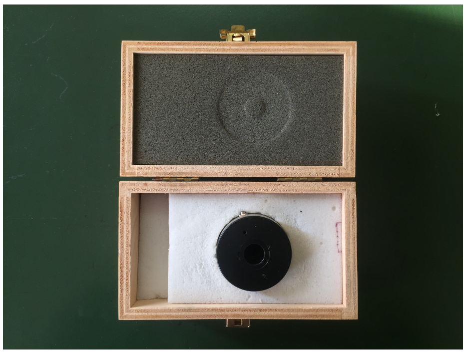

Figure 52: *active coupler WA0817*

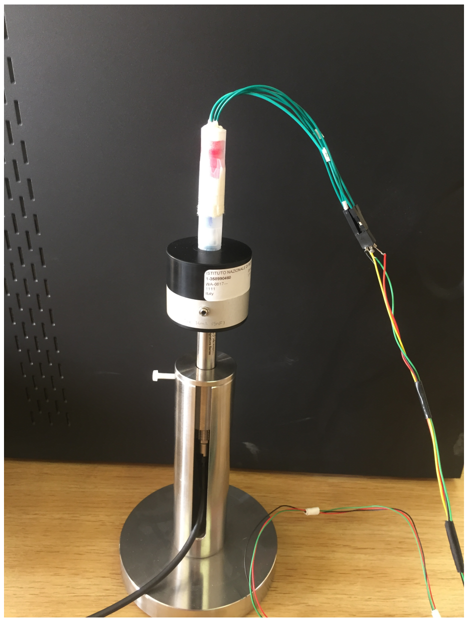

Figure 53: *MEMS calibration with active coupler and 4180*

For theory concept refer to 2.3.2. The measurement environment was a silence office so that it is not need of remote connection as for sound calibrator calibration. The instrument used in this case was an active coupler. This object has two holes where the reference microphone and the microphone under test are fitted in. Inside there is a build-in sound source which supplies essentially equal sound pressures to the two inserted microphones. The two microphone are close enough to sound source, see figure 28 to consider the sound in a pressure-field.
The build-in source has not a pre-imposted frequency so a sine signal generator and source amplifier has to be provided. Furthermore since a reference microphone is used, a sound analyzer, a microphone pre-amplifier and two PCs were necessary. The active coupler used was the Bruel & Kjaer WA0817. The reference microphone used in this case is the *Bruel & Kjaer 4180*. This last is high quality condenser microphones used as laboratory standard microphones for all the primary calibration. The frequency response of this microphone is almost flat between 0-20kHz, see figure 54.

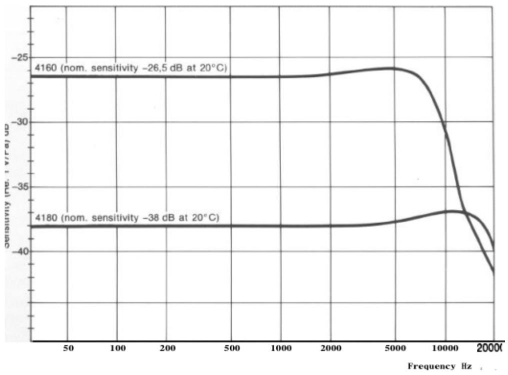

Figure 54: *Typical frequency response for 4160 and 4180 microphones*

The MEMS microphone with the adapter is inserted in the active coupler and as for anechoic calibration for each frequency chosen the value of the reference microphone is recorded in a text file and the value of digital MEMS is then analyzed from the binary file. The input frequencies are generated by the sine generator and driven into the build-in sound source. The selected frequencies are the same for the hemi-anechoic calibration, but in this case the number of MEMS orientation were just two 90 and 270 degrees since the coupling problem with the MEMS microphone are present and it was not useful consider more than two positions. A better explanation of this problem is described in the next section 4. As for the anechoic calibration, the frequency range that is chosen is the following.

- from 20 Hz to 1kHz - 1/3 *octave band step*
- from 1kHz to 6 kHz - 1/6 *octave band steps*
- from 6kHz to 20kHz - 1/12 *octave band steps*

3.5 Frequency Response at Low Frequencies (1 Hz - 100 Hz)

INSTRUMENT	VALUE	MANUFACTURER	TIC. TYPE	U(y)
reference microphone	L_p	Bruel & Kjaer	4191	0.2 dB
MEMS microphone UT	LSB/Pa - dBFS	ST	MP34DT05-DS	
sound source	L_p	pierced loud speaker	INRIM	
spectrum analyzer	Hz/L_p	Onosokki	DS-3200	0.015 dB
signal generator	Hz	Bruel & Kjaer	1049	0.001 Hz
sound source amplifier		Rotel	RA-05-SE	
microphone amplifier		Bruel & Kjaer	5935	
cables RGB				
2 PCs				

Table 5: *Test Bench for Low Frequency Calibration*

Figure 55: *Punctured Speaker with Microphones*

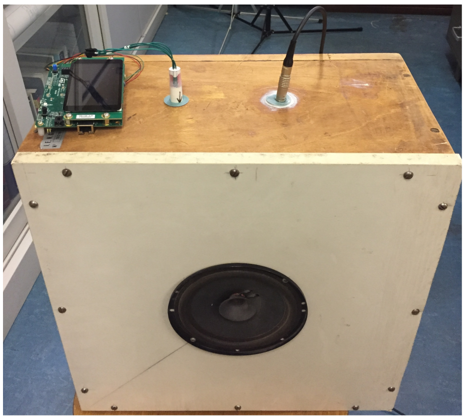

Figure 56: *Punctured Speaker without Microphones*

One of the possible microphone MEMS application is the biomedical engineering (see figure 1). Human bodies acoustic signals, like blood pressure or heartbeat are between 1 and 20 Hz. To calibrate microphone at very low frequencies the easier way is in a pressure field. A squared wooden sound speaker is perforated with two holes on the same lateral face in which the MEMS microphone with its adapter and the reference microphone is inserted. To improve the grip avoiding air leakage, a strip of spongy material is fitted in, as shown in figure 55, 56. When an acoustic signal is generated by a sound speaker, it propagates front and back the diaphragm. So in this case the sound of interest is the one propagated inside the wooden speaker.since in this case the waveform generated were at very low frequency. The sound-field could be considered uniform in all the points inside the speaker because the wavelengths, recalling the law

$$\lambda = \frac{c}{f}$$

and

$$c = 340m/sec$$

are between 170-17 m. As consequence, even if the microphone are not face-to-face the receive the same pressure levels. The frequency range selected is the following:

- from 1 Hz to 100 - 1/3 *octave band step*

The acquisition time was about 2-3 minutes for measure due to the fact that with very low frequencies is necessary more time to acquire a significant number of periods of the sine wave. The acquisition process was the same for anechoic calibration. The test bench implemented was quite similar to the one used in anechoic room, except for remote connection and tripod boom that are not necessary since the ambient was a silent office and the microphones were fitted directly in the speaker.

3.6 Total Harmonic Distortion

Refer to section 2.2.5 for theory concept.
The *THD* of digital MEMS microphones is measured in anechoic room. The signals generated were all at 1 kHz. The signal L_p was from 100 dBSPL where the distortion is about 0 % until 120 dBSPL. According to IEC normative from 100 dB to 115 dB the signal are generated by steps of 1 dB of difference between one and the next. From 115 dB to 120 dB, where the THD has a exponential behavior the step was of 0.1 dB in order to better describe the evolution. The correct value of L_p is controlled by the reference microphone, Bruel & Kjaer 4191, which for all the values of L_p, it works in linear range. In fact, 3% of distortion is given with acoustic pressure bigger than 162 dBSPL.
Since the signal generated were all at 1kHz, the sound source that is chosen was an horn. THD measure was done to evaluate the microphone distortion as consequence, the distortions coming from the source should be avoid. Horn sound sources are built to generated sound filed with reduced distortions for middle-high frequency which means from 800 Hz and 2 kHz that is the case of this measure. The acquire method and the test bench were the same of frequency response in anechoic room, see 3.4.1.

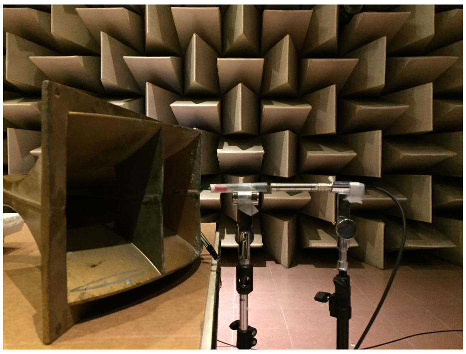

Figure 57: *digital MEMS distortion with Horn as sound source*

Figure 58: *Acoustic Horn*

3.6.1 *Matlab* Implementation

Since the analysis of digital MEMS was carried out with Matlab, also the THD computation was implemented with the same software. Two kind of THD were analyzed, THD standard and THD + N (see section 2.2.5).
The **THD+N** is computed started from the spectrum of the signal calculated with the algorithm describe in 3.2. First of all, a maximum and minimum threshold are defined. The maximum value was the amplitude of the fundamental harmonic and the minimum value was the maximum minus *80 dB*. Those two value are necessary to include all the significant lines of the fft spectrum which give an energy contribution to the computation of the fundamental harmonic. By looking the figure 59it is possible to notice that the global value of the fundamental harmonic is not the energy contribution of just one line but is the sum of all the line which make up the harmonic, that in this case are 5. So the power of the fundamental is calculated computing the energy of this line and the energy of the other harmonic plus noise which are computed as difference between all the spectrum energy minus the energy of the fundamental harmonic. To find the value of the first 5 lines of the fft before and after the line of the fundamental, an *index research* is implemented, see the code in the Appendix A 6.

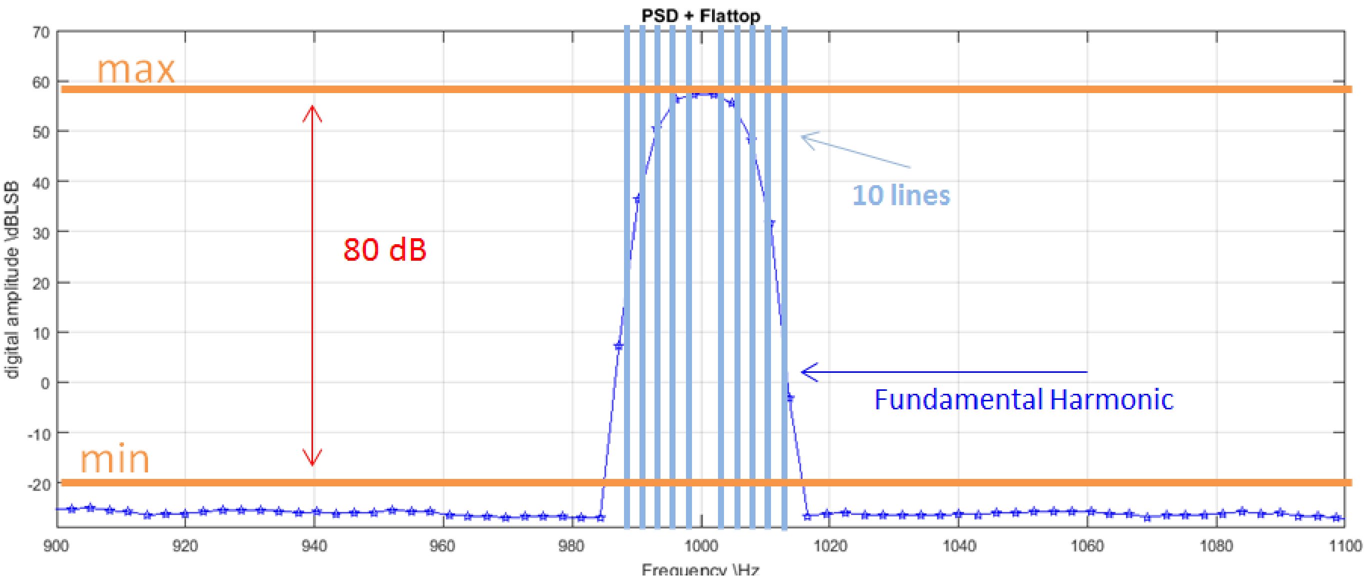

Figure 59: *Graphic Algorithm for the Computation of the Harmonic Fundamental Energy*

The standard **THD** is computed finding the value of the fundamental and the successive harmonics. Those value is carried out by computing the maximum value of the fundamental frequency and the first 3 multiple harmonics. The maximum value is obtained with the max function of all the samples contained in the interval centered in $f_C \pm \Delta f$. Where f_C is the correct value of the fundamental frequency or of the successive harmonic, and the the Δf was a frequency difference. This difference is taking into account since the value of the maximum harmonic could be not exactly centered at the correct frequency because this value depends on the number of sampling point of the fft. In example a signal of 1kHz should have the fundamental and successive harmonic at respectively 1kHz, 2kHz, 3kHz etc... . Because of the sampling points those value could be centered in example at 1005 Hz, 1990 Hz, 3010 Hz. The value of Δf is chosen small for low frequency and bigger for high frequency, the exact value are describe in the code in the Appendix A 6. This code is verify by calculating the THD of an ideal square wave with duty cycle of 50 % which has from the theory a distortion of 48.3 %.

3.7 Level Linearity

The level linearity (see section 2.2.7) measure was done in anechoic room since in necessary a very silent ambient to test the lowest L_p value of the MEMS dynamic range. The test bench used was the same of the THD measure. Digital MEMS microphone and reference microphone are placed face-to-face as usual and the sound source was the speaker. This measure was done following the IEC 61094-3. The value analyzed covered all the range of the digital MEMS microphone, from the residual noise, that is about 30 dBA to the AOP that is 120 dBA. The step between one value and the next one is of 1 dB from 30 to 35 dB, then step of 10 dB from 35 until 105 dB, and then again 1 dB from 115 until 120 dB. The frequency for all the sound levels was 1kHz. The normative IEC 61094-3 refers to a global value with A-weighted filter, so the OnoSokki and the MEMS analysis were impostred to do a 1/3 octave band spectrum. For each measure the value of the reference microphone and the value of the digital MEMS are recorded and then analyzed.

3.8 $\frac{1}{3}$ Octave Band Analysis

3.8.1 *Pink Noise 20Hz-20kHz*

As described in chapter 1, digital MEMS microphone could be used also as sound meter. To evaluate this behavior the octave band, previously describe in section 3.2.3, was done. In anechoic room a random noise of 100 dB from 20-20kHz is generated. Then with the reference microphone and the Onosokki spectrum analyze the 1/3 octave band is calculated recording the global level and the global level A-weighted. In parallel the MEMS acquisition is done. The acquisition time was about 1 minute. The signal is then elaborate with the process described in section 3.2.3. The scope of this measure is to compare the two spectrum with their global level and understand how much the MEMS analysis is different from the laboratory sound meter. The results will be shown in the next chapter.

3.8.2 Digital MEMS Equivalent Input Noise - Self-generated Noise

Refer to section 2.2.4 for theory concept.
This measure was done to evaluate how the noise is distributed over the frequency bands and how much is the lowest signal captured by digital MEMS. The measurement environment was the anechoic room since a very quite ambient is necessary because if the sound pressure level to be measured is about 30 dB, a minimum noise signal coming from the surrounding environment can corrupt the measure. The acquisition was done without any sound signal, and was about 30 seconds. The global level was acquired in linear and A-weighted. This last is required for the SNR measure.

3.9 Signal-to-Noise Ratio

Refer to section 2.2.3 for theory concept.
The environment chosen is the anechoic room. The signal at *1kHz* is generate with the sound speaker used for the frequency response and is acquired for 30 seconds. The residual noise is the global level A-weighted calculated in the equivalent input noise.

3.10 Stability

Refer to section 2.2.9 for theory concept.

3.10.1 Short Term Stability

The measurement environment used was the anechoic-room with the configuration equal to the frequency response (see section 3.4.1), a signal at 1kHz with 94 dBSPL is generated for 30 minutes and in parallel acquired by the digital MEMS.

3.10.2 Long Term Stability

To evaluate a sort of long term stability the sound calibrator was used. The period of time was four months. A 1kHz waveform at 94 dBSPL is generated with the sound calibrator 4226 and acquired with the digital MEMS microphones. The sensitivity in $Dec\hat{i}mal_{16-bit-signed}$ Pa and in $dBFS$ acquired in the first month is compared with the sensitivity acquired in the last month.

3.11 Influence of Temperature

INSTRUMENT	VALUE	MANUFACTURER	TIC. TYPE	U(y)
reference microphone	L_p	Bruel & Kjaer	4180	0.2 dB
MEMS microphone UT	LSB/Pa - dBFS	ST	MP34DT05-DS	
spectrum analyzer	Hz/L_p	Onosokki	DS-3200	0.015 dB
signal generator	Hz	Bruel & Kjaer	1049	0.001 Hz
sound source	L_p	Tweeter Motorola		
sound source amplifier		Rotel	RA-05-SE	
microphone amplifier		Bruel & Kjaer	5935	
cables RGB				
2 PCs				

Table 6: *Test Bench for Temperature Measure*

Refer to section 2.2.10 for theory concept.
Those measures are done in the climatic chamber of INRiM shown in figure 60. Inside the chamber the reference microphone and the MEMS microphones are placed one in front to the other distant 1 mm in order to acquire the same L_p. On one corner of the chamber the sound sources is placed. This last is a piezoelectric tweeter since the piezoelectric material is more stable with temperature changes than coil speaker. The temperature range selected are chosen trying to make an hysteresis loop. They were:

- $+20$,$+10$,0,$-10°$
- 0,$+10$,$+20$,$+30$,$+40$,50°
- $+40$,$+30$,20°

At every temperature a signal at 2kHz is generated. The choice of 2kHz instead the standard 1kHz was made because the piezoelectric tweeter sound speaker is linear starting from 1kHz, so in order to avoid pressure attenuation due to non-linear response, the signal frequency was 2kHz. The L_p was about between 90-100 dBSPL. To reach a constant temperature in the environment measurement the climatic chamber is on for an hour per every temperature range. While the sound source is on for 30 minutes since the piezoelectric tweeter requires more time to be stabilized than coil speaker. The acquisition with MEMS microphone is done for about 1 minutes. The L_p value generated by the sound speaker is acquired by the reference microphone. The sensitivity is obtained by comparison as usual.

Figure 60: *Climatic chamber with 4191 reference microphone, digital MEMS and piezoelectric sound speaker*

4 Measurement Results and Uncertainty Assessment

In this chapter the results obtained from the measurements described in the previous chapter and their uncertainties assessment are presented.

4.1 Uncertainty Assessment

The uncertainty evaluated is the expanded uncertainty with a significant level of 95%. The way of computing it is based on GUM and it is described in section 4.10.

4.2 Frequency Response

Frequency response is obtained by comparison with a reference microphone. Two kind of sensibility are evaluated: one referred to a sensitivity in $Dec\hat{i}mal_{16-bit-signed}/Pa$ and an other referred to a sensitivity in *dBFS*. The first is carried out by considering the RMS value of the waveform in time domain, see section 3.2.1, the other by considering the peak value of PSD achieved from the computation explained in section 3.2.2. Before computing the frequency response, the Chauvenet's criterion is applied in order to exclude the outliers value. calculations are computed using a *Matlab* algorithm.

4.2.1 Sensitivity in $Dec\hat{i}mal_{16-bit-signed}/Pa$ or *dBFS*

$Dec\hat{i}mal_{16-bit-signed}$ /Pa

The step processes to calculate the frequency response in the case of $Dec\hat{i}mal_{16-bit-signed}/Pa$ are the following. Starting from sound pressure level L in dB (refered to $20\mu Pa$) of the reference microphone, or the reference sound pressure for sound calibrator, is necessary to convert it in $Pascal$ with formula:

$$\hat{p} = p_0 \cdot 10^{\frac{L}{20}}$$

When the B&K 4191 reference microphone is used, a correction factor is applied since this kind of microphone is a free-filed type and the frequency responses are done in pressure-filed, so, in order to have a flat response at all frequency, is necessary to correct its sensitivity. The sensitivity in $Dec\hat{i}mal_{16-bit-signed}/Pa$ is obtained by taking the ratio of the rms value of the reference microphone converted in $Pascal$ and the rms value of the digital MEMS microphone in $Dec\hat{i}mal_{16-bit-signed}$.

$$DigitalMicSens = \frac{Dec\hat{i}mal_{16-bit-signed}}{\hat{p}}$$

The value of the digital MEMS microphone is the averaged value of the all positions (8 position for anechoic-room, 4 positions for sound calibrator, 2 positions for active coupler) after the Chauvenet's criterion is applied to avoid outliers. Then, as usual in the frequency response, the sensitivity values are normalized by the the sensitivity at 1kHz, converted in dBSPL and plotted over the acoustic frequency range *20Hz-20kHz*.

dBFS

The step processes to calculate the frequency response in the case of *dBFS* are the following. The value in *dBFS* of the digital MEMS is firstly converted in dBSPL with the formula:

$$dBSPL = AOP + dBFS$$

The value of the AOP used in the case is *119.19*(the reason of that will be explained in the section 4.5). Then the difference in dBSPL between the MEMS microphone and the reference microphone previously corrected due to the pressure filed, or the sound source of the sound calibrator is taken. The value so obtained is converted in linear scale in order to apply the Chauvenet's criterion and exclude the outliers. The averaged over all the MEMS positions is carried out and a normalization by the sensitivity at 1 kHz is performed. In the end the value are reconverted again in dBSPL and plotted over the acoustic frequency range *20Hz-20kHz*.

4.2.2 Hemi-Anechoic Room

Table 7: *Sensitivity Values for Digital MEMS microphone obtained in Hemi-Anechoic Room*

frequency \Hz	*sensitivity ref.* $/Decimal_{16-bit-signed}/Pa$	*sensitivity ref.* $2^{15}-1$/dB	*Expanded (k=2) uncertainty/dB*
25.1	992	-30.38	0.23
31.6	1053	-29.86	0.22
39.8	1111	-29.39	0.22
50.1	1187	-28.82	0.44
63.1	1189	-28.81	0.29
79.4	1204	-28.70	0.22
100.0	1239	-28.45	0.33
125.9	1227	-28.53	0.24
158.5	1228	-28.52	0.22
199.5	1250	-28.37	0.26
251.2	1237	-28.46	0.22
316.2	1235	-28.48	0.22
398.1	1246	-28.40	0.23
501.2	1240	-28.44	0.21
631.0	1236	-28.47	0.22
794.3	1225	-28.55	0.38
1000.0	1216	-28.61	0.38
1059.3	1232	-28.50	0.29
1188.5	1232	-28.50	0.23
1333.5	1229	-28.52	0.21
1496.2	1216	-28.61	0.37
1678.8	1231	-28.50	0.21
1883.6	1240	-28.44	0.22
2113.5	1240	-28.44	0.38
2371.4	1242	-28.43	0.38
2660.7	1253	-28.35	0.22
2985.4	1247	-28.39	0.23
3349.7	1245	-28.41	0.23
3758.4	1252	-28.36	0.22
4217.0	1258	-28.32	0.24
4731.5	1266	-28.26	0.24
5308.8	1275	-28.20	0.22

frequency \Hz	*sensitivity ref.* $/Decimal_{16-bit-signed}/Pa$	*sensitivity ref.* $2^{15}-1$/dB	*Expanded (k=2) uncertainty/dB*
5956.6	1278	-28.18	0.24
6683.4	1292	-28.08	0.27
7286.2	1306	-27.99	0.22
7717.9	1328	-27.84	0.22
8175.2	1328	-27.84	0.23
8659.6	1345	-27.73	0.23
9172.8	1354	-27.68	0.24
9716.3	1353	-27.68	0.45
10292.0	1417	-27.28	0.36
10901.8	1450	-27.08	0.39
11547.8	1486	-26.87	0.47
12232.1	1521	-26.67	0.53
12956.9	1558	-26.46	0.55
13724.6	1599	-26.23	0.76
14537.8	1651	-25.95	0.69
15399.3	1699	-25.70	0.87
16311.7	1881	-24.82	0.82
17278.3	1692	-25.74	2.74
18302.1	1925	-24.62	2.36
19386.5	1788	-25.26	4.18

Table 7 shows the sensitivity value in $Dec\hat{i}mal_{16-bit-signed}/Pa$ for every sine waves generated in the hemi-anechoic room. The number of frequency are 51 and the positions are 8: 4 in which microphones are positioned in one way (L_{12}) and 4 with interchanged positions (L_{21}). Taking into account the binary format data of digital MEMS, that is 16-bit signed. The sensitivity, expressed in dB, is given by

$$SensMic_{dB} = 20 \cdot log_{10}(\frac{Decimal_{1\hat{6}-bit-signed}/Pa}{2^{15}-1})$$

where $2^{15}-1$ is arbitrary chosen as reference values in Decibel. The value of uncertainty is just listed, the way of calculating it will be explained in the section 4.10. The figure 61 shows the frequency response for the two different sensitivity.

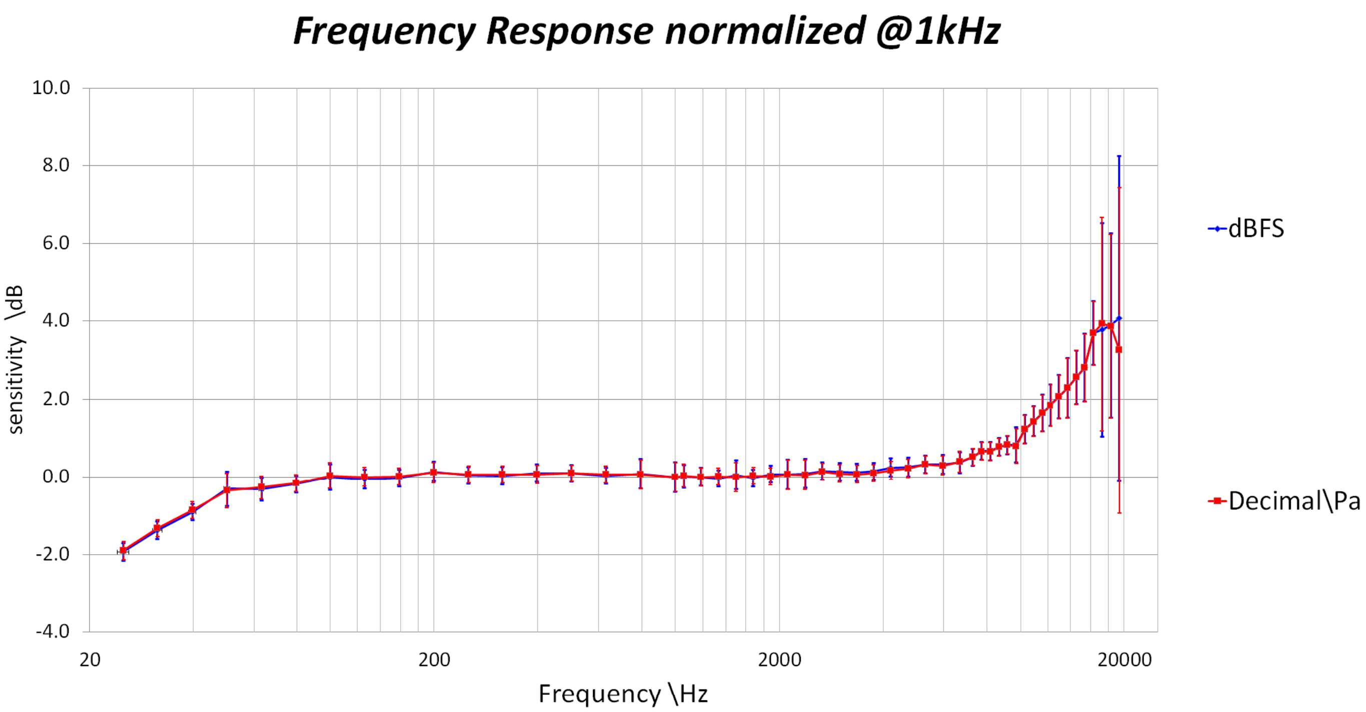

Figure 61: *Frequency Response expressed in* $\hat{Decimal}_{16-bit-signed}/\mathrm{Pa}$ *and* dBFS *for Digital MEMS microphone obtained in Hemi-Anechoic Room*

Frequency response is almost flat from 100 Hz to 4 kHz. Under 100 Hz the frequency response starts to roll off due to the ventilation hole in the back cavity, the geometry parameters of the holes in the backplate and an high-pass filter before the amplifier, necessary to exclude the noise coming from electronic component. The maximum attenuation is about 2 dB at 25 Hz. For frequencies above 4 kHz it starts to increase, reaching the resonance peak caused by the inlet at 17.2 kHz with an increment of about 4 dB.
Frequency response calculated with the two different sensitivities is almost the same except for the last point where in the case of $\hat{Decimal}_{16-bit-signed}/Pa$ is lower. According to frequency response of B&K microphone, after the resonance peak the response should decrease, so the reference in $\hat{Decimal}_{16-bit-signed}/Pa$ seems to be more correct. However the sound diffraction, and the uncertainties, at this frequency are too high to repute it more correct than the other.
The expanded uncertainties are under 0.2 dB until 10 kHz, than starts to increase due to the small wavelength of the sound at high frequencies which becomes comparable with the dimension of microphone diaphragm, causing diffractions. The highest uncertainty is, ax expected, at frequencies between *17 kHz and 20 kHz* where it reaches the value of 2 dB and 5 dB.

4.2.3 B&K 4226 Sound Calibrator

Table 8: *Sensitivity Values for Digital MEMS microphone obtained in Sound Calibrator*

frequency /Hz	*sensitivity ref.* $/Decimal_{16-bit-signed}/Pa$	*sensitivity ref.* $2^{15}-1$/dB	*Expanded (k=2) uncertainty/dB*
31.50	1072	-29.71	0.51
63	1207	-28.67	0.51
125	1247	-28.39	0.51
250	1257	-28.32	0.50
500	1258	-28.32	0.50
1000	1259	-28.31	0.52
2000	1261	-28.29	0.53
4000	1278	-28.18	0.51
8000	1349	-27.71	4.07
12500	1494	-26.82	3.20
16000	1621	-26.11	2.97

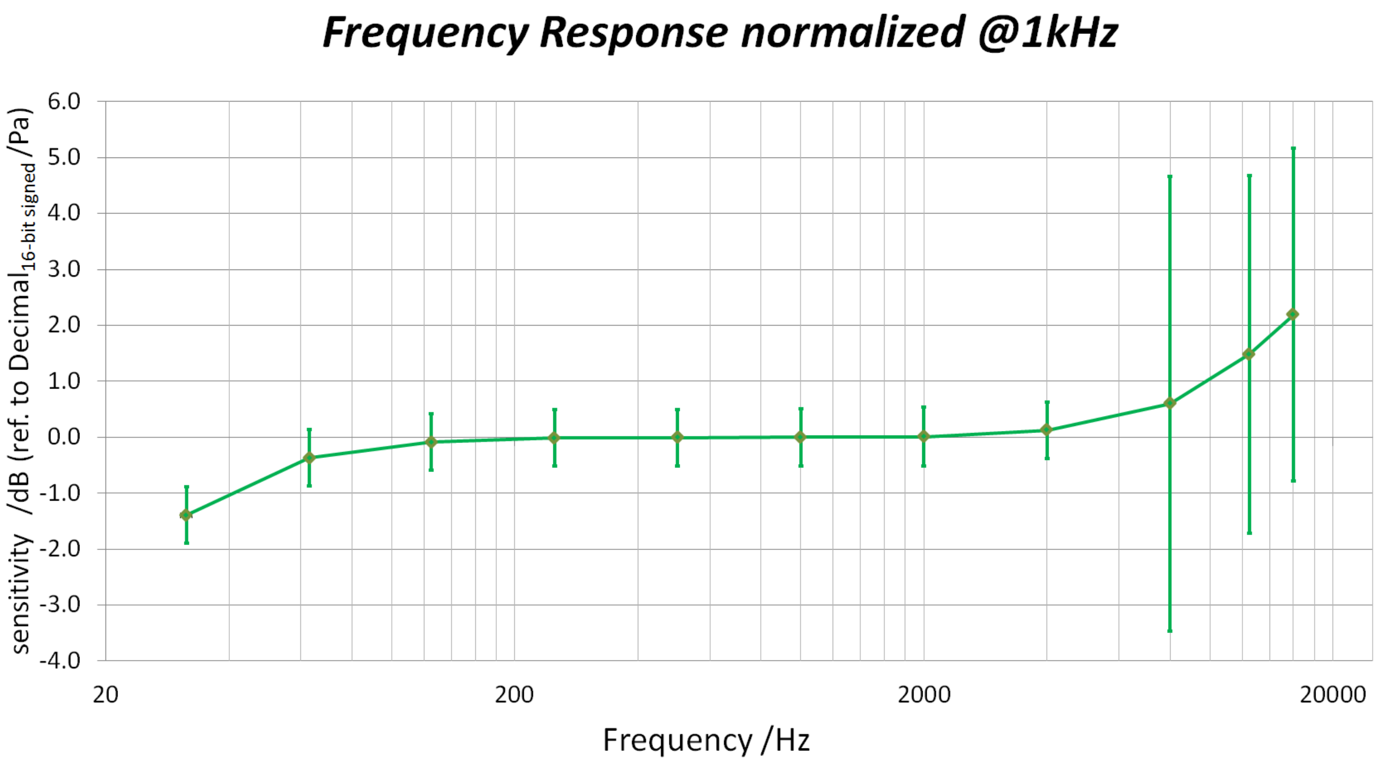

Figure 62: *Frequency Response expressed in* $\hat{Decimal}_{16-bit-signed}/Pa$ *for Digital* MEMS *microphone obtained with the Calibrator 4226*

Table8 shows the sensitivity value in $\hat{Decimal}_{16-bit-signed}/Pa$ for the 10 frequencies generated by the sound calibrator B&K

4226 and the frequency response is shown in figure 62.
It is possible to see again a flat behavior from 100 Hz to 4 kHz, the cut-off region and the resonance peak respectively at low and high frequencies. The expanded uncertainty become relevant at high frequencies due to air leakages and also due to the less number of positions. Unlike the hemi-anechoic room, in this case they just 4 rotated position are considered. The lees is the number of acquired data the more is the uncertainty, in fact for the same frequency, the uncertainty in this case is about 0.3 dB bigger. Moreover, the sine wave generated are limited by the possible pre-imposted frequencies in the 4226 sound calibrator which are 11 in total between 20 Hz and 20 kHz. In this case is not possible to see the resonance peak at 17 kHz. The frequency response expressed in $Dec\hat{i}mal_{16-bit-signed}/Pa$ or in $dBFS$ is the same and for simplicity only the first is shown in the figure 62.

4.2.4 Active Coupler

Table 9: *Sensitivity Values for Digital MEMS microphone obtained in Active Coupler*

frequency /Hz	*sensitivity ref.* $/Decimal_{16-bit-signed}/Pa$	*sensitivity ref.* $2^{15}-1$/dB	*Expanded (k=2) uncertainty/dB*
25.1	1108	-29.42	6.15
31.6	1146	-29.13	5.68
39.8	1185	-28.83	5.46
50.1	1221	-28.57	6.56
63.1	1169	-28.95	7.23
79.4	1210	-28.65	8.96
100.0	1183	-28.85	11.92
125.9	1233	-28.49	15.38
158.5	1334	-27.81	19.67
199.5	1228	-28.53	24.65
251.2	1279	-28.17	29.86
316.2	1278	-28.18	39.23
398.1	1220	-28.58	36.36
501.2	1274	-28.21	34.67
631.0	1216	-28.61	25.86
794.3	1260	-28.30	15.16
1000.0	1209	-28.66	0.22
1059.3	1404	-27.36	0.22
1188.5	1314	-27.94	9.61
1333.5	1309	-27.97	9.61
1496.2	1224	-28.55	9.61
1678.8	1221	-28.57	34.67
1883.6	1405	-27.36	25.86
2113.5	1271	-28.23	15.16
2371.4	1227	-28.53	0.22
2660.7	1308	-27.98	0.30
2985.4	1257	-28.32	3.16
3349.7	1214	-28.62	3.16
3758.4	1428	-27.21	2.93
4217.0	1328	-27.85	2.93
4731.5	1312	-27.95	0.37

frequency \Hz	*sensitivity ref.* $/Decimal_{16-bit-signed}/Pa$	*sensitivity ref.* $2^{15}-1$/dB	*Expanded (k=2) uncertainty/dB*
5308.8	1235	-28.48	0.37
5956.6	1255	-28.34	0.37
6683.4	1199	-28.73	0.26
7286.2	1442	-27.13	2.83
7717.9	1454	-27.06	2.83
8175.2	1275	-28.20	2.83
8659.6	1334	-27.81	2.83
9172.8	1463	-27	2.83
9716.3	1368	-27.59	2.83
10292.0	1331	-27.83	0.80
10901.8	1410	-27.32	14.44
11547.8	1472	-26.95	14.44
12232.1	1394	-27.42	14.44
12956.9	1623	-26.10	14.44
13724.6	1687	-25.77	14.44
14537.8	1797	-25.22	25.89
15399.3	1664	-25.89	25.89
16311.7	2630	-21.91	25.89
17278.3	1967	-24.43	17.97
18302.1	2324	-22.98	17.97
19386.5	2716	-21.63	17.97

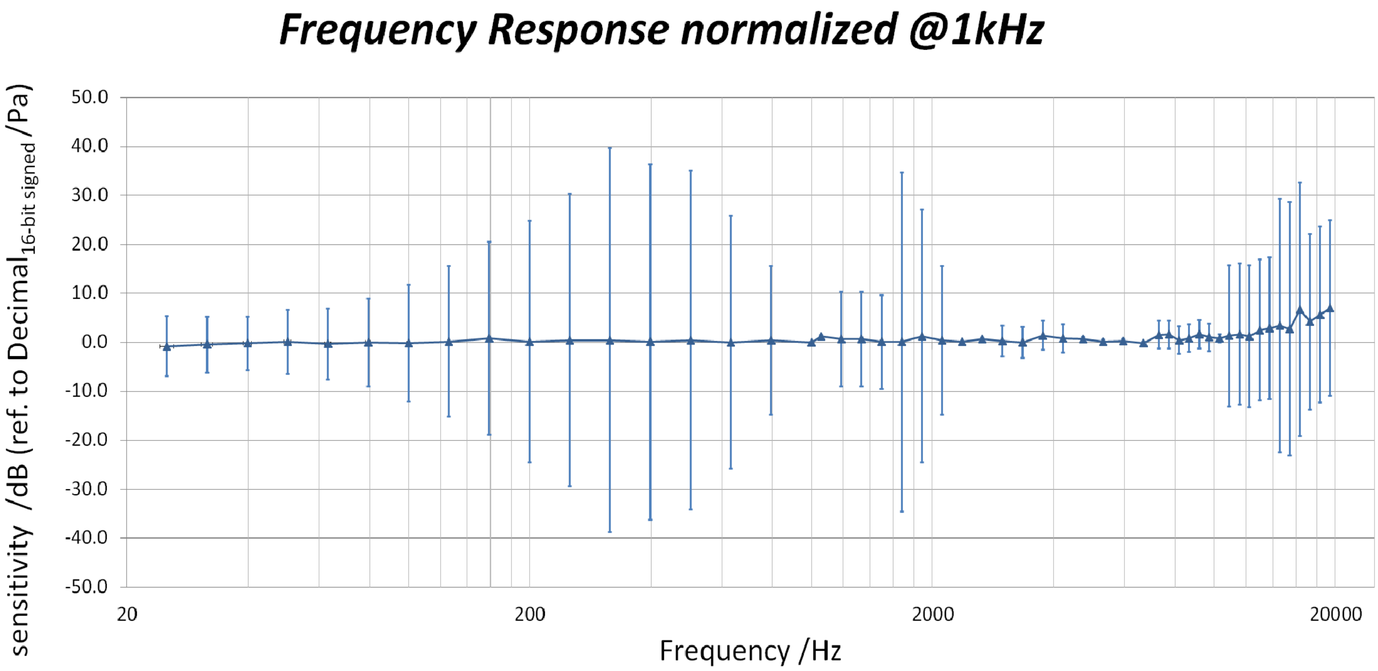

Figure 63: *Frequency Response expressed in* $\hat{Decimal}_{16-bit-signed}$/Pa *for Digital MEMS microphone obtained with the Active Coupler*

Table ?? shows the sensitivity value in $\hat{Decimal}_{16-bit-signed}/Pa$ and the frequency response is shown in figure 63.
First of all is possible to see the high uncertainties content for frequencies. The mean value is about 12 dB while in certain cases it reaches also 40 dB. Even if the response is almost flat, as obvious, with this lack of accuracy those measure can not be considered reliable. In fact the cut-off region and the resonance peak are not present. The reason of those uncertainties is that with the active coupler the digital MEMS microphone does not correctly couple and consistent air leakages are present although the realization of a proper PVC adapter has been implemented. Typically when two B& K reference microphone are inserted in the active coupler the inside L_p generated by the built-in sound source is almost constant. Instead, when the MEMS microphone with its adapter is inserted, the inside sound pressure level is about 10-15 dB lower. This means that the sound field is not well closed inside the active coupler and leakages are present. As consequence, the value read from the MEMS microphone is not constant and entails a high uncertainties. This result is the same for the sensitivity expressed in *dBFS*.

4.3 Frequency Response at very Low Frequencies (1 Hz - 100 Hz)

Table 10: *Sensitivity Values for Digital MEMS microphone obtained for Very Low Frequencies Response*

frequency /Hz	*sensitivity ref.* $/Decimal_{16-bit-signed}/Pa$	*sensitivity ref.* dBSPL
1	565.0	•_•
1.26	596.0	•_•
1.58	333.0	•_•
2	197.0	-24.26
2.51	167.0	-20.76
3.16	221.0	-17.87
3.98	229.0	-15.76
5.01	299.0	-12.99
6.3	461.0	-9.09
7.94	471.0	-8.84
10	554.0	-7.36
12.58	743.0	-4.72
15.84	773.0	-4.34
19.95	896.0	-3.05
25.11	1076.0	-1.46
31.62	1085.0	-1.40
39.81	1234.0	-0.26
50.11	1266.0	-0.04
63.09	1322.0	0.34
79.43	1250.0	-0.15
100	1192.0	-0.29
125.9	*1227*	*-0.35*
158.5	*1228*	*-0.31*
199.5	*1250*	*-0.14*
251.2	*1237*	*-0.24*
316.2	*1235*	*-0.26*
398.1	*1246*	*-0.19*
501.2	*1240*	*-0.19*
630	*1236*	*-0.25*
794.3	*1225*	*-0.20*
1000	*1216*	*-0.29*

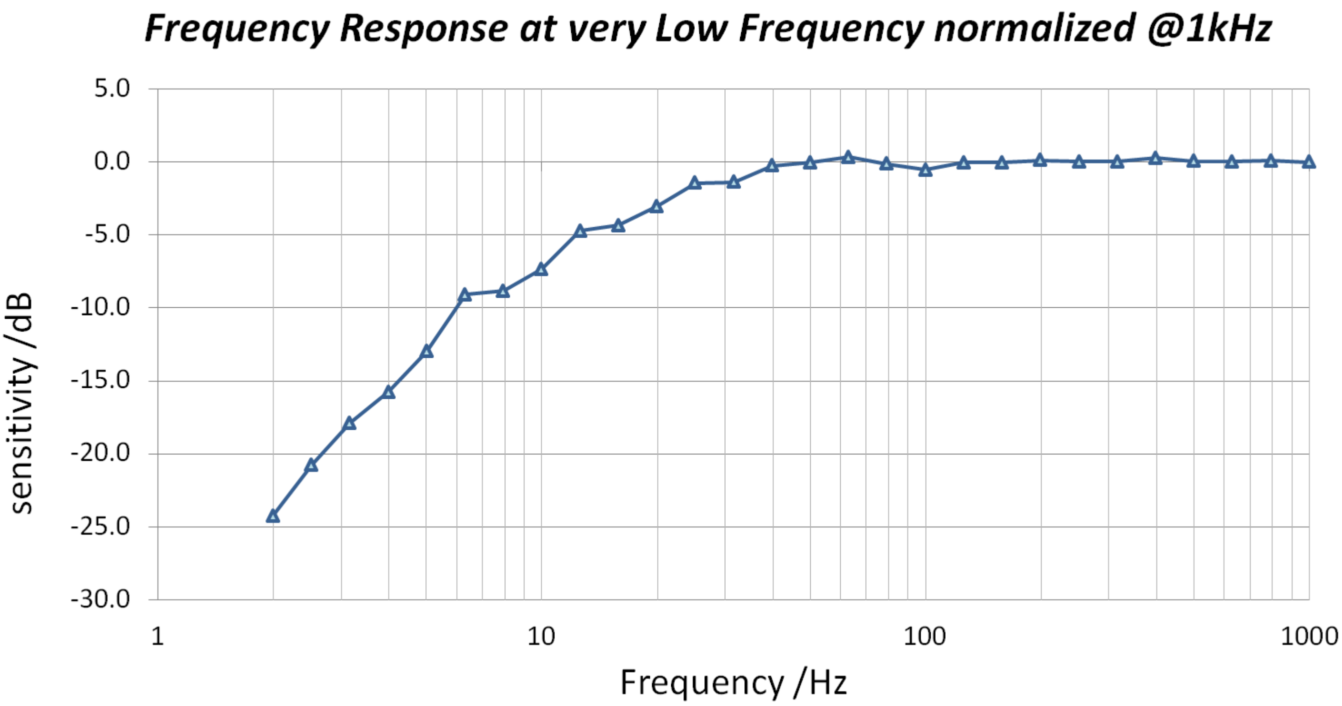

Figure 64: *Very Low (1 Hz - 100 Hz)Frequency Response expressed in* dBFS *for Digital MEMS microphone*

The results obtained with the frequency response at very low frequencies are shown in table 10 and in figure 64. The line with cursive font are the values taken from the calibration in hemi-anechoic room used just to plot the frequency response. The value expressed in •_• in the *dBFS* column means that the value for this frequency is not possible to be computed.
In order to deal with very low frequencies the value of the sensitivity is carried out considering the Power Spectrum Density with Flat-Top filter described in section 3.2.2. The sensitivity in $Dec\hat{i}mal_{16-bit-signed}/Pa$ is not possible to evaluate correctly since the algorithm to calculate it deals with a digital filter in time domain 3.2.1 and when, the frequency is very low, it is inefficiency. As consequence, the value expressed in $Dec\hat{i}mal_{16-bit-signed}/Pa$ with frequency below 10 Hz reported in table 10 are not reliable.
Moreover, even if the frequency is analyzed using a frequency spectrum analysis, under 2 Hz the microphone is not able to acquire any signals. The figures 66 and 65 shows the *PSD* for one signal at 1 Hz and 3 Hz. The former is completely cut-off by the MEMS microphone and is not present in the spectrum, the latter appears strongly attenuated. In particular the value is 21 dB that are *21 mPa*. The frequency response shown in figure 64 evaluates a significant roll off starting from 20 Hz with -5 dB to 2 Hz with - 25 dB. This strong attenuation could be due to an high-pass filter at the input of the operational amplifier, used to amplify the acoustic signal before the ADC, which discriminates the electrical noise signal at low frequency.

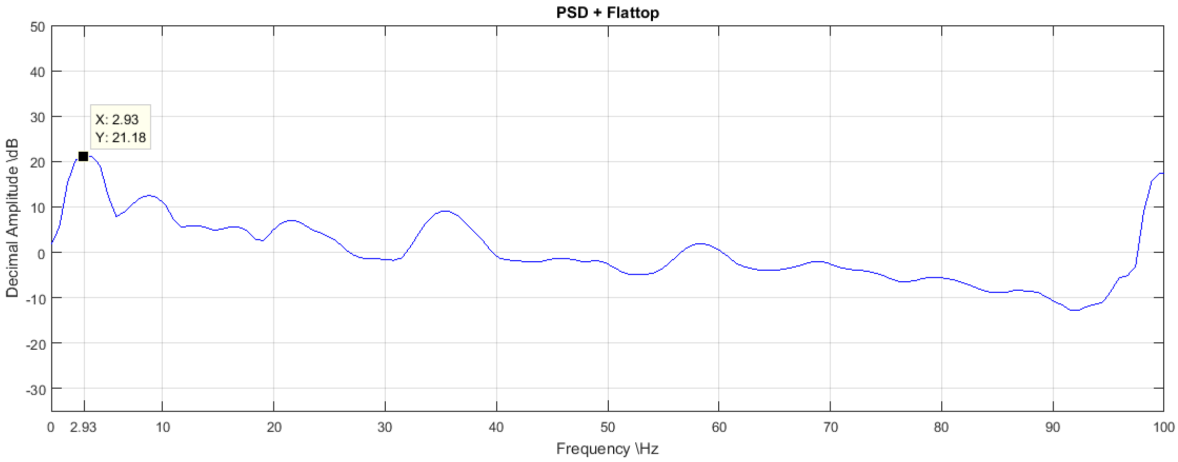

Figure 65: *Spectrum of 3 Hz Acoustic Signal*

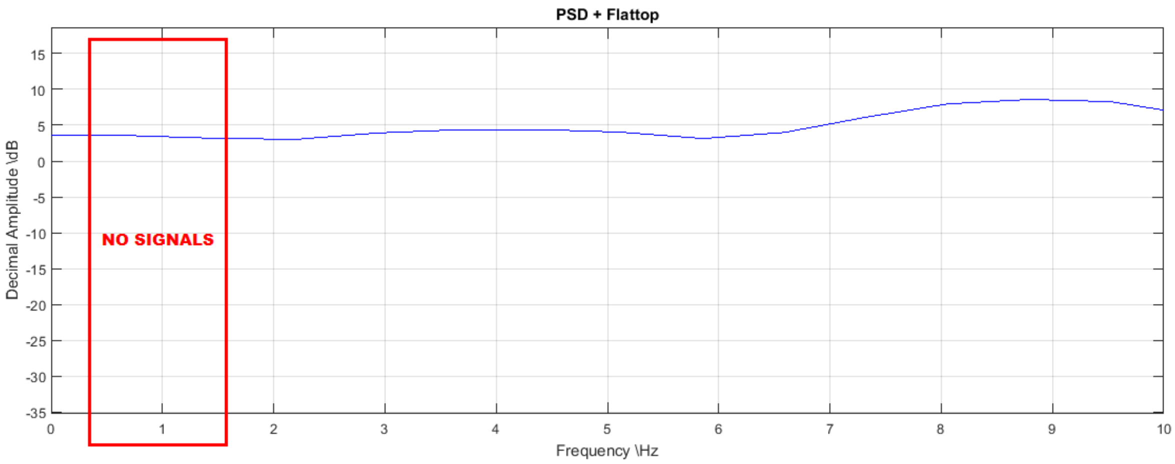

Figure 66: *Spectrum of 1 Hz Acoustic Signal*

4.4 Total Harmonic Distortion

Table 11: *Total Harmonics Distortions and Total Harmonic Distortions plus Noise Values for Digital MEMS microphone*

dBSPL	THD + N %	THD %
100	1.36	1.36
105	1.48	1.47
106	1.47	1.46
107	1.46	1.44
108	1.43	1.41
109	1.40	1.37
110	1.32	1.28
111	1.24	1.19
112	1.13	1.07
112.5	1.06	0.99
113	1	0.92
113.5	0.95	0.84
114	0.92	0.80
114.5	1.02	0.88
114.6	1.05	0.92
115	2.08	1.65
115.5	3.20	2.67
116	4.69	4.07
116.5	6.38	5.67
117	8.14	7.44
117.5	9.83	9.10
118	11.47	10.79
118.5	13.04	12.45
119	14.51	13.82
119.5	15.77	15.06
120	17	16.36

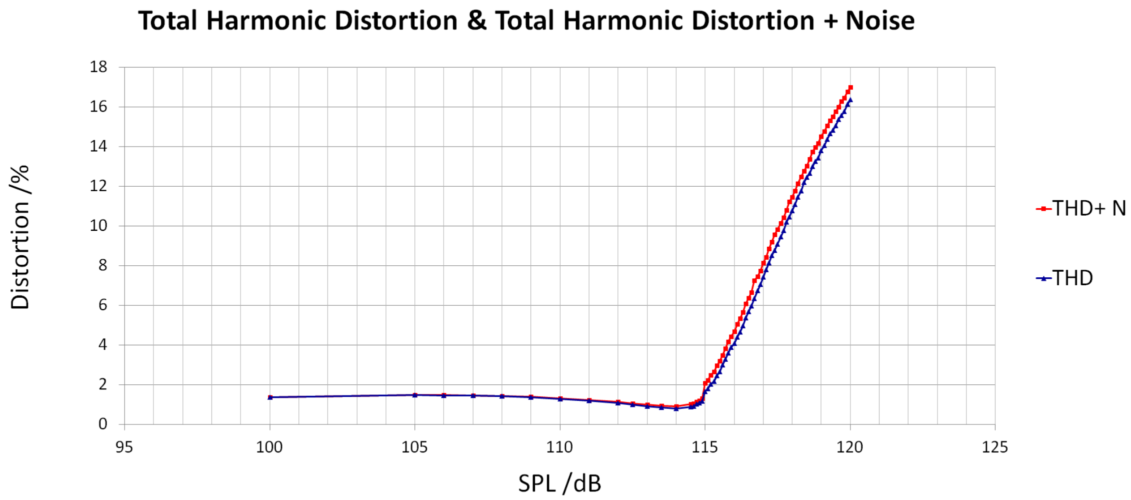

Figure 67: *THD and THD+N for Digital MEMS microphone*

The distortion of digital MEMS microphone is expressed by the standard total harmonic distortion (THD) and the total harmonic distortion plus noise ($THD + N$). In figure 67 the result are plotted and in table 11 are listed. On the y-axis is the percentage distortion value and on the x-axis is the L_p expressed in / dB . The distortion is about 1 % from below 115 dBSPL. After this point it starts to increase with an exponential behavior. At the Acoustic Overload Point declared by the constructor, that is 120 dBSPL, the distortion with noise is 17 %. While the 10% of distortion is reached at 117.6 dBSPL. In order to consider a microphone measure reliable, the distortion should be declared at 3 %, as explained in the normative IEC-63094-4 [1].So the maximum acoustic pressure point without significant distortions, measurable with digital MEMS microphone is:

$$AOP_{THD \leq 3\%} = 115.5$$

.

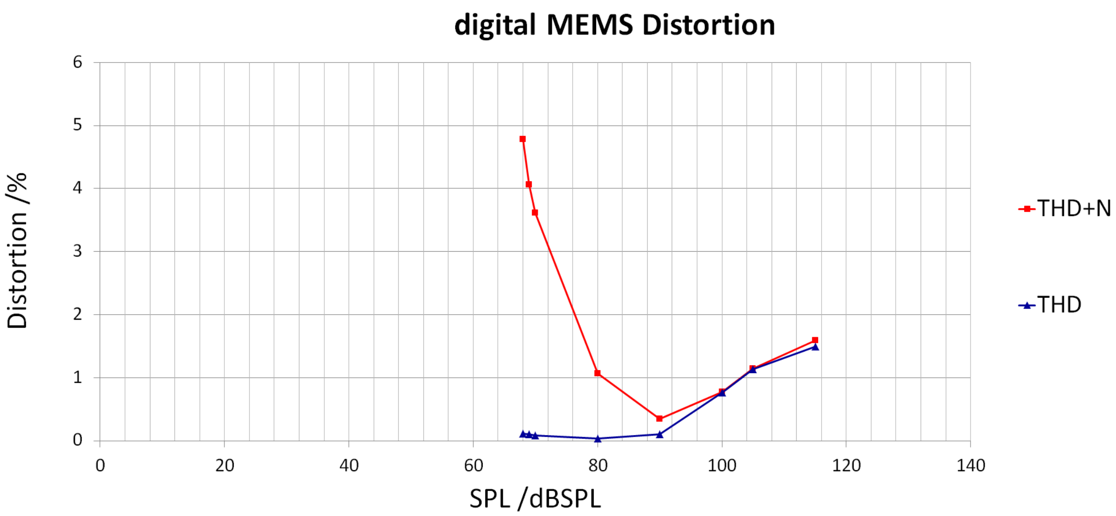

Figure 68: *Noise Distortion for Digital MEMS microphone*

The meaning of THD+N is that with digital MEMS microphone it is impossible to separate the noise-floor coming from the electrical component (pre-amplifier and ADC) from the acoustic signal. This is because the sound field acquired by digital

MEMS is always first amplified by the pre-amplifier and sampled by the ADC. This kind of noise, that is the residual noise, seems to increase while the L_p decreases until a certain value. Figure 68 shows that while THD, which considers just the signal and its harmonic content, reduces, as expected, while reduces the L_p. Instead THD+N increases while the L_p reduces. This means that the noise coming from the electrical component is not more negligible when the L_p reaches value lower than 80 dBSPL. As consequence, to understand the MEMS microphone distortion the THD+N parameter is more accurate than just THD.

4.5 Level Linearity

Table 12: L_p *values for Digital MEMS obtained with Level Linearity measure*

$L_{Aeq} ref.mic.$ /dB(A)	L_{Aeq} MEMS /dB(A)	L_p /dBFS
33	33.08	-84.16
34	34.11	-84.41
35	35.41	-84.99
36	36.10	-84.77
37	37.23	-83.94
45	45.19	-74.58
55	55.29	-64.28
65	62.74	-56.82
70	69.53	-50.02
80	80.19	-39.36
90	90.20	-29.35
100	100.26	-19.29
105	105.37	-14.19
115	114.92	-4.63
116	115.74	-3.82
117	116.45	-3.13
118	117.10	-2.51
119	117.73	-1.92
120	118.33	-1.37
121	118.84	-0.89
122	119.21	-0.55
123	119.47	-0.32
124	119.67	-0.16
125	119.83	-0.04
126	119.96	0.05
127	120.06	0.11
128	120.15	0.15
129	120.21	0.18
130	120.26	0.20

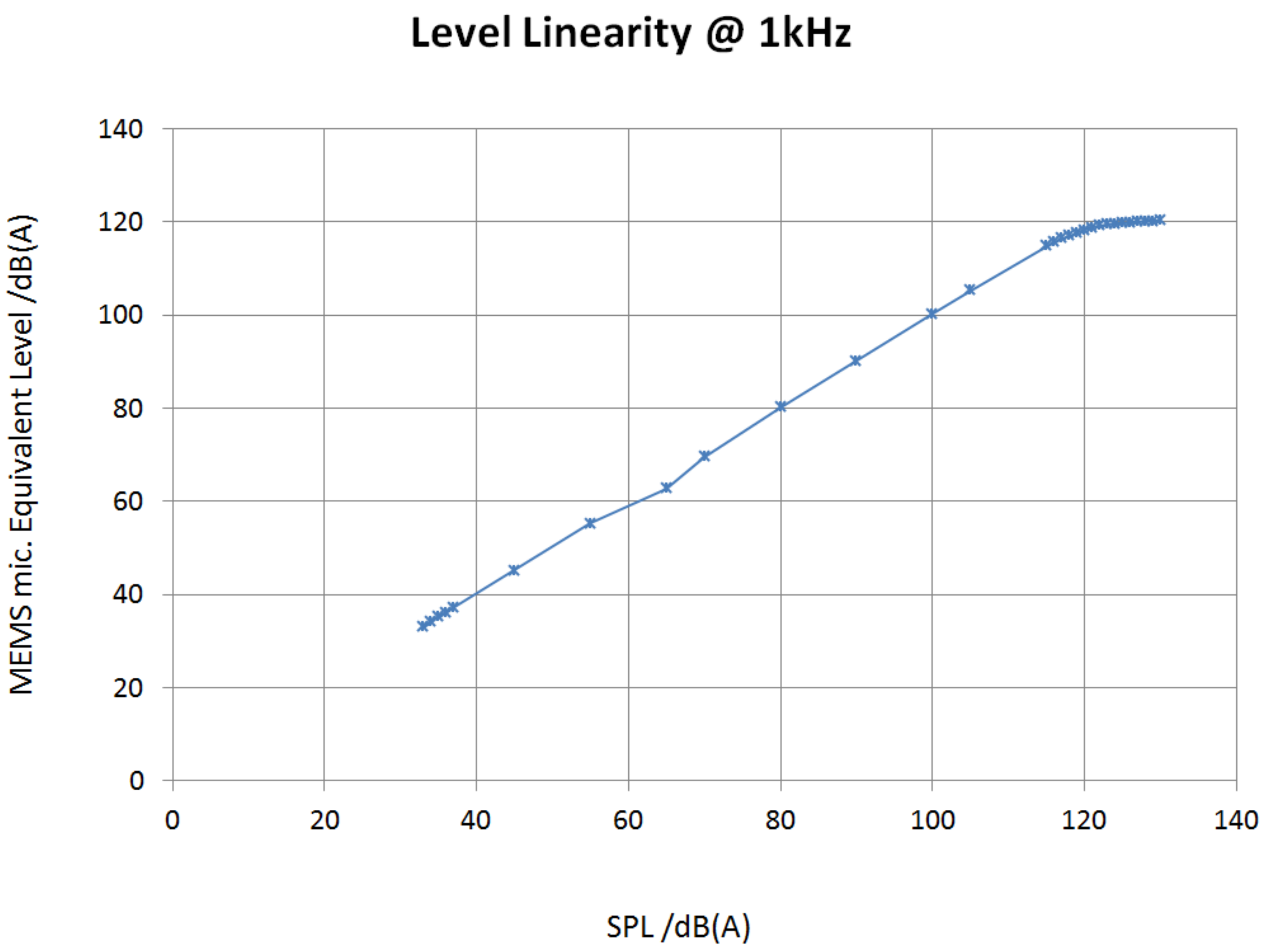

Figure 69: *Level Linearity of Digital MEMS microphone*

Values in table 12 in the first column show the value of L_{Aeq} measured by the reference microphone, in the second and third the equivalent level read by the MEMS in dB(A) and the L_p in dBFS respectively. The linear behavior is achieved until 118 dB where the difference from the value generated and the value read by the MEMS microphones is about 1 dB. After this point the MEMS microphone saturates and reaches the plateau at 120 dB. The difference from the value read by the MEMS and the L_p value generated by the sound source, from 33 to 118 dB, is tens of dB. From 119 dB the difference increase due to distortions. The 65 dB values show a strong non-linearity in MEMS which shows a value of 62.74. This results could be consider an error of the operator during the measure, since at this lower values of L_p the behavior must be linear, considering that, upper and lower values show a linear behavior.

Acoustic Overload Point

The acoustic overload point is an important parameter of digital MEMS microphones since it needs to convert in dB the sensitivity expressed in dBFS, as explained in section 2.2.1. Although in this thesis a sensitivity expressed in $Dec\hat{i}mal_{16-bit-signed}/Pa$ is presented, main MEMS microphones manufacturer continue to expressed the sensitivity in *dBFS*. As consequence, a rigorous way of computing it must be carried out. The correct value of acoustic overload point could be obtained in two different ways. The first is experimentally evaluated with the level linearity measure, that should be between 125 and 126 dB (table 12). This is because between this two values the ADC converter reaches the +0 dBFS. The problem of this computation is that the ADC is obtained taking into account the peak value of the digital sinewave that, with this higher value of L_p, is saturated as shown in figure 70:

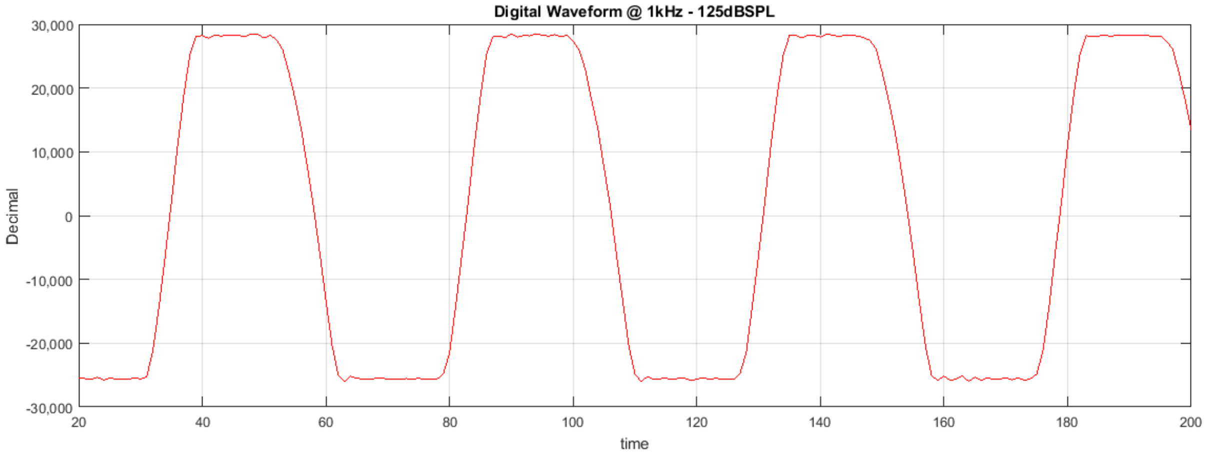

Figure 70: *1kHz - 125 dB Digital Sine-Wave*

As consequence, the peak value and so the dBFS result attenuated due to the clipped waveform and the AOP results bigger than it is.
Another way to compute it is to use the digital full scale expressed in *Decimal* and divided it by the sensitivity expressed in $Decimal_{16-bit-signed}/Pa$, calculated with 1 Pa signal at 1 kHz . Note that in this special case the reference is not the RMS value but the peak value of digital waveform. The AOP in Pascal is equal to:

$$\frac{\frac{FS=32767}{1807}}{1}\frac{Decimal_{16-bit-signed}}{\frac{Decimal_{16-bit-signed}}{Pa}} = 18.13Pa$$

and the AOP in dBSPL is equal to:

$$AOP_{dBSPL} = 20 \cdot log_{10}(\frac{18.13Pa}{20\mu Pa}) = 119.14dBSPL$$

The common value expressed for the AOP is 120 dB but it should be computed every time since is different for all microphones. The figure 71 shows the frequency response obtained with the two types of AOPs. The tow plot are quite the same. The table 13 shows the two AOPs expressed for a 94 dB signal at 1 kHz acquired with MEMS microphones in hemi-anechoic-room and measured with a B&K reference microphone. Is possible to notice that with the 120 AOP the L_p is 94.78 instead of 94, and with 119.14 is 93.92. So in the first case the error is about 0.8 dB while in the second case is 0.08 dB. This last result is more accurate.

Table 13: L_p of 94 dB - 1kHz input signal computed with different AOPs

AOP /dB	***sens /dBFS***	L_p ***of input signal /dB***
120	-25.22	94.78
119.14	-25.22	93.92

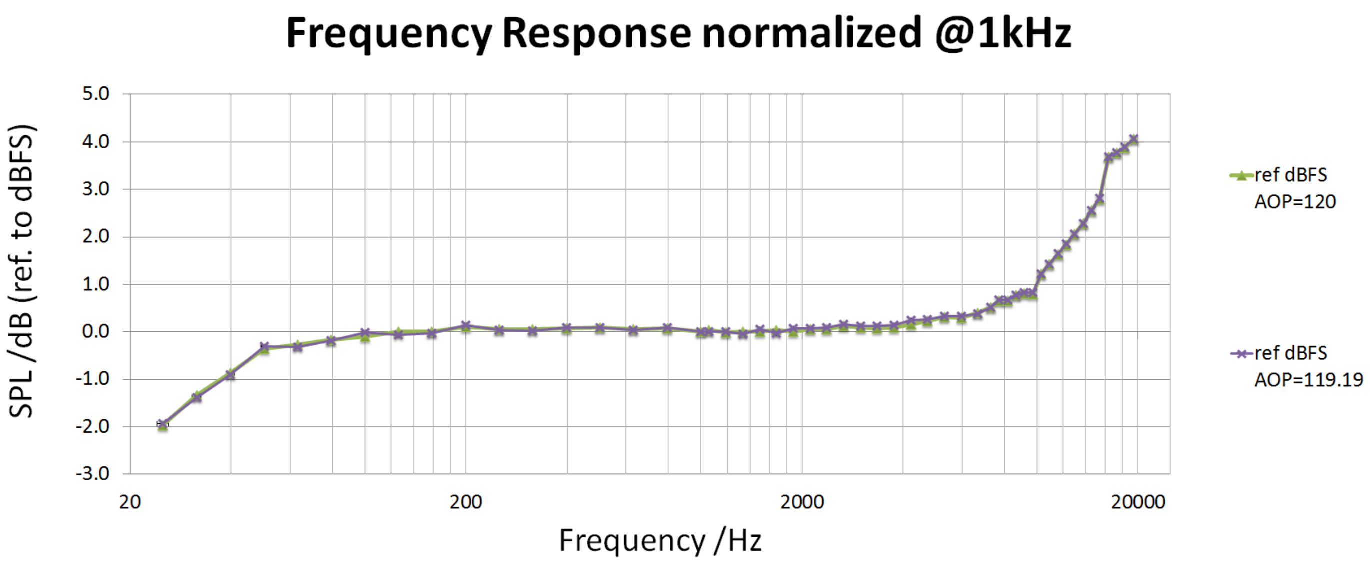

Figure 71: *Two Different Way of Frequency Response obtained with AOP=120 and AOP=119.14.*

4.6 1/ 3 Octave Band Analysis

To compute the 1/3 octave band the algorithm described in section 3.2.3 has been implemented. This measure is done to analyze a pink noise and compare it with B&K results, and also to evaluate the residual noise of digital MEMS microphone.

4.6.1 *Pink Noise 20Hz-20kHz*

Table 14: *Equivalent Levels with 1/3 Octave Bands Spectrum fro Pink Noise 20-20kHz*

MEMS		***B&K 4191***	
Equivalent Level Linear	*Equivalent Level A-Weighted*	*Equivalent Level Linear*	*Equivalent Level A-Weighted*
100.51 dB	100.11	100.57 dB	100.16

Table 14 shows the *Leq* and the *LeqA* value for a 100 dB pink noise signal from 20 Hz to 20 kHz acquired for 1 minute. Is possible to see that the global level read by the MEMS microphone is almost the same of B&K microphone. For linear levels the difference is 0.06 dB and for a-weighted levels is 0.05 thus completely negligible.

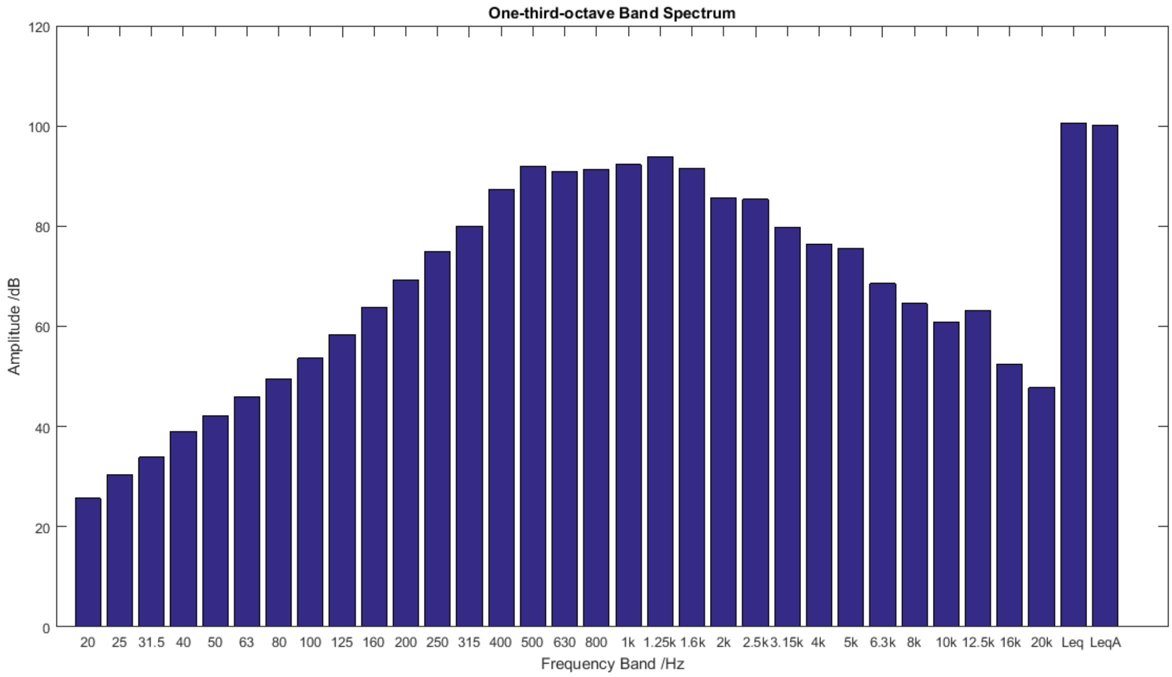

Figure 72: *1/3 octave band spectrum of digital MEMS microphone* for a 100 dB Pink Noise

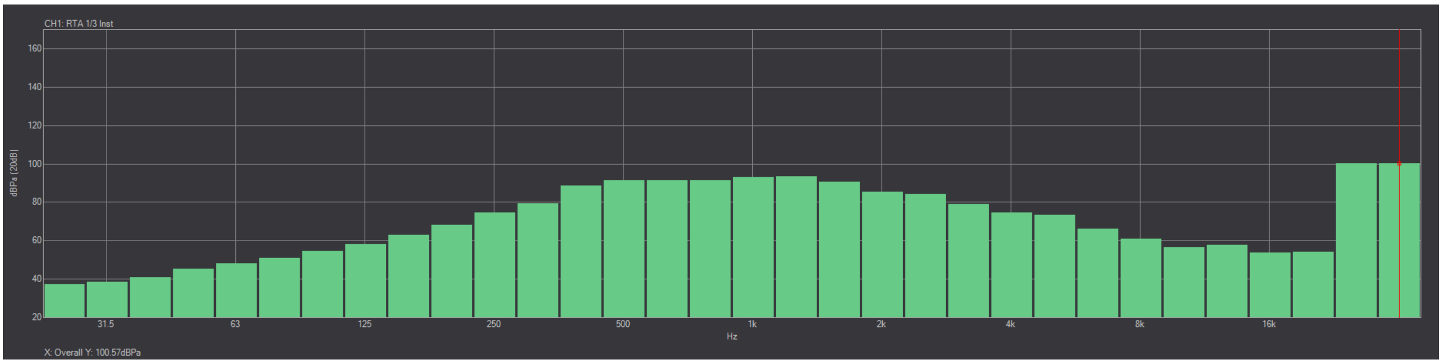

Figure 73: *1/3 octave band spectrum of B&K microphone*

Figure 72 and 73 compare the two octave band analysis. It is possible to notice that there no significant differences. Levels are the highest between 400 Hz and 2 kHz for both microphones. Out of this zone the energy band start to decrease gradually except for the band at 12.5 kHz that is bigger than the previous. Anyway this behavior is present in both microphone so is not an error of digital MEMS microphone.

4.6.2 Digital MEMS Residual Noise (EIN)

Table 15: Equivalent Levels with 1/3 Octave Bands Spectrum for Residual Noise of Digital MEMS Microphone

Frequency Band /Hz	L_p ***/dB***
20	5.9
25	8.3
31.5	11.9
40	16.5
50	16.9
63	19.0
80	19.0
100	17.9
125	18.0
160	17.9
200	17.0
250	16.5
315	15.7
400	14.9
500	15.0
630	14.9
800	15.1
1000	15.6
1250	16.1
1600	16.9
2000	17.5
2500	18.4
3150	19.3
4000	20.2
5000	21.1
6300	22.1
8000	23.0
10000	23.9
12500	24.8
16000	24.8
20000	25.0
Leq	34.7
LeqA	31.3

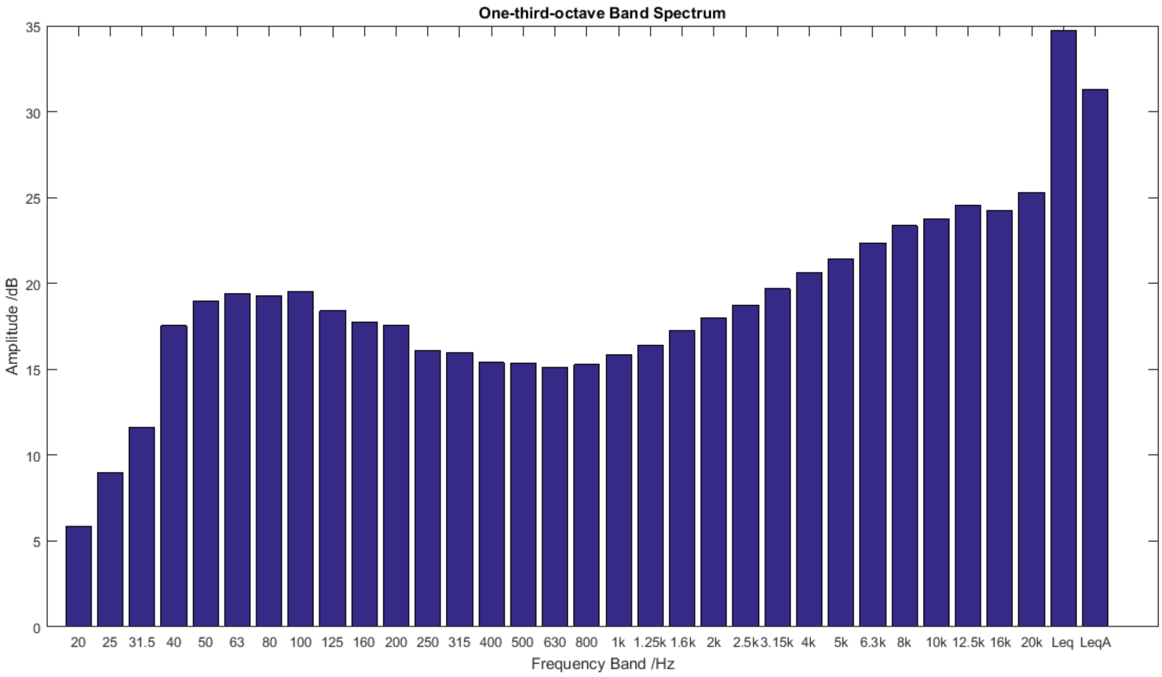

Figure 74: *1/3 octave band spectrum of digital MEMS microphone* for Residual Noise

The digital MEMS has a A-weighted and linear residual noise level of 31.29 dB(A) and 34.33 dB respectively, see tab. 15. The residual noise over the band spectrum is lower than 17 dB before 50 Hz due to the cut-off caused by high-pass filter inside the MEMS. From 60 Hz to 160 Hz remains constant between 18 and 19 dB, then starts to decrease until 400 Hz where it reaches its lowest values equal to 15 dB. From 1kHz to 8 kHz the residual noise increases until 25 dB at 20 kHz. This increase at high frequency could be due to the sigma-delta converter which moves the quantization noise at high frequencies. As mentioned in the previous chapter the sound pressure level at each frequencies could be evaluated starting from the sensitivity expressed in $Dec\hat{i}mal_{16-bit-signed}/Pa$ carried out for each frequency or starting from the sensitivity in $Dec\hat{i}mal_{16-bit-signed}/Pa$ carried out just at 1 kHz and use this last for all.

Table 16: *Equivalent Level evaluted by using the MEMS microphone sensitivity computed for each frequencies and using just the sensitivity at 1kHz*

	L_{Aeq} **/dB(A)**	L_{eq} **/dB**
sens1kHz	31.266	34.717
sensAllfreq	31.832	36.085
differences	**0.567**	**1.367**

Tab. 16 shows the equivalent level computed with the two types of sensitivities, the difference in LeqA is negligible while in the Leq linear is about 1.3 dB.

4.6.3 Dynamic Range

According the Acoustic overload point and the residual noise the dynamic range is:

$$DynamicRange = 119.14dB - 31.26dB(A) = 87.88$$

and converted in Pascal is:

$$DynamicRange = 18.11Pa - 1mPa$$

4.7 Signal-to-Noise Ratio

The SNR is obtained with the formula:

$$SNR = \frac{Sensitivity_{1kHz-94dB}}{ResidualNoise(EIN)}$$

where the EIN is equal to *31.26 dB(A)*.

Table 17: *Digital MEMS microphone SNR with sensitivity in dBFS and* $\hat{Decimal}_{16-bit-signed}/Pa$

EIN	***Sensitivity of signal @ 1kHz - 94 dB***					
dB(A)	*dBFS*		$\hat{Decimal}_{16-bit-signed}$	*Pa*	*sens @ 1kHz*	*dBSPL*
31.29	-25.35	94.64	1250.50	1	1216	94.22
SNR/dB		63.35				62.93

Table 17 shows the value of the EIN, and the value of the two different sensitivities carried out from 1kHz signal at 94 dBSPL. Since the sensitivity in *dBFS* is higher of 0.64 dB than $\hat{Decimal}_{16-bit-signed}/Pa$, the SNR is higher too and is equal to 63.35. By considering the sensitivity in $\hat{Decimal}_{16-bit-signed}/Pa$ the SNR is 62.93, quite the same value. It is possible to conclude that the SNR of digital MEMS microphone with HIGH MODE setting is 63 dB.

4.8 Stability

4.8.1 Short Term Stability

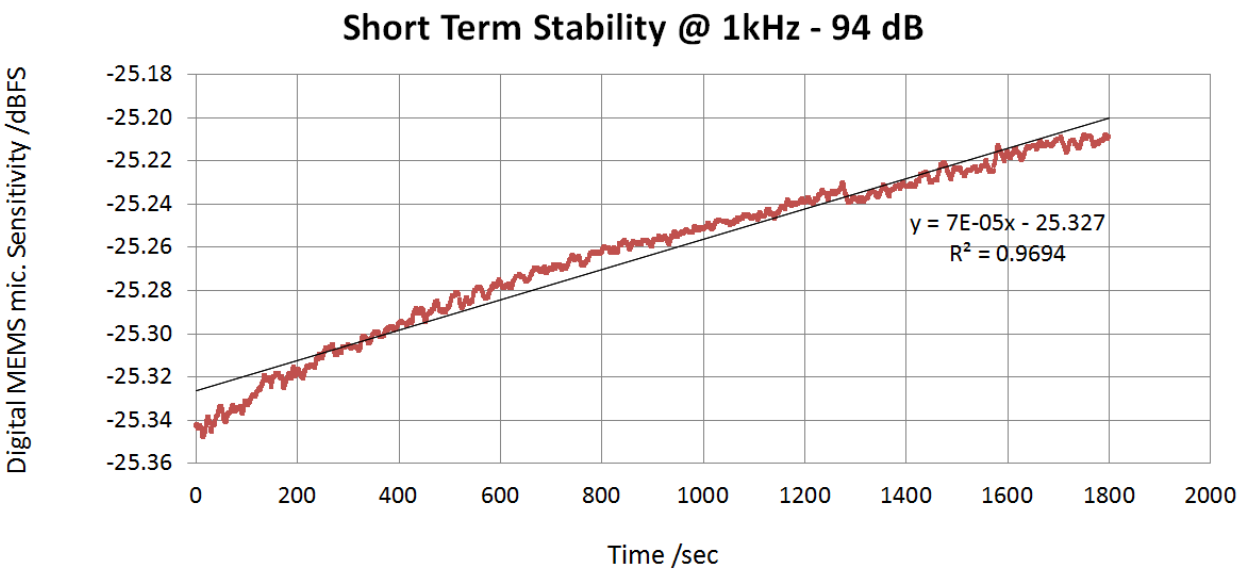

Figure 75: *Short Term Stability - 30 minutes - for Digital MEMS microphone*

The short term stability is computed acquiring a 1kHz signal at 94 dBSPL for 30 minutes. The figure 75 shows the behavior. On the y-axis is figured the sensitivity in $dBFS$ at 1kHz on x-axis the time in seconds. The sensitivity apparently increases of 0.14 dB, from -25.34 to -25.20. The linear fit model generated a linear equation equal to:

$$y = 70\mu \cdot x - 25.327$$

with an $R^2 = 0.96$ that means that the goodness of the model is accurate. This means that the sensitivity of digital MEMS microphones increases of $70\mu dBFS$ per second.

4.8.2 Long Term Stability

The long term stability takes into account 4 months from November to February. Only two measures are performed: one in the first month an other in the last. The results are shown in figure 76 which describes the sensitivity in dBFS on the y-axes and the month on the x-axes. It is possible to see that sensitivity increase of 0.1 dB in four months and that the trendline computes a changes of 0.04 dB per month. This results demonstrate that the change in sensitivity in a 4 months is quiet negligible, however it is important to improve this measure considering a longer period of time such as 1 year.

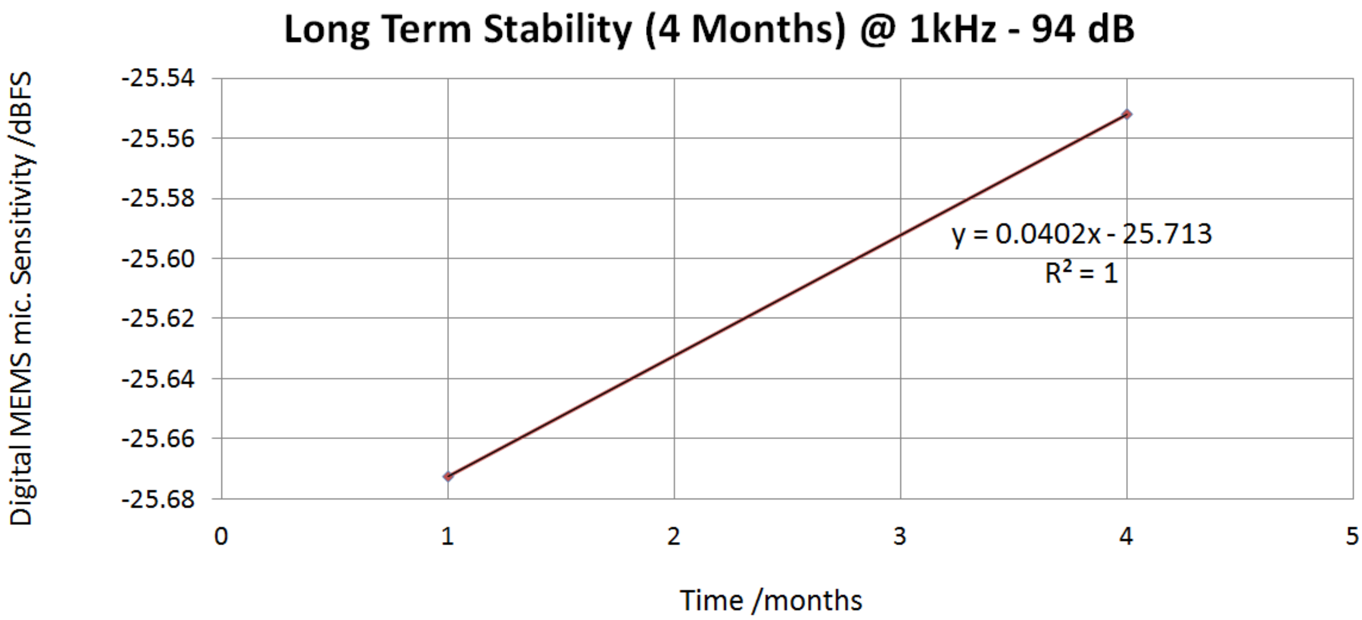

Figure 76: *Long Term Stability - 4 Months - for Digital MEMS microphone*

4.9 Influence of Temperature

Table 18: *Influence of Temperature on Frequency Response Values fro Digital MEMS*

Temperature $/^\circ C$	***Humidity %***	L_p ***/dB***
20	34.1	1.28
10	31.8	1.52
0	42	-0.10
-10	43.4	1.70
0	34.4	-0.34
10	38.9	0.75
20	37	0.37
30	39.1	-2.85
40	26.7	1.14
50	23.5	0.65
40	27.3	1.70
30	27.3	0.35
20	27.4	1.31

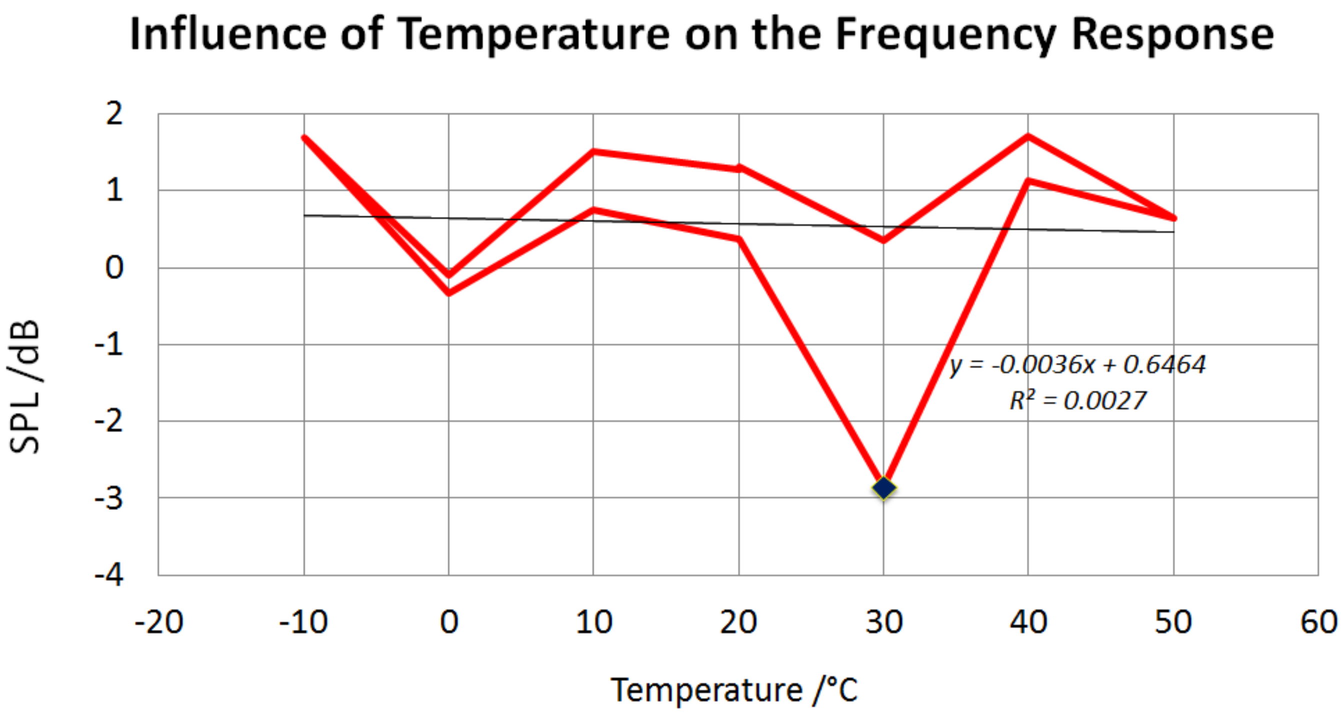

Figure 77: *Influence of Temperature for Digital MEMS microphone*

The influence of temperature is evaluated considering the frequency response at 2 kHz for the reason explained in section 3.11. The values of temperature are chosen in order to generate an hysteresis loop. The frequency response is computed by comparison in the same way of hemi-anechoic room. Furthermore in this case a temperature correction factor is also applied to the reference microphone B&K 4191, since its frequency response is temperature dependent, as describe in section ??. The value computed are anyway affected by a high uncertainties, in fact is possible to see in figure 77 that the L_p computed at 30° is first time of the hysteresis loop 0.35 dB and -2.3 dB the second time. As for standard microphones the microphone sensitivity seems to decrease while temperature increases, the fit interpolation describes a linear equation whit a slope of *036*. This means that the digital MEMS sensitivity decrease of about 0.004 dB/°C anyway the R^2 value is 0.0027 which means very low accuracy.

4.10 Uncertainty assessment Computation

The uncertainty computation is done just for the measures where multiple data have been acquired. The uncertainty evaluated is the expanded uncertainty at a significant level of 95% and is the results of type A and B uncertainties. The type A uncertainties contributions are mainly the standard deviations of digital MEMS microphone carried out from all the different positions and the accuracies of B&K reference microphone and the 4226 sound calibrator. The type B uncertainties are derived from manufacturer's specifications and are listed in table 19:

Variable	***Type B Uncertainty***
thermometer, temperature	0.05 dB/°C
barometer	5μ dB/ kPa
thermometer, humidity	0.05 dB/°%
onosokki spectrum analyzer	0.015 dB

Table 19: *Type B uncertainties*

The table 20 shows the uncertainty computation for the hemi-anechoic frequency response. In this case the values listed refers to the acquired data at 25 Hz. The table is divided in six subtables: in the first are contained the variables and their units of measure, in the second and third the type A and type B standard uncertainties, in the fourth the parameters, in the fifth the variance contributions and the t-distribution with the *Welch-Satterthwaite* formula, in the sixth subtable, on the bottom-left, the final expanded uncertainty. The type A uncertainties are the standard deviation of all the positions, 8 number of data which means 7 degrees of freedom, and the accuracy of reference microphone, just 1 data which means maximum number of degrees of freedom. The uncertainties of the reference microphones is an expanded uncertainty with coverage factor equal to 2 and a standard deviation equal to 0.1. The type B uncertainties are the ones listed in table 19, and are evaluated with a k factor equal to 3. For each type B uncertainties in the column a_i are listed the semi-fields. The global expanded uncertainty is carried out considering all the singles variance $u_i^2(y)$ which are evaluated by the formula:

$$u_i^2(y) = c_i^2 \cdot u_i^2(x_i)$$

where $u_i^2(x_i)$ is the input variance (type A and type B) and c_i^2 is the sensitivity coefficient. The total variance is the sum of the single variances and are equal in this case to to 0.012.

$$u^2(y) = \sum_{i=1}^{N} u_i^2(y) = 0.012$$

The total standard uncertainty is the square root of the total variance

$$u(y) = \sqrt{u^2(y)}$$

and the expanded uncertainty is the standard uncertainty multiple by the coverage factor

$$U(y) = k \cdot u(y)$$

and equal, in this case to 0.21 dB.

Table 20: *The uncertainty table for hemi-anechoic room frequency response for 25 Hz sine wave*

Variable x_i			**Cat. A**					**Cat. B**		**Paramteres**						
Symbol	Value	Note	U_i	P_{di}	ν_{di}	k_{di}	s_i	a_i	k_{ai}	$\ni_i$	n_{di}	n_{ri}	$u^2(x_i)$	$c_i = \Delta y/\Delta x$	$u_i^2(y)$	$u_i^4(y)/\ni_i$
$Decimal_{16-bit-signed}/Pa$	991.95	*st. Dev.*					14.03		3	7	1	8	24.62	0E+00	-	-
dB		*unc. Bruel Microphone*	0.20			2.0	0.1		3	100	1	1	0.01	1.00E+00	0.0100	0.00
										100	1	1		1.00E+00	-	-
dB\C		*temperature*						0.05	3	100	1	1	0.00	1.00E+00	0.0008	0.00
dB		*humidity*						0.05	3	100	1	1	0.00	1.00E+00	0.0008	0.00
dB\kPa		*static pressure*						5.0E-03	3	100	1	1	0.00	1.00E+00	0.0000	0.00
dB		*onosokki amplitude*						0.015	3	100	1	1	0.00	1.00E+00	0.0001	0.00
y	-36.400	dB														

Varianza di y, $u^2(y)$	1.2E-02	1.0E-06
Incertezza tipo di y, u(y)	1.1E-01	
Degrees of Freedom of y, $n(y)$	136	
Significant Level	95.0%	
Coverage Factor	2.0E+00	
Expanded Uncertainty $U(y)$	**2.1E-01**	dB

This computation is done for all frequencies and also for the other two frequency response, one with 4226 sound calibrator and an other with active coupler. The main difference with the hemi-anechoic frequency response is the lack of the reference microphone and different value of type B uncertainties depending on the used instruments. The results are listed in the previous section's tables (table **??**, 7, 8).

5 Conclusions

Digital MEMS microphone have been characterized and calibrated with the comparison method. Many advantages have been carried out and some other measure have to be done as future work in order to complete the characterization.

5.1 Frequency Responses

Three different pressure field measurement methods for sensitivity and frequency response have been investigated: in a hemi-anechoic chamber, with a B&K 4226 sound calibrator, with an active coupler. For the hemi-anechoic room frequency response, high frequency resolution and low uncertainties are reached. Anyway temperature and humidity are difficult to control due to large volume (300 m^3) and the time measuring is very long, about 2 days. The frequency response in this case has the lowest averaged uncertainty within 0.20 dB and 4.18 dB, with an average value of 0.49 dB. Uncertainties at higher frequencies are larger than lower frequencies due to diffraction effects. The sensitivity at 1 kHz is 1216 $Dec\hat{i}mal_{16-bit-signed}/Pa$. For frequency response computed with the Bruel and Kjaer 4226 calibration less frequency resolution and bigger uncertainties are reached. Temperature and humidity are controlled since the measuring environment was a quite office and short measuring times are required, about 2 hours. The uncertainty is within 0.5 dB and 4.07 dB, the averaged value is 1.30 dB. In this case, uncertainties at higher frequencies are larger than lower frequencies due, especially, to air leakages in the cavity, which means that MEMS microphones and in its adapter are not perfectly coupled in the hole cavity. The sensitivity at 1 kHz is 1259 $Dec\hat{i}mal_{16-bit-signed}/Pa$. Thanks to its simplicity this kind of calibration could be implemented when many microphone have to be calibrated and a it is not needed a very high frequency resolution. The active coupler calibration present an high frequency resolution, good control of temperature and humidity and middle time duration, about half a day. Nevertheless, it is not reliable since it is affected by very high uncertainties caused by significant air leakages in the cavity of the active coupler. The uncertainty values are within 0.22 dB and 39.23 dB with an average of 12.8 dB. The sensitivity at 1 kHz is 1209 $Dec\hat{i}mal_{16-bit-signed}/Pa$. Table 21 summarizes the advantages and disadvantages of the three types of calibrations.

	Hemi-Anechoic Room	*B&K 4226 Sound Calibrator*	*Active Coupler*
Adavatages	high frequency resolution lowest uncertainty very high precision	short measuring time low uncertainty good control of temperature and humidity	high frequency resolution good control of temperature and humidity
Disadavantages	long measuring time bad controll of temperature and humidity	Low frequency resolution Low precision	lowest precision highest uncertainty

Table 21: Advatages and Disadvatages for the frequency response in three differenet environments

In figures 78 and 79 the frequencies response of the 3 calibration methods are compared (first figure considers all the three environment, the latter just the hemi-anechoic and sound calibrators).

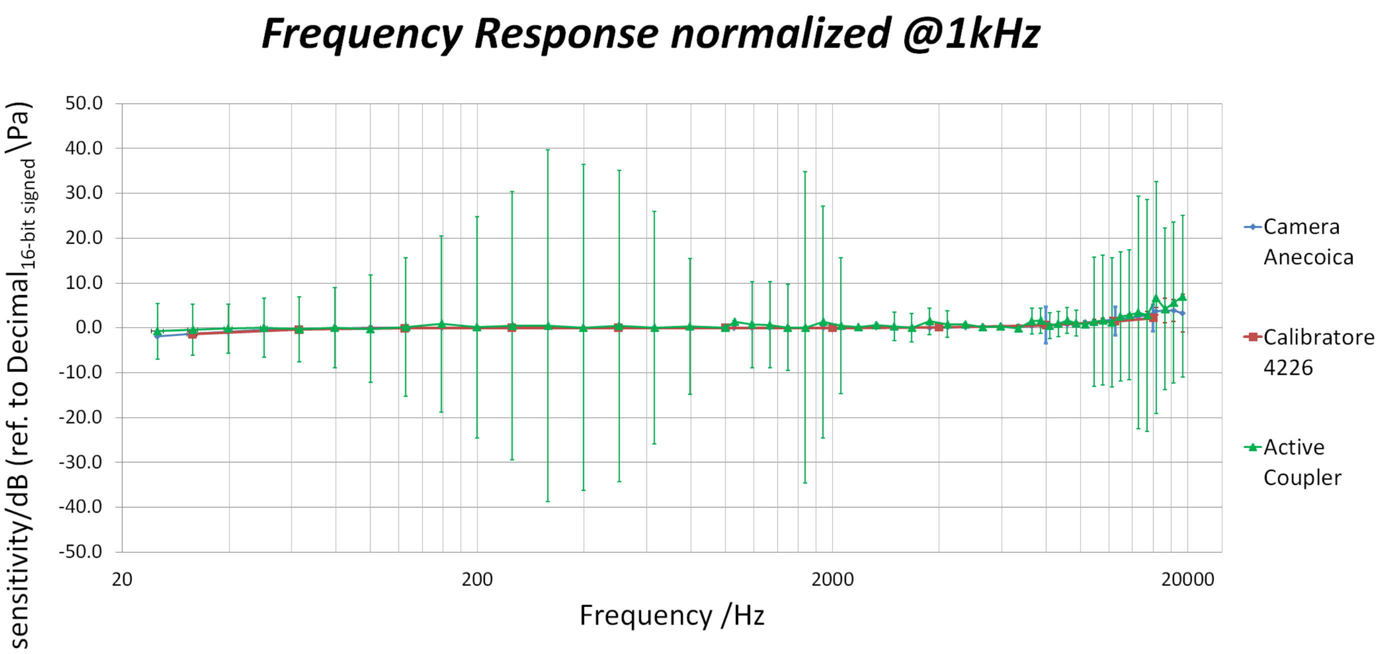

Figure 78: *Comparison between the three types of frequency response*

In figure 78 it is possible to notice that the active coupler frequency response entails high uncertainties, however it describes a flat frequency response.
Figure 79, instead, shows that the frequency response with the B&K 4226 calibrator which requires less time, is almost the same of the one in the hemi-anechoic room. This result demonstrates the accuracy of the calibration with B&K 4226 calibrator compared to the hemi-anechoic response.

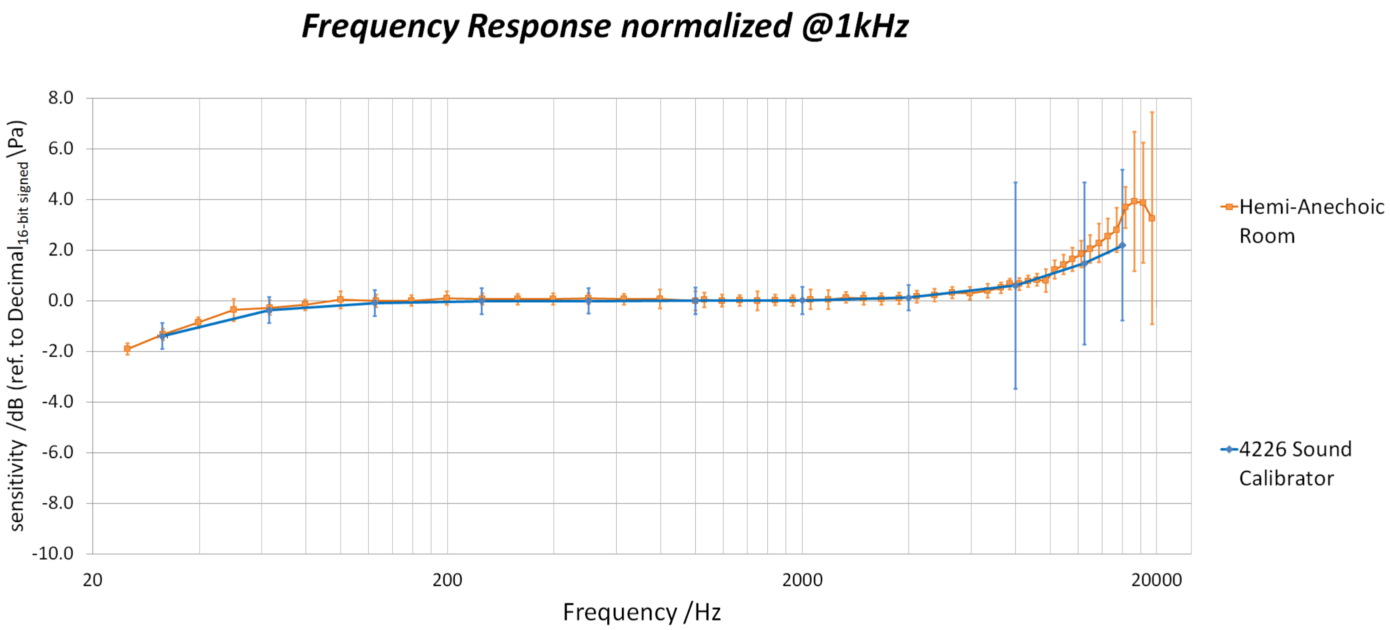

Figure 79: *Comparison between the frequency response carried out with B&K 4226 sound calibrator and in Hemi-anechoic room*

This high performances of MEMS microphones demonstrate that they could be used as measuring devices, as examples for noise monitoring, health-care applications, automotive and so on. The lack of a normative is nowadays a problem to be overcome. The three methods shown in this thesis could be a starting point to write a normative for digital MEMS microphones calibration. In particular, according to the uncertainty reached, different calibration methods could be studied. One where the simplicity of the method is preferred, carried out with the sound calibration. An other where high frequency resolution and high precisions are required, carried out in the hemi-anechoic room.

5.2 Sensitivity of the Digital MEMS microphones

Two types of sensitivity have been reported, one referred to the digital full scale expressed in *dBFS* and another referred to the RMS value of the digital sine wave, expressed in $\hat{Decimal}_{16-bit-signed}/Pa$. The main problem of the sensitivity expressed in *dBFS* is the computation of the Acoustic Overload Point. This value represent the maximum acoustic pressure expressed in dBSPL, which should be equal to digital full scale of the ADC (*0 dBFS*). However, computing the AOP is a hard task because when the acoustic pressure reaches high values, MEMS microphones is out of the linear range and relevant saturations are involved. Manufacturer's datasheets refers the AOP as the value in which the microphone reaches the 10% of THD+N. Anyway this value results very imprecise and less accurate, furthermore the IEC 61094-3 Normative expresses the maximum acoustic pressure level for standard microphone as the **3%** of the distortion. Moreover, since the sensitivity expressed in dBFS is referred to the peak value, it is impossible to characterize an acoustic random noise because its peaks values could be very variable. For all those reasons it is preferred to express the sensitivity in $\hat{Decimal}_{16-bit-signed}/Pa$ and obtain the value in pascal by considering the RMS value of the digital sine wave. Moreover when it deals with random stationary signal like noise, is more accurate to compute the RMS value than the peak.

5.3 Digital MEMS microphone parameter

The main parameters of the digital MEMS are compared with the tolerances expressed for sound level meter to classify a microphones in Class 1, in Class 2 or neither.

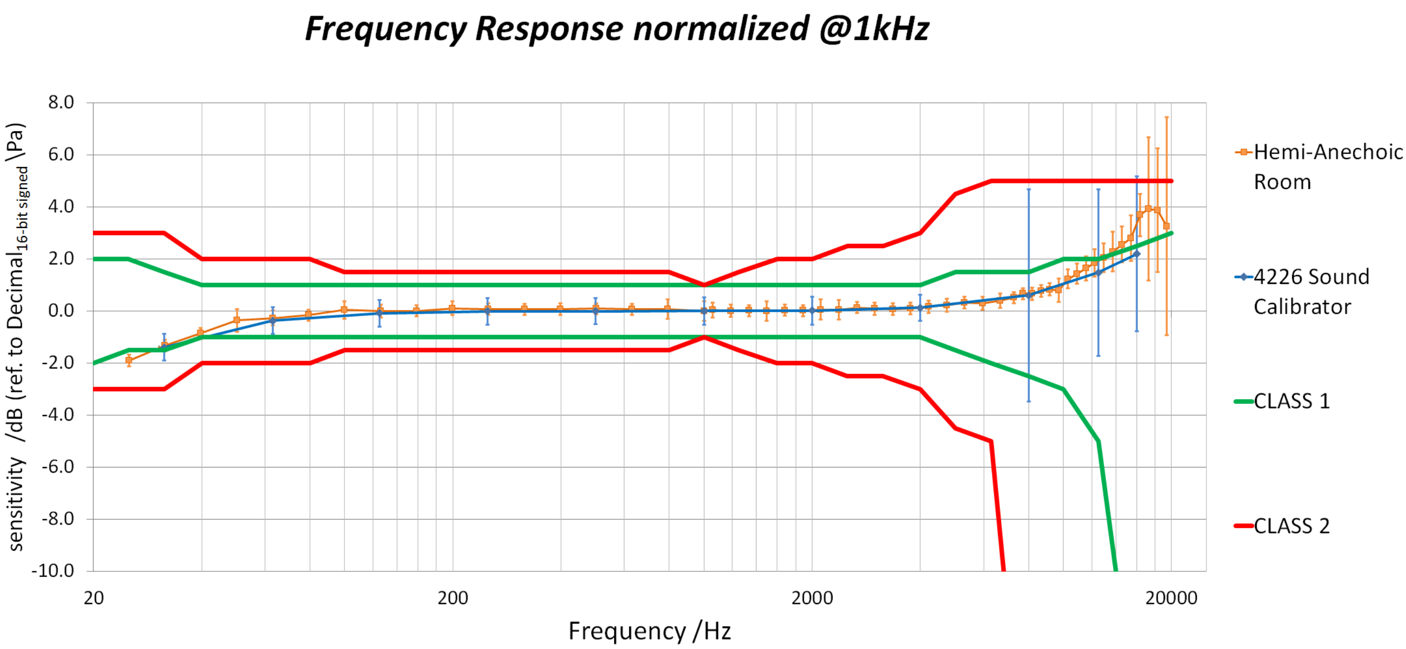

Figure 80: *Comparison between the frequency response and Class 1 and 2 level meters*

In general the results obtained for the digital MEMS microphones tested are under the limits of the Class 2 and sometimes under the Class 1. Figure 80 shows that, between 30 Hz and 7 kHz both the frequencies response of 4226 sound calibrator and hemi-anechoic room are between the upper and lower limit of class 1 level meter. From 8 kHz to 10 kHz the uncertainties of 4226 sound level calibrator is out of class 1 tolerance but within class 2, while hemi-anechoic response is again within class 1. From 12.5 kHz to 20 kHz the response is out of the upper limit of class 2.

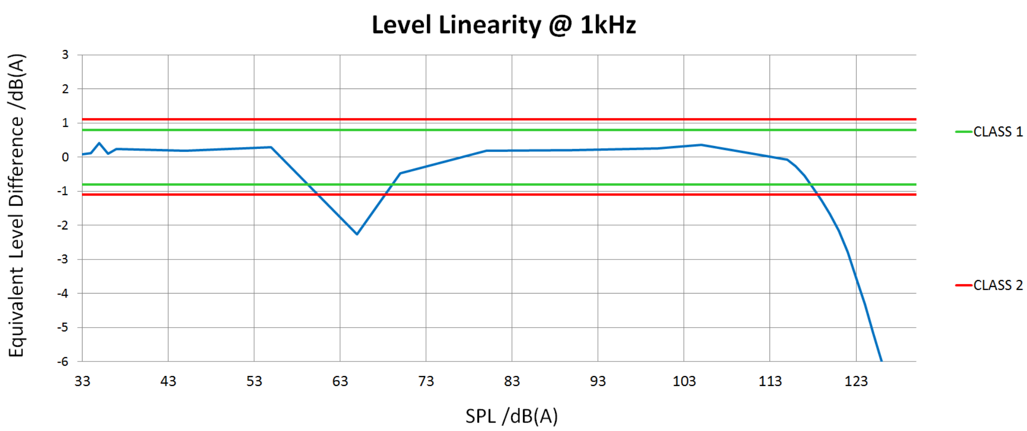

Figure 81: *Level Linearity Compared with class 1 and class 2 sound level meter tolerances*

The level linearity shown in figure 81 is between class 1 until 119 dB(A), after this point digital MEMS sarts to saturate. There is an outlier value at 65 dB(A) which is probably due to an error of the operator.

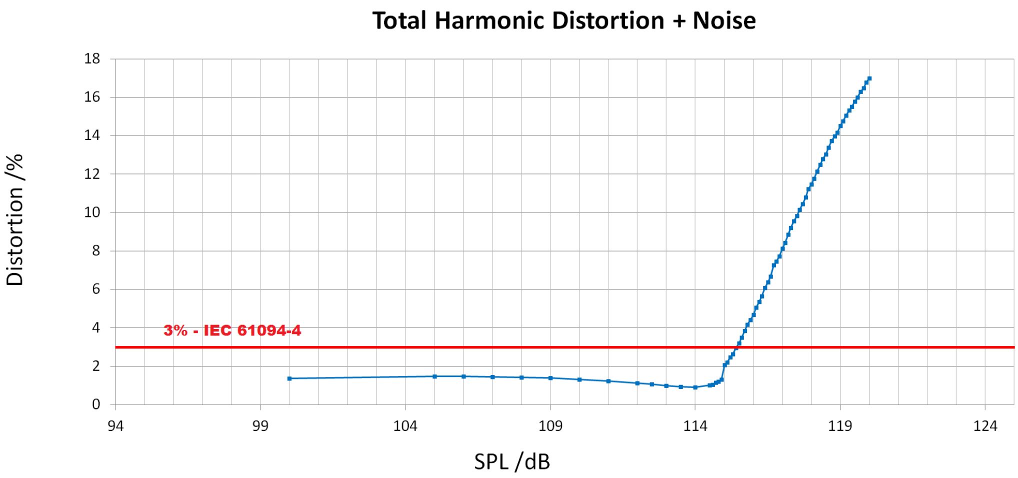

Figure 82: *Total Harmonic Distortion compared with normative IEC 61094-4*

Total harmonic distortion tolerance for the standard microphone is 3%. For digital MEMS microphone this limit of distortion is achieved at 115.4 dB as shown in figure 82. As consequence the dynamic range, according to normative, is 115.4-31.0 = 84.4 dB.

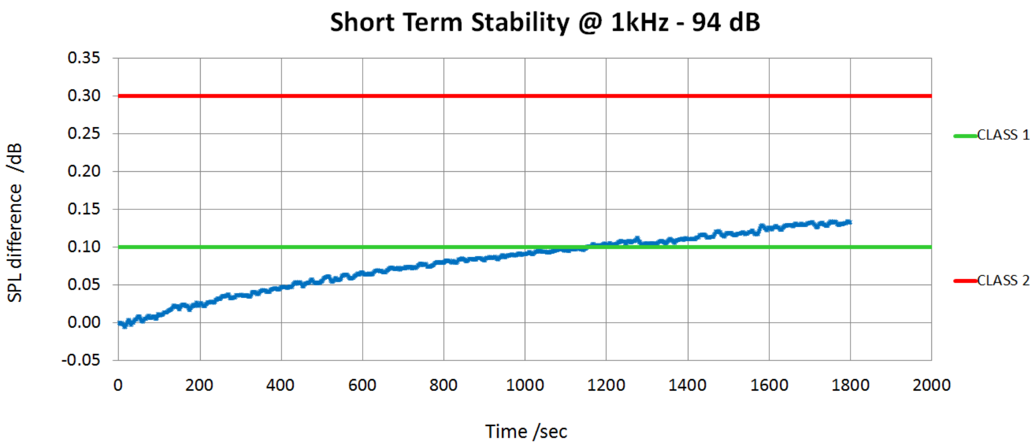

Figure 83: *Short Term Stability Compared with class 1 and class 2 sound level meter tolerances*

Figure 83 shows sound pressure level differences between 30 minutes computed with digital MEMS. It is possible to notice that the values are only under tolerance of class 2.

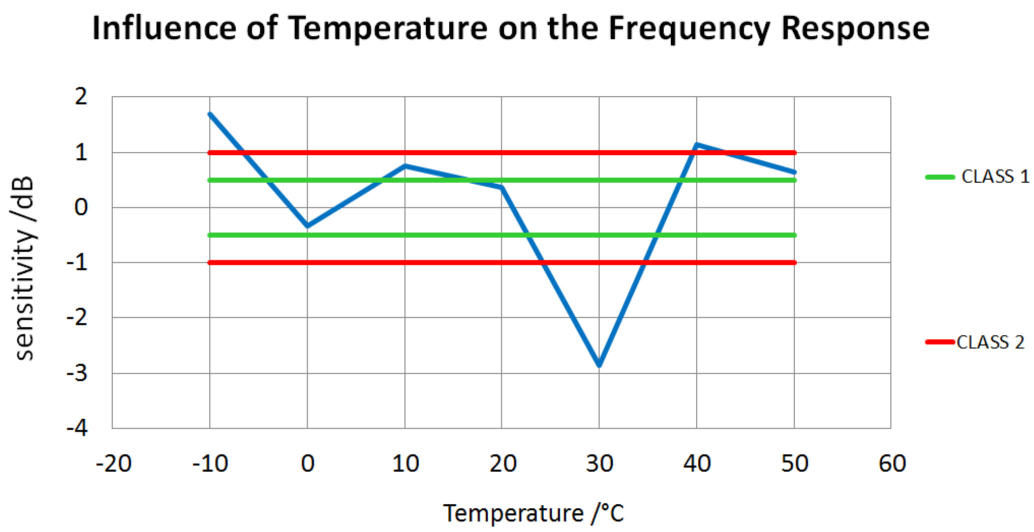

Figure 84: *Influence of Temperature Compared with class 1 and class 2 sound level meter tolerances*

The temperature response, see figure 84, is out of all classes due to the outlier at 30°, shown in section 3.11. If this point is not considered the microphone is almost under the class 2 tolerance.

5.4 Future Work

In the future works the long term stability should be firstly evaluated (such as 1 year). If MEMS microphones will be used as measuring devices one of the most significant parameter to be evaluated is aging. Understanding, in city noise monitoring, how many times MEMS devices have to be recalibrated and how much their sensitivity changes is a crucial point.
Moreover it is important to estimate the humidity and pressure dependency since MEMS microphones could be used also for outdoors measures.
Manufacturer's datasheet certifies that MEMS microphones are omnidirectional, due to their small, almost point source, diaphragm. Anyway a characterization following the IEC standard has to be preferred to obtain more accurate results.
Understanding the acoustic parameter differences from the same MEMS microphones is important since those sensors are produced in stack of big quantities and referring a single calibration for every one is hard and long. The cost for a calibration by comparison, following the IEC 61094-4, is about 800 € while for one MEMS microphone is about 1 €. This price difference should be overcome by considering a trade off between an accurate calibration and low cost. One possible solution could be adopt the calibration with the B&K 4226 calibrator which gives sufficient precise results and require a calibration cost acceptable for the MEMS's price. The lack of a IEC normative for the both digital and analog MEMS microphone calibration has to be overcome. Without this document, MEMS microphones can not be used for legal measures such as, for cities monitoring or in health care contest. The first step to do is to raise awareness the scientific community on this theme and to give a metrological support, in acoustic measure, to the industries that work with MEMS microphone.

6 Appendix A

```
clc
clear

%%%%% definire il percorso della cartella contente i file
cd 'C:...'
name='name.bin';
fileID = fopen(name);
precision = 'int16';
A = fread(fileID,precision);

%%%%% costanti
dmic= A(1:2:end);   %odd matrix - digitale
amic=A(2:2:end);    %even matric - analogico
fc=48000;
sf=1/0.21558;       %fattore di scala flattop
sh=1/0.5;           %fattore di scala hanning
ii=1;
res = 2^15-1;       %fondoscale 16-bit signed
p0=20*10^-6;        %pressione atomosferica


%%%%% FREQUENZA SEGNALE IN INGRESSO

if(strcmp(name,'fondo')==1)       %controllo per salvare il fondo
      fs=0;
  else
      fs=sscanf(name,'%f');
end


%%%%%%%%%%%%%%%%%%%%%%%%%%%%%%%%%%%%%%%%%%%%%%%%%%%%%%%%%%%%%%%%%%%%%%%%%%%%%%%%%%%%%%%%%%%%%%%%%%
%%%%% SENSIBILITA' IN DECIMAL\PASCAL. BANDA DEL FILTRO NEL TEMPO +/- 10% DELLA FREQUENZA %%%%%
%%%%%%%%%%%%%%%%%%%%%%%%%%%%%%%%%%%%%%%%%%%%%%%%%%%%%%%%%%%%%%%%%%%%%%%%%%%%%%%%%%%%%%%%%%%%%%%%%%

bpfilt = designfilt('bandpassfir','FilterOrder',80,'CutoffFrequency1',fs-fs/10,'CutoffFrequency2',fs+fs/10,'SampleRate',fc);
dmic_filtrato = filter (bpfilt,dmic);
dmic_RMS = sqrt((sum(dmic.^2))/length(dmic));


%%%%% WINDOWING

n_samples = length(dmic);
winSize = 8192*2;

OverlapStep = 50;   %50% overlap or 0 to not use overlap

if OverlapStep > 0

    Overlap = floor((OverlapStep*winSize) / 100);
    nFrames=floor(n_samples/Overlap)-1;
else
```

```
    Overlap= winSize;
    nFrames=floor(n_samples/Overlap)-1;
end


k=1;
i=1;

%%%%% inizializzazione array

spettro=zeros(nFrames,Overlap+1);
spettrow=zeros(nFrames,Overlap+1);
spettroh=zeros(nFrames,Overlap+1);
spettropsd=zeros(nFrames,Overlap+1);
spettrowpsd=zeros(nFrames,Overlap+1);
spettrohpsd=zeros(nFrames,Overlap+1);
valoredipicco=zeros(nFrames,1);
%THD_N=zeros(nFrames,Overlap+1);

%%%%%%%%%%%%%%%%%%%%%%%%%%%%%%%%%%%%%%%%%%%%%%%%%%%%%%%%%%%%%%%%%%%%%%%%%%%%%%%%%%%%%%%%%%%%%
%%%%% CALCOLO DEI DIFFERENTI TIPI DI SPETTRO. FFT/PSD CON HANNING E FLATTOP            %%%%%
%%%%%%%%%%%%%%%%%%%%%%%%%%%%%%%%%%%%%%%%%%%%%%%%%%%%%%%%%%%%%%%%%%%%%%%%%%%%%%%%%%%%%%%%%%%%%

while ( (k+winSize-1) <= n_samples )

    FrameSignal = dmic(k:k+winSize-1);
    N=length(FrameSignal);
    fn = fc*(0:(N/2))/N;


    %windowing flattotp + hanning
    w = flattopwin(winSize);
    wdata = FrameSignal(:).*w;
    h = hanning(winSize);
    hdata = FrameSignal(:).*h;

    %fft normale
    y = fft(FrameSignal);
    y=abs((y)/(N/2));
    P1 = y(1:N/2+1);

    %fft hanning
    yh = fft(hdata);
    yh=abs((yh*sh)/(N/2));
    P1h = y(1:N/2+1);

    %fft FLATTOP
    yw = fft(wdata);
    yw=abs((yw*sf)/(N/2));
    P1w = yw(1:N/2+1);

    %PSD
    ypsd = (y.*conj(y));
    P1psd = ypsd(1:N/2+1);
```

```

    %PSD hanning
    yhpsd = (yh.*conj(yh));
    P1hpsd = yhpsd(1:N/2+1);

    %PSD flattop
    ywpsd = (yw.*conj(yw));
    P1wpsd = ywpsd(1:N/2+1);


    %% vettori spettri e autospettri

    spettro(i,:)=P1;
    spettroh(i,:)=P1h;
    spettrow(i,:)=P1w;

    spettropsd(i,:)=P1psd;
    spettrohpsd(i,:)=P1hpsd;
    spettrowpsd(i,:)= P1wpsd;

    valoredipicco(i,:)=max(FrameSignal);


    k=k+Overlap;
    i=i+1;
end

P1_mean=sum(spettro)/(i-1);
P1psd_mean=sum(spettropsd)/(i-1);

P1wpsd_mean = sum(spettrowpsd)/(i-1);
P1w_mean=sum(spettrow)/(i-1);

P1h_mean=sum(spettroh)/(i-1);
P1hpsd_mean=sum(spettrohpsd)/(i-1);

valoredipicco_mean=sum(valoredipicco)/(i-1);
%valoreRMS_mean=sum(valoreRMS/(i-1));

%%%%%%%%%%%%%%%%%%%%%%%%%%%%%%%%%%%%%%%%%%%%%%%%%%%%%%%%%%%%%%%%%%%%%%%%%%%%%%%%%%%%%%%%%%%%%
%%%%% TOTAL HARMONIC DISTORTION AND TOTAL HARMONIC DISTORTION + NOISE                   %%%%%
%%%%%%%%%%%%%%%%%%%%%%%%%%%%%%%%%%%%%%%%%%%%%%%%%%%%%%%%%%%%%%%%%%%%%%%%%%%%%%%%%%%%%%%%%%%%%

%%%%% THD + N

P1wpsdlog=(10*log10(P1wpsd_mean))';         %serve 10 logaritmo perche' si parla di potenza
massimo=max(P1wpsdlog);
minimo=massimo-65;

index_max = find(P1wpsdlog == massimo);
index = find(P1wpsdlog >= minimo & P1wpsdlog <= massimo);
di=7;                                       %numero di indici prima e dopo l'indice della
     fondamentale
index=index(index >= index_max-di & index <=index_max+di);
```

```
energia_fund = sum(P1wpsd_mean(index));
THD_N=(((sum(P1wpsd_mean)-energia_fund)/energia_fund).^.5)*100;

sens = 20*log10((max(P1wpsd_mean)^.5)/(res));
sens_peak = 20*log10(valoredipicco_mean/(res));
%THDN=THD_N*100;

%%%%% THD STABDARD

if(fs<=8000)          %la frequenza massima e' 24kHz non e' possibile calcolare
                       %la THD per tutte le frequenze
     harm_max=armoniche(P1wpsdlog,fn,fs);
    harm_max_lin=10.^(harm_max(:,1)/10);
     THD_std = ((sum(harm_max_lin(2:end))/(harm_max_lin(1))).^0.5)*100;
 end

%%%%% AOP

AOP_Pa = res/sqrt(max(P1wpsd_mean));
AOP_dB = 20*log10(AOP_Pa/p0);

%%%%% GRAFICI


xmin = -inf;
xmax = 10;
ymin = -inf;
ymax = +inf;

figure(1)
plot(dmic,'r')
title('Signal')
xlabel('time')
ylabel('Decimal')

figure(2)
subplot(221)
plot(fn,P1h_mean,'black');
title('FFT + Hanning')
xlabel('Frequency \Hz')
ylabel('digital amplitude \LSB')
subplot(222)
plot(fn,P1w_mean,'r');
title('FFT + Flattop')
xlabel('Frequency \Hz')
ylabel('digital amplitude \LSB')
subplot(223)
plot(fn,P1hpsd_mean,'g');
title('PSD + Hanning')
xlabel('Frequency \Hz')
ylabel('power digital amplitude \LSBe2')
subplot(224)
plot(fn,P1wpsd_mean,'blue');
```

```
title('PSD + Flattop')
xlabel('Frequency \Hz')
ylabel('power digital amplitude \LSBe2')

figure(3)
subplot(221)
plot(fn,20*log10(P1h_mean),'black');
axis([xmin xmax ymin ymax])
grid on;
title('FFT + Hanning')
xlabel('Frequency \Hz')
ylabel('digital amplitude \dBLSB')
subplot(222)
plot(fn,20*log10(P1w_mean),'r');
axis([xmin xmax ymin ymax])
grid on;
title('FFT + Flattop')
xlabel('Frequency \Hz')
ylabel('digital amplitude \dBLSB')
subplot(223)
plot(fn,10*log10(P1hpsd_mean),'g');
axis([xmin xmax ymin ymax])
grid on;
title('PSD + Hanning')
xlabel('Frequency \Hz')
ylabel('digital amplitude \dBLSB')
subplot(224)
plot(fn,10*log10(P1wpsd_mean),'blue');
axis([xmin xmax ymin ymax])
grid on;
title('PSD + Flattop')
xlabel('Frequency \Hz')
ylabel('digital amplitude \dBLSB')

figure(4)
plot(fn,10*log10(P1wpsd_mean),'blue');
axis([xmin xmax ymin ymax])
grid on;
title('PSD + Flattop')
xlabel('Frequency \Hz')
ylabel('Decimal Amplitude \dB')
```

```
clc
clear

%%%%%%%%%%%%%%%%%%%%%%%%%%%%%%%%%%%%%%%%%%%%%%%%%%%%%%%%%%%%%%%%%%%%%%%%%%%%%%%%%
%il programma calcola il livello equivalente pesato A e non pesato A come
%valore efficace della serie temporale e come livello equivalente totale
%filtrato sulle bande di 1/3 di ottava
%%%%%%%%%%%%%%%%%%%%%%%%%%%%%%%%%%%%%%%%%%%%%%%%%%%%%%%%%%%%%%%%%%%%%%%%%%%%%%%%%

%%%% load files %%%%
name='name.bin';
fileID = fopen(name);
precision = 'int16';
A = fread(fileID,precision);
load('sensMEMS.mat');


fc=48000;
F = [ 20, 25 31.5 40, 50 63 80, ...
    100 125 160, 200 250 315, 400 500 630, 800 1000 1250, ...
    1600 2000 2500, 3150 4000 5000, 6300 8000 10000, 12500 16000 20000 ];
sens1k = 1216.3236;
p0=20*10^-6;
dmic= A(1:2:end);    %odd matrix - digitale

%%%%% filtro da 22.4Hz a 22390 Hz %%%%%%%
Fs=fc;
Fc=1000;
N=3;
pi = 3.14159265358979;
f1 = 22.4;
f2 = 22390;
Qr = Fc/(f2-f1);
Qd = (pi/2/N)/(sin(pi/2/N))*Qr;
alpha = (1 + sqrt(1+4*Qd^2))/2/Qd;
W1 = Fc/(Fs/2)/alpha;
W2 = Fc/(Fs/2)*alpha;
[B,A] = butter(N,[W1,W2]);

%%%%% livello globale tra 20 e 20k %%%%%%
dmic_filtrato = filter (B,A,dmic);
Leq_temp = 20*log10((rms(dmic_filtrato)/sens1k)/p0);

%%%%%%%%%%% One Third Octave Band %%%%%%%%%%%%%%%%%%%%%%%%%%%%%%%%%%%%%%%%%%%%%%%%%
%rincavo i Pa usando la sensibilita' LSB/Pa per ogni terzo di ottava e
%calcolo il livello equivalente come RADICE DELLA SOMMA AL QUADRATO
%%%%%%%%%%%%%%%%%%%%%%%%%%%%%%%%%%%%%%%%%%%%%%%%%%%%%%%%%%%%%%%%%%%%%%%%%%%%%%%%

[dmic_RMS_filtr, f_filtr] = oct3bankmod(dmic_filtrato);
dmic_one_third = [f_filtr',dmic_RMS_filtr'];
dmicPa_eqvl = sqrt(sum((dmic_one_third(:,2)./sensMEMS(:,2)).^2));
dmic_one_third_dB=20*log10(dmic_one_third(:,2)./sensMEMS(:,2)/p0);
Leq_oct3 = 20*log10((dmicPa_eqvl)/p0);

```

```
%%%%%%%%%%%% A Wheigthing Filter %%%%%%%%%%

[C,D] = adsgn(fc);
dmic_A = filter(C,D,dmic_filtrato);

LeqA_temp = 20*log10((rms(dmic_A)/sens1k)/p0);
[dmic_RMS_filtr_A, f_filtr] = oct3bankmod(dmic_A);
dmic_one_third_A = [f_filtr',dmic_RMS_filtr_A'];


dmic_one_third_dBA=20*log10(dmic_one_third_A(:,2)./sensMEMS(:,2)/p0);
dmicPa_eqvl_A = sqrt(sum((dmic_one_third_A(:,2)./sensMEMS(:,2)).^2));
LeqA_oct3 = 20*log10((dmicPa_eqvl_A)/p0);

%%%%%%%%%%% usando la sensibilita' a 1kHz per tutte le frequenze %%%%%%%%%
dmicPa_eqvl_A_sens1k = sqrt(sum((dmic_one_third_A(:,2)./sens1k).^2));
LeqA_oct3_sesn1k = 20*log10((dmicPa_eqvl_A_sens1k)/p0);

dmicPa_eqvl_sens1k = sqrt(sum((dmic_one_third(:,2)./sens1k).^2));
Leq_oct3_sens1k = 20*log10((dmicPa_eqvl_sens1k)/p0);

%%%%%%%%%%%%%%%%%%%%%%%%%%%%%%%%%%%%%%%%%%%%%%%%%%%%%%%%%%%%%%%%%%%%%%%%%%%
%%%% aggiungo il livello equivalente e il livello equivalente pesato A %
%%%%%%%%%%%%%%%%%%%%%%%%%%%%%%%%%%%%%%%%%%%%%%%%%%%%%%%%%%%%%%%%%%%%%%%%%%%
dmic_one_third_dB(end+1)=Leq_oct3;
dmic_one_third_dB(end+1)=LeqA_oct3;

%%%%%%% plot %%%%%%%

name={'20';'25';'31.5';'40';'50';'63';'80';'100';'125';'160';'200';'250';'315';'400';'500';'630
    ';'800';'1k';'1.25k';'1.6k';...
    '2k';'2.5k';'3.15k';'4k';'5k';'6.3k';'8k';'10k';'12.5k';'16k';'20k';'Leq';'LeqA'};
figure
bar(dmic_one_third_dB);
set(gca,'XTick',1:1:33);
set(gca,'xTickLabel',name)
xlabel('Frequency Band /Hz'); ylabel('Amplitude /dB');
title('One-third-octave Band Spectrum')
```

```
function [p,f] = oct3bank(x);
% OCT3BANK Simple one-third-octave filter bank.
%     OCT3BANK(X) plots one-third-octave power spectra of signal vector X.
%     Implementation based on ANSI S1.11-1986 Order-3 filters.
%     Sampling frequency Fs = 44100 Hz. Restricted one-third-octave-band
%     range (from 100 Hz to 5000 Hz). RMS power is computed in each band
%     and expressed in dB with 1 as reference level.
%
%     [P,F] = OCT3BANK(X) returns two length-18 row-vectors with
%     the RMS power (in dB) in P and the corresponding preferred labeling
%     frequencies (ANSI S1.6-1984) in F.
%
%     See also OCT3DSGN, OCT3SPEC, OCTDSGN, OCTSPEC.

% Author: Christophe Couvreur, Faculte Polytechnique de Mons (Belgium)
%         couvreur@thor.fpms.ac.be
% Last modification: Aug. 23, 1997, 10:30pm.

% References:
%     [1] ANSI S1.1-1986 (ASA 65-1986): Specifications for
%         Octave-Band and Fractional-Octave-Band Analog and
%         Digital Filters, 1993.
%     [2] S. J. Orfanidis, Introduction to Signal Processing,
%         Prentice Hall, Englewood Cliffs, 1996.


pi = 3.14159265358979;
Fs = 48000;                     % Sampling Frequency
N = 3;                    % Order of analysis filters.
F = [ 100 125 160, 200 250 315, 400 500 630, 800 1000 1250, ...
    1600 2000 2500, 3150 4000 5000 ]; % Preferred labeling freq.
ff = (1000).*((2^(1/3)).^[-10:7]);  % Exact center freq.
P = zeros(1,18);
m = length(x);

% Design filters and compute RMS powers in 1/3-oct. bands
% 5000 Hz band to 1600 Hz band, direct implementation of filters.
for i = 18:-1:13
   [B,A] = oct3dsgn(ff(i),Fs,N);
   y = filter(B,A,x);
   P(i) = rms(y);
end
% 1250 Hz to 100 Hz, multirate filter implementation (see [2]).
[Bu,Au] = oct3dsgn(ff(15),Fs,N);    % Upper 1/3-oct. band in last octave.
[Bc,Ac] = oct3dsgn(ff(14),Fs,N);    % Center 1/3-oct. band in last octave.
[Bl,Al] = oct3dsgn(ff(13),Fs,N);    % Lower 1/3-oct. band in last octave.
for j = 3:-1:0
   x = decimate(x,2);
   m = length(x);
   y = filter(Bu,Au,x);
   P(j*3+3) = rms(y);
   y = filter(Bc,Ac,x);
   P(j*3+2) = rms(y);
   y = filter(Bl,Al,x);
```

```
   P(j*3+1) = rms(y);
end

% Convert to decibels.
% Pref = 1;                    % Reference level for dB scale.
% idx = (P>0);
% P(idx) = 10*log10(P(idx)/Pref);
% P(~idx) = NaN*ones(sum(~idx),1);

% Generate the plot
if (nargout == 0)
  bar(P);
  ax = axis;
  axis([0 19 ax(3) ax(4)])
  set(gca,'XTick',[2:3:18]);          % Label frequency axis on octaves.
  set(gca,'XTickLabels',F(2:3:length(F)));  % MATLAB 4.1c
%  set(gca,'XTickLabel',F(2:3:length(F)));  % MATLAB 5.1
  xlabel('Frequency band [Hz]'); ylabel('Power [dB]');
  title('One-third-octave spectrum')
% Set up output parameters
elseif (nargout == 1)
  p = P;
elseif (nargout == 2)
  p = P;
  f = F;
end
```

```
function [p,f] = oct3bank(x);
% OCT3BANK Simple one-third-octave filter bank.
%    OCT3BANK(X) plots one-third-octave power spectra of signal vector X.
%    Implementation based on ANSI S1.11-1986 Order-3 filters.
%    Sampling frequency Fs = 44100 Hz. Restricted one-third-octave-band
%    range (from 100 Hz to 5000 Hz). RMS power is computed in each band
%    and expressed in dB with 1 as reference level.
%
%    [P,F] = OCT3BANK(X) returns two length-18 row-vectors with
%    the RMS power (in dB) in P and the corresponding preferred labeling
%    frequencies (ANSI S1.6-1984) in F.
%
%    See also OCT3DSGN, OCT3SPEC, OCTDSGN, OCTSPEC.

% Author: Christophe Couvreur, Faculte Polytechnique de Mons (Belgium)
%         couvreur@thor.fpms.ac.be
% Last modification: Aug. 23, 1997, 10:30pm.

% References:
%    [1] ANSI S1.1-1986 (ASA 65-1986): Specifications for
%        Octave-Band and Fractional-Octave-Band Analog and
%        Digital Filters, 1993.
%    [2] S. J. Orfanidis, Introduction to Signal Processing,
%        Prentice Hall, Englewood Cliffs, 1996.


pi = 3.14159265358979;
Fs = 48000;                    % Sampling Frequency
N = 3;                  % Order of analysis filters.
F = [ 20, 25 31.5 40, 50 63 80, ...
    100 125 160, 200 250 315, 400 500 630, 800 1000 1250, ...
    1600 2000 2500, 3150 4000 5000, 6300 8000 10000, 12500 16000 20000 ];% Preferred labeling
        freq.
% exact frequency
xx=-100:100;
fr=10^3;
b=3;
G = 10^(3/10);
alfa=G.^(xx/b);
fm=(alfa*fr)';
fm=fm(fm>=19 & fm<=20000);

ff=fm;

%ff = (1000).*((2^(1/3)).^[-10:7]);     % Exact center freq.
P = zeros(1,31);
m = length(x);

% Design filters and compute RMS powers in 1/3-oct. bands
% 5000 Hz band to 1600 Hz band, direct implementation of filters.
for i = 31:-1:7
    [B,A] = oct3dsgn(ff(i),Fs,N);
    y = filter(B,A,x);
    P(i) = rms(y);
```

```
end
% 1250 Hz to 100 Hz, multirate filter implementation (see [2]).
    [Bu,Au] = oct3dsgn(ff(9),Fs,N);     % Upper 1/3-oct. band in last octave.
    [Bc,Ac] = oct3dsgn(ff(8),Fs,N);     % Center 1/3-oct. band in last octave.
    [Bl,Al] = oct3dsgn(ff(7),Fs,N);     % Lower 1/3-oct. band in last octave.
for j = 1:-1:0
   x = decimate(x,2);

   y = filter(Bu,Au,x);
   P(j*3+3) = rms(y);
   y = filter(Bc,Ac,x);
   P(j*3+2) = rms(y);
   y = filter(Bl,Al,x);
   P(j*3+1) = rms(y);
end

% Convert to decibels.
% Pref = 1;                  % Reference level for dB scale.
% idx = (P>0);
% P(idx) = 10*log10(P(idx)/Pref);
% P(~idx) = NaN*ones(sum(~idx),1);

% Generate the plot
% if (nargout == 0)
%   bar(P);
%   ax = axis;
%   axis([0 19 ax(3) ax(4)])
%   set(gca,'XTick',[2:3:30]);      % Label frequency axis on octaves.
%   set(gca,'XTickLabels',F(2:3:length(F)));  % MATLAB 4.1c
% %  set(gca,'XTickLabel',F(2:3:length(F)));  % MATLAB 5.1
%   xlabel('Frequency band [Hz]'); ylabel('Power [dB]');
%   title('One-third-octave spectrum')
% % Set up output parameters
% elseif (nargout == 1)
%   p = P;
% elseif (nargout == 2)
  p = P;
  f = F;
end
```

```
function [B,A] = oct3dsgn(Fc,Fs,N);
% OCT3DSGN  Design of a one-third-octave filter.
%    [B,A] = OCT3DSGN(Fc,Fs,N) designs a digital 1/3-octave filter with
%    center frequency Fc for sampling frequency Fs.
%    The filter is designed according to the Order-N specification
%    of the ANSI S1.1-1986 standard. Default value for N is 3.
%    Warning: for meaningful design results, center frequency used
%    should preferably be in range Fs/200 < Fc < Fs/5.
%    Usage of the filter: Y = FILTER(B,A,X).
%
%    Requires the Signal Processing Toolbox.
%
%    See also OCT3SPEC, OCTDSGN, OCTSPEC.

% Author: Christophe Couvreur, Faculte Polytechnique de Mons (Belgium)
%         couvreur@thor.fpms.ac.be
% Last modification: Aug. 25, 1997, 2:00pm.

% References:
%    [1] ANSI S1.1-1986 (ASA 65-1986): Specifications for
%        Octave-Band and Fractional-Octave-Band Analog and
%        Digital Filters, 1993.

if (nargin > 3) | (nargin < 2)
  error('Invalide number of arguments.');
end
if (nargin == 2)
  N = 3;
end
if (Fc > 0.88*(Fs/2))
  error('Design not possible. Check frequencies.');
end

% Design Butterworth 2Nth-order one-third-octave filter
% Note: BUTTER is based on a bilinear transformation, as suggested in [1].
pi = 3.14159265358979;
f1 = Fc/(2^(1/6));
f2 = Fc*(2^(1/6));
Qr = Fc/(f2-f1);
Qd = (pi/2/N)/(sin(pi/2/N))*Qr;
alpha = (1 + sqrt(1+4*Qd^2))/2/Qd;
W1 = Fc/(Fs/2)/alpha;
W2 = Fc/(Fs/2)*alpha;
[B,A] = butter(N,[W1,W2]);
```

References

[1] Iec 61094-1/2/3/4/5/6/7, measurement microphones, series of microphone and calibration standards.

[2] Alfons Dehé, Martin Wurzer, M. F., and Krumbei, U. The infineon silicon mems microphone. *Infineon Technologies AG, 81726 Munich, Germany.*

[3] Christen, T. A 15-bit 140- w scalable-bandwidth inverter-based modulator for a microphone with digital output. *IEEE JOURNAL OF SOLID-STATE CIRCUITS* (2013).

[4] Girardin, G. Acoustic mems and audio solutions market and technology report. *Yole Développement* (2017).

[5] Jarman, D. A brief introduction to sigma delta conversion. *INTERSIL, Application Note* (1995).

[6] Lewis, J. Analog and digital mems microphone design considerations. *Technical Article ANALOG DEVICES MS-2472* (2013).

[7] Loibl, M. Measurement of digital mems microphones. *Sensoren* (2016).

[8] Michael Loibl 1, Sebastian Walser 1, J. K. . G. F. . C. S. Measurement of digital mems microphones. *University of Applied Sciences Munich, Lothstraße 64, 80335 Munich, Germany* (2016).

[9] Qiao, D. H., T. J. X. L., and Wang, C. H. *A micromachined condenser microphone with polysilicon diaphragm.* 2005.

[10] Retenrghem, T. V. On the ability of consumer electronics microphones for environmental noise monitoring. *Journal of Dynamic Article LinksC Environmental Monitoring* (2011).

[11] Rongshan Wei, J. W. An energy-efficient multistage charge pump for mems microphone. *IEICE Electronics Express, Vol.* No.*,*-** (2017).

Ringraziamenti

Desidero ringraziare tutti coloro che mi hanno aiutato e sostenuto nello svolgimento di questo tesi e in questa mia esperienza a Torino.

Ringrazio il mio relatore, il Prof. Carullo per avermi accettato come tesista, senza di Lui questo lavoro non sarebbe stato possibile.

Ringrazio Andrea per avermi seguito con pazienza ed impegno, nonché per avermi trasmesso molto delle sue conoscenze ed avermi sempre dimostrato una grande disponibilità durante tutti questi sei mesi. Lo ringrazio anche per avermi talvolta ritenuto un amico con cui bere una birra vedendosi un bel concerto dal vivo, magari di musica italiana...

Ringrazio Alessandro per avermi sempre considerato come un collega più che come un tesista coinvolgendomi anche in altri progetti al di fuori del mio lavoro di tesi, nonché per avermi insegnato molto sia in campo acustico che non. Ora so esattamente com'è una bagna cauda!!

Ringrazio Claudio che con le sue vaste conoscenze e grande esperienza mi ha aiutato a superare i primi ostacoli seguendomi con passione e disponibilità ed indirizzandomi verso il raggiungimento di un'autonomia lavorativa.

Ringrazio Andrea P.B. per avermi sempre sostenuto, trasmettendomi molto delle sue conoscenze ed interessi. Purtroppo non siamo riusciti a combinare la gita a Saluzzo ma penso che un'altra occasione ricapiterà, inoltre non ho ancora visto il tuo sintetizzatore analogico!!

Ringrazio i ragazzi del dipartimento vibrazioni, Fabrizio, Claudio, Alessandro per la simpatia e l'ospitalità sempre fornita a me... "essere inutile". Inoltre li ringrazio ufficialmente anche per tutti i caffè che mi hanno offerto. Ringrazio ancora in particolare Fabrizio anche per essersi reso disponibile ad effettuare misurazioni riguardante il mio lavoro di tesi.

Ringrazio i ragazzi del dipartimento di acustica, Mario e Antonio per essersi resi generosamente disponibili ogni volta che mi sono rivolto loro per domande o favori.

Ringrazio anche Giuseppe, Simona, Rugiada, Raffaella, Ezio per i pranzi insieme e la loro simpatia.

Ringrazio soprattutto i miei genitori che con il loro affetto e generosità mi hanno permesso di studiare a Torino e completare il mio percorso di formazione. Ringrazio anche mia nonna per avermi sempre fornito consigli preziosi per affrontare la mia esperienza lontano da casa, nonché per avermi sempre messo in guardia a "quelli coi coltelli nei treni"...

Ringrazio Claudia per essermi sempre stata vicino, nonostante la distanza, nella buona e cattiva sorte, sostenuto, incoraggiato ed anche sopportato nei momenti più difficili. Senza di lei questo lavoro non sarebbe stato possibile. La ringrazio anche per tutte le memorabili esperienze passate insieme in questi tre anni sia qui a Torino che a casa.

Ringrazio i miei tre "robosi" coinquilini, Andre Matte e Spana, per tutto il supporto, simpatia e generosità regalatomi in questi tre anni di piacevolissima convivenza, i fratelli che non ho mai avuto. Che la nostra amicizia continui anche negli anni futuri! Ringrazio Gianluca, mio collega di studi e soprattutto amico che ha reso questi 3 anni di Politecnico sempre piacevoli. Il mio terrone preferito potrei dire... peccato non averti festeggiato a dovere per la tua laurea, ma direi che si potrebbe rimediare facendolo con la mia? che ne dici?

Ringrazio anche Lorenzo S., Lorenzo P. e Carlo Alberto per l'aiuto e tutti i felici momenti passati insieme.

Ringrazio i Nashira, la mia band, per tutta la musica suonata, il disco registrato e tutti i concerti fatti, compresi quelli con 3 persone!!

Ringrazio infine tutti i miei amici di Casalmaggiore il cui ricordo delle avventure passate insieme mi ha sempre accompagnato in questi anni.

Nicola
30 Marzo 2018